Membrane potential responses of neurons in the optic tectum during visual object processing in amphibians: Top-down influences, the role of GABA and influences on behaviour

Dissertation

To achieve the academic grade of doctor rerum naturalium – Dr. rer. nat.

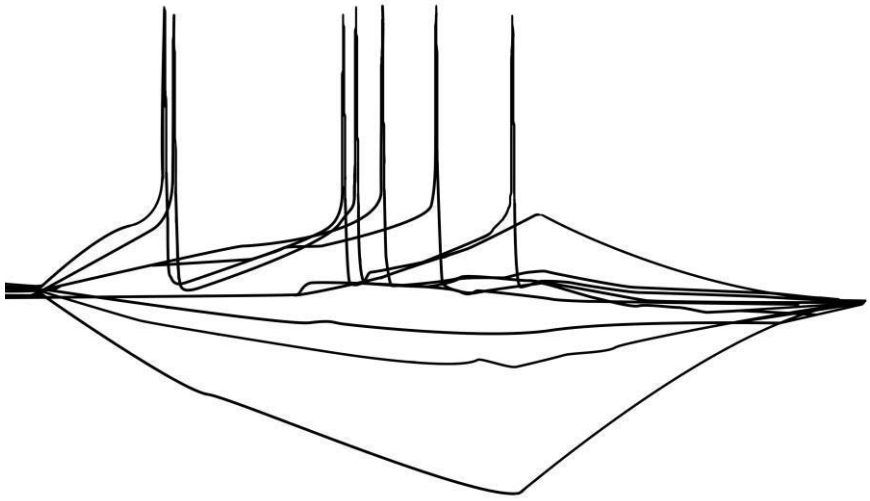

University of Bremen – Department of Biology and Chemistry

By Nikola Jovan Misevic

Berlin, June 2020

Advisor: Prof. Dr. Ursula Dicke

Evaluator 1: Prof. Dr. Ursula Dicke

Evaluator 2: Prof. Dr. Dr. Gerhard Roth

Date of defence: 23rd October 2020

Acknowledgements

My first thanks go to Prof. Dr. Ursula Dicke for providing with the topic of my dissertation, the excellent advice and assistance with planning of the experiments and analysis of data.

I would like to thank Prof. Dr. Dr. Gerhard Roth for his advice and being available as an assessor. I would like to thank Prof. Dr. Michael Koch for being available as an assessor.

I would like to thank Swetlana Baichel, Johanna Radziejewski and Oliver Wetjen for their invaluable encouragement, discussion, and lovely atmosphere.

I would like to thank the technical assistants Barbara Klazura and Dorothea Kittlaus for their excellent support in the lab and warm and welcoming atmosphere in the workplace.

My thanks also go to Paul Freudenberger and Maja Misevic for their helpful encouragement and friendship.

I would like to thank my wife, Maria Misevic-Kallenbach for her unending support, patience, and advice. Without her, this work would not have been possible.

Table of contents

1. Introduction

1.1 Phylogeny of amphibians

Modern amphibians or *Lissamphibia* are organized into three orders. They are a sister group to all terrestrial vertebrates and constitute around one-fifth of all currently living tetrapod species (Frost *et al.*, 2006). Jetz and Pyron (2018) provide data for a total number of 7238 species of amphibians, however a total number of 7700 species is assumed to be found globally. The order *Anura*, which is the largest group within *Lissamphibia* contains frogs and toads. The order is organized into 29 families and approximately 6700 species. The order *Caudata (*former *Urodela)* consists of 10 families and approximately 545 species. Species of this order are commonly described as newts and salamanders. The third order of *Lissamphibia* is *Gymnophiona*, which are legless, terrestrial animals found most commonly in South America and southern China (amphibiaweb.org, 2019). The order *Gymnophiona* consist of 6 families, in which 170 species are found (amphibiaweb.org, 2019).

Most studies of the phylogeny of *Lissamphibia* suggest that they constitute a monophyletic group with lungfishes as the closest non-tetrapod living sister group to *Lissamphibia* (Brinkmann, et al 2004). The *Lissamphibia* are a phylogenetically old group and even though not a large fossil record has been found, it is assumed that the three living amphibian groups evolved during the Palaeozoic or the Mesozoic area. A study by San Mauro and colleagues (2005) suggests that the three groups of *Lissamphibia* radiated rapidly, which resulted in a lacking and paradoxical early fossil record

Large anatomical differences are apparent among extant amphibian species. *Caudata* closely resemble ancient amphibians, whereas *Anura* possess a reduced vertebral column and strongly developed hind limbs. *Gymnophiona* on the other hand mostly have highly ossified skulls and miss limbs (Pough, 2016).

1.2 The organization of the amphibian brain

Most vertebrates live in a visually dominated world. They rely on their eyes to navigate in their environment, feed on prey or flee from predators. Complex and dynamically structured information is perceived with the eyes and processed in the visual system of the brain; even the smallest tadpoles are able to distinguish light from dark and food from non-food. Animals detect sensory signals, process relevant information, and dynamically adapt their behaviour. Among the sensory modalities, the visual system of vertebrates seems to be the most complex, organized in parallel pathways processing shape, colour, structure, movement, depth information and other features of visual objects. Furthermore, the brain has the capability to learn and adapt to changes in the environment. Animals dynamically make decisions on a multitude of factors and thereby improve their probability of survival and reproduction.

These observed behavioural patterns found in all vertebrates are organized by neuronal networks of the central nervous system. They are highly structured, although the organization and functional connectivity is not easily discernible. Of particular interest is the contribution of single neurons or neuronal ensembles. More precisely, their electrical behaviour and the cellular structures constituting the membrane of a neuron. A deeper understanding of the mechanism leading to such a dynamic and adaptive network will help to understand the complex behaviours observed in vertebrates.

1.2.1 Background of amphibian neurophysiology

In neuroscience, amphibians were considered a classical model animal used for a description of simple behaviours. However, that picture has changed with a body of recent works, where it was found that amphibians are also capable of dynamic, complex behaviour (Schuelert & Dicke, 2005), decision making (Ruhl & Dicke, 2012) and learning (Jenkin & Laberge, 2010). Traditionally, the amphibian brain, especially the brain of several frog species, has been extensively studied and described (Gaze, 1958; Maturana, 1959; Grusser-Cornehls *et al.*, 1963). Amphibians possess a relatively simply organized brain with a comparatively small number of neurons. However, by the use of modern methods such as single-cell labelling, retrograde labelling and electrophysiology, the amphibian brain is an ideal candidate to investigate brain structure and connectivity and further advance the knowledge on the functional organization of brain and behaviour.

1.2.2 The amphibian central nervous system

In the following section, an overview of the different parts of the central nervous system is given. However, the visual sense and visual system of amphibians will be the key subject of investigation. Several amphibian species rely on the olfactory and/or acoustic sense in order to navigate in their environment, hunt or reproduce; however, these sensory modes were not experimentally investigated (Baugh & Ryan, 2010). The description of anatomical details and functional connection of the amphibian brain will focus mainly on structures related to the visual system and brain centres controlling and guiding behaviour. Despite the fact that most frogs use phonotaxis to find a mate, they still use their visual senses to identify potential partners and to engage in mating behaviour (Muntz, 1963; Endepols *et al.*, 2000).

The central nervous system comprises the brain and spinal cord and serves as the basis for all motor and sensory functions in vertebrates. Sensory cells provide input from the outside world to the central nervous system, mediated by neurons and fibres of the peripheral and/or the central nervous system. Control of the muscular system is organized by motor centres of the brain and spinal cord and transmitted by motor neurons of the brainstem and spinal cord projecting to the peripheral nervous system. The central nervous system of all vertebrates is divided into five anatomical structures, named from rostral to caudal: The telencephalon, the diencephalon, the mesencephalon, the medulla oblongata, the cerebellum and the spinal cord.

1.2.2.1 The telencephalon

The telencephalon of amphibians consists of a pair of elongated hemispheres, connected by a bridge, also referred to as the telencephalon impar (Wada *et al.*, 1980). In anurans, the telencephalic lobes are clearly separated from each other, whereas in salamanders and newts, the border between the two hemispheres of the telencephalon are indicated only by a shallow groove. The telencephalon in amphibians is usually referred to as the pallium and subdivided into several anatomical regions, such as the dorsal pallium, lateral pallium and medial pallium (Roth *et al.*, 2007). A lamination of the pallium comparable to the cortical layers of the mammalian cortex is not present in the brain of frogs and salamanders. Migrated neurons inside the white matter are common. The dorsal border of the medial pallium is topic of some discussion because chemical markers for a distinction between dorsal and medial boundaries were not found so far. Authors commonly draw the border between the medial and dorsal pallium at the level of the

dorsomedial telencephalic sulcus (Northcutt, 1974; Scalia *et al.*, 1991). However, tracer application studies of the medial pallium suggest a more medial border (Roth, unpublished).

Anatomically, the telencephalon is separated by the diencephalon by the nucleus preopticus (Dicke & Roth, 2007; Nieuwenhuys *et al.*, 2014). Recent studies have also shown that the rostral portion of the pallium is a region of its own due to its connectivity. The rostral pallium receives a large amount of dorsal thalamic afferents and has projection patterns that differ from those of neurons of the posterior pallium (Roth, unpublished).

Subpallial structures are located centrally in the telencephalon. Ventral to the medial pallium, the nucleus accumbens and the ventral striatum are situated. More rostrally, ventral to the ventromedial telencephalon and the septal region, the shell-like ventral pallidum is located. The amygdala of anurans is located ventral to the caudal, ventral telencephalon by the mediocentral amygdala and more laterally by the lateral, also called vomeronasal and cortical amygdala (Roth *et al.*, 2004). The striatopallidal complex is located in the ventrolateral part of the telencephalon.

Some homologies were described between the structures of the amphibian pallium and the vertebrate telencephalon. Agreement exists that the medial pallium is homologous to the mammalian hippocampus, despite the fact that characteristic features of neurons of the mammalian dentate gyrus were not found in the amphibian brain (Westhoff & Roth, 2002). Behavioural studies in amphibians suggest that the medial pallium is also involved in the formation of memory and learning (Wenz & Himstedt, 1990; Papini *et al.*, 1995). The function of the dorsal pallium remains unclear, since it receives sensory afferents similar to the medial pallium but lacks extra-telencephalic efferents. Roth and Dicke (2007) suggest that the dorsal pallium has an integrative-associative and limbic function and might share some characteristics with the cortical structure of mammals.

The lateral pallium including the ventral pallium, is considered to be homologous to the mammalian piriform cortex, even though a majority of projections of the olfactory tract project to the caudal portion. Therefore, the function of the rostral and intermediate portion remains to be discussed.

1.2.2.2 The diencephalon

The diencephalon of amphibians, as well as that of other vertebrates is divided into the epithalamus, thalamus and the hypothalamus (Roth *et al.*, 2003). In the caudal part a transition zone between the diencephalon and the mesencephalon exists, referred to as the pretectum, which is located dorsally to the posterior commissure (Kuhlenbeck, 1967). The thalamus itself is further subdivided into a dorsal and ventral part by a recess, referred to as the sulcus medialis. The ventral thalamus and the hypothalamus are anatomically divided by the sulcus hypothalamicus. The thalamus of anurans has been studied in detail by Neary and Northcutt (1983) and was divided into several nuclei. The dorsal thalamus comprises three nuclei close to the ventricle. An anterior, central and posterior nucleus. Furthermore, a lateral nucleus has been described, which itself comprises three sub-nuclei (Neary & Northcutt, 1983). The ventral thalamus is anatomically divided by a ventromedial nucleus and exhibits several migrated nuclei. These nuclei are termed the ventrolateral nucleus, the neuropil of Bellonci and the superficially situated ventral nucleus (Neary & Northcutt, 1983; Roth *et al.*, 2003). All of these diencephalic nuclei are found in a similar configuration in most of the other frog species. Salamanders have a compact diencephalon with a dense cellular layer surrounding the third ventricle and very few migrated neurons. Therefore, nuclei cannot be discerned by simple staining and observation. Retrograde labelling techniques have partly shown such nucleation (Dicke & Roth, 2007); however, more studies are needed in order to visualize the diencephalic nuclei (Roth *et al.*, 2004).

1.2.2.3 The mesencephalon

The mesencephalon is one of the key structures investigated in this thesis, and therefore, the anatomy and circuitry of the midbrain will be discussed in detail in chapter 1.3. The following is a general overview. The isthmic nucleus in the caudal mesencephalon is a very compact and prominent nucleus and has a specific connectivity with the tectum. It is divided from the ventral tegmentum by the sulcus isthmi, which is located ventral to the dorsocaudal tegmentum. The tegmentum itself has a dorsal and ventral part. The ventral tegmentum includes the oculomotor and trochlearmotor nucleus. Both ascending and descending pathways of the brain cross through the fibre layer of the ventral and dorsal tegmentum. Neurons of the tegmental nuclei are likely to receive input from these pathways, because laterally directed dendrites of tegmental neurons are found in this region. However, the tegmental relay stations are currently still not well understood. It is

a highly complex anatomical region, where sensory, motor and limbic systems interface with each other (Szekely *et al.*, 1973; Roth *et al.*, 1988; Nieuwenhuys *et al.*, 1998)

The torus semicircularis is an important nucleus of the mesencephalon and located ventrally to the dorsal structure of the mesencephalon, the tectum. In anurans, three major nuclei are described, a principal nucleus, a laminar nucleus and a magnocellular nucleus. The structure serves as the centre of the ascending auditory pathways, as well as pathways of the vestibular and somatosensory system and if present that of the lateral line system (Potter, 1969; Wilczynski, 1981; Feng *et al.*, 1990; Kulik & Matesz, 1997) The roof of the midbrain is referred to as the mesencephalic tectum and forms two bulbous hemispheres. The region of the optic tectum comprises the superficial layers of the bulb, containing in- and outputs from the visual system. In salamanders, these bulbs may also be wide and flat. The tectum serves as a centre for visual perception and visuomotor function. Amphibians require an intact function of the tectum to localize and recognize objects (Ingle, 1973a; Finkenstadt, 1980; Kostyk & Grobstein, 1982; Schuelert & Dicke, 2005). Furthermore, depth perception is processed within the tectum. Anatomical studies revealed separate pathways that ascend and descend to the thalamus and pre/motor centres in the medulla oblongata and the spinal cord, respectively (Wiggers & Roth, 1994). Also, the ability to accurately orient is a behaviour mediated by the tectum (Kostyk & Grobstein, 1982; Finkenstädt & Ewert, 1983)

1.2.2.4 The cerebellum and the medulla oblongata

The cerebellum of amphibians is small, however, the types of cerebellar neurons and its microcircuitry as found in other vertebrates is present in amphibians as well. Inside the cerebellum, Purkinje cells are aligned at the boundary between the molecular and granular layer, which serve as the afferent and efferent fibre layers. The cerebellum receives input from the diencephalon and mesencephalon, and substantial afferents to the cerebellum originate in the medulla oblongata. Mainly fibres from the trigeminal and trochlear nerve terminate in the cerebellum as well as input comes from the vestibular nuclear complex and the glossopharyngeal system. Efferent projections extend to the lateral medulla oblongata and then mainly to the vestibular complex. The cerebellum of amphibians serves as a sensorimotor integration system and motor coordination centre (Antal *et al.*, 1980; Fite *et al.*, 1988; Dicke & Muhlenbrock-Lenter, 1998). The medulla oblongata of amphibians is divided into three longitudinal zones based on the density and arrangement of cells and characteristic distribution of neurotransmitters. The zones are referred to as the median, medial and lateral zone. The cranial nerves V–XII terminate in the rhombencephalic part of the medulla oblongata. The medulla oblongata serves as a relay station for somato- and viscerosensory information; it also processes inputs from the inner ear or in some species from the lateral line organs or the ampullary organs. The medulla oblongata also comprises an extended network, the reticular formation, which is a functionally heterogeneous zone. Groups of neurons control vital bodily functions such as respiration and blood circulation, generate motor commands or control vigilance and attention (Dicke & Roth, 2007).

1.2.2.5 The spinal cord

The most caudal part of the central nervous system is the spinal cord, in which the afferent and efferent fibres enter and leave the central nervous system via the spinal nerves. Primary somatosensory afferent fibres enter through the dorsal roots and bifurcate into descending or ascending fibre bundles. A substantial part of these fibres crosses the midline and terminate in the contralateral grey matter. From there, projections reach the cerebellum, hindbrain or the medulla oblongata (Antal *et al.*, 1980; Dicke & Muhlenbrock-Lenter, 1998). Characteristically, in tetrapods the spinal cord consists of a cervical, thoracical, lumbar and sacral part, and contains a cervical and lumbar enlargement because of the increased mass of sensory and motor neurons for the control of the limbs. In frogs, the spinal cord is divided into a dorsal, lateral, central, ventromedial and

ventrolateral field, with the dorsal horn separated into dorsal funiculi. Motor neurons are found in the ventral zone and are arranged along motor columns in a rostrocaudal axis (Matesz & Szekely, 1978; Wake *et al.*, 1988; Kim & Hetherington, 1993).

1.3 The visual system

1.3.1 The anatomy of the eye

A large number of amphibian species rely on their visual sense to hunt prey (Larsen & Guthrie, 1975). Most amphibians also represent prey for larger predators in their environment. For these two behavioural patterns, predation and predator avoidance, large, well developed eyes increase visual perception and thereby provides survival advantage. Well-developed eyes are a good indicator for a well-structured visual system. Amphibians, as most other vertebrates, possess a typical structure of the eye. Light passes and is focussed through the cornea and lens into the hyaloid canal. Photoreceptors in the retina are excited by light and propagate their excitation to retinal ganglion cells, which pre-process visual information and transmit it to the brain (Roth, 1987). Typically, the majority of fibres of the visual nerve cross to the contralateral hemisphere with only rare projections to the ipsilateral side.

The retina consists of a five-layered structure, which is commonly found in vertebrates. In the most distal layer, the outer segments of the photoreceptors are found. Rods, single cones and double cones are distinguished in amphibians. The outer segments of these photoreceptors are separated from their nuclei by the outer limiting membrane. The outer nuclear layer contains the nuclei of the photoreceptors. Bipolar and horizontal cells interconnect the photoreceptors through the outer plexiform layer (Dowling & Werblin, 1969) with their nuclei being part of the inner nuclear layer. The most central layer is the retinal ganglion cell layer; the retinal ganglion cells project their axon via bundles across the inner surface of the eye toward the optic disk. These axons then form the optic nerve.

Even though no specialized regions on the retina such as the fovea are found, the number of receptors and retinal ganglion cells are large. For example, *Rana esculanta* has approximately 1 million photoreceptors and approximately 500,000 retinal ganglion cells (Maturana *et al.*, 1959). Retinal ganglion cells were studied in detail and using electrophysiological recording techniques; three distinct classes were described according to their responses to specific visual stimuli (Dicke & Roth, 2009):

- Small-field cells mainly respond to objects with a relatively high contrast either moving or non-moving. P-cells in primates and X cells in cats display comparable characteristics.
- Medium-field cells respond mostly to small dislocations of edges and movement. They correspond with M cells and Y cells of the primate and cat retina, respectively.
- The large-field cells respond most strongest to large objects presented to the retina or changes to illumination over large parts of the retina.

The optic nerve contains both myelinated and unmyelinated fibres. It enters the brain at the level of the diencephalon and forms the optic chiasm, where fibre bundles cross towards the contralateral hemisphere. Projections of the retinal ganglion cells are mainly topographically organized and largely reach the contralateral diencephalon and mesencephalon (Maturana, 1959; Lazar, 1969; Scalia & Fite, 1974; Montgomery & Fite, 1989).

1.3.2 Projection targets of the retinal ganglion cells

The retinal ganglion cells of amphibians mainly have axonal terminations within the diencephalon and mesencephalon (Maturana, 1959; Lazar, 1969; Scalia & Fite, 1974; Montgomery & Fite, 1989). For neurons projecting toward the contralateral diencephalon, four distinct neuropils have been described: The neuropil of Bellonci, the corpus geniculatium thalamicum, the nucleus preopticus and the posterior thalamic neuropil (Rettig & Roth, 1986). Retinal ganglion cells that project to the optic tectum terminate extensively in several fibre layers, at least in three or four, depending on the species of amphibian (Roth, 1987). The axons of retinal ganglion cells also run to the basal optic neuropil, which is located in the tegmentum of the brain (Fritzsch, 1980).

Only a small percentage of retinal ganglion cells were found to project to the ipsilateral diencephalon or mesencephalon (Singman & Scalia, 1990, 1991). The basal optic root is divided into a lateral and medial fascicle. In *Rana pipiens*, the lateral fascicle innervates the terminal field of the nucleus of Bellonci. The central and mediodorsal portions are innervated by the medial fascicle, while the ventrolateral portion of the nucleus of Bellonci is innervated by the lateral fascicle. Both fascicles innervate the medial region (Fite *et al.*, 1988).

The major target for retinal ganglion cells is the optic tectum of the mesencephalon. Of the axons terminating in the optic tectum, a majority of synaptic endings were found inside the superficial layers (Singman & Scalia, 1990; Wiggers, 1999). Furthermore, a small number of retinal ganglion cells project to the basal optic neuropil, which is located within the tegmentum in the mesencephalon (Fritzsch & Himstedt, 1980; Rettig & Roth, 1986; Wiggers, 1999).

The axonal terminations of retinal ganglion cells in the optic tectum of salamanders has been studied in detail. Wiggers (1999) investigated the terminations of retinal ganglion cells using an *in vitro* labelling approach of single cells. In most cases, axons arborize in dense and complex bushes with high variability. Roughly 20 % of terminals reach in the subpial layer. The corresponding fibres are also located directly below the tectal surface and commonly form a dense plexus. Almost 60 % of retinal terminals were found in intermediate layers of the tectum. Axons projecting to the deep layers of the tectum additionally form axonal terminals inside the thalamus and pretectum. The axonal terminals of retinal ganglion cells have also been studied in frogs using horse-radish peroxidase labelling (Wiggers, 1999). Stirling and Merrill (1987) found that the axons of retinal ganglion cells branch out at the level of the pretectum before terminating inside the tectum. In all superficial layers of the tectum, terminals were found. However, the extent and morphology of these arborizations were variable. In general, small and dense arborizations with beaded terminals were found in the superficial layers, whereas in the deeper tectal layers larger arborizations with only a few branches were present (Stirling & Merrill, 1987; Hughes, 1990).

1.3.3 Ascending visual projections in the amphibian brain

The vertebrate brain processes information by using bottom-up processing, where incoming sensory information is sorted and processed according to certain criteria as well as top-down modulation, where certain internal states regulate informational flow among brain centres. Anatomically, three ascending visual pathways are described in the amphibian brain. These are also the major pathways of visual information processing of other vertebrates. Namely they are the retino-thalamo-telencephalic, the retino-tecto-thalamo-telencephalic and the retino-tectal-pretectal pathway (Dicke & Roth, 2009). While in the primate brain the functional roles of these ascending pathways are reasonably well known, in amphibians the functional significance is still a matter of discussion. An important role appears to fall to the dorsal thalamus, which mediates

visual information to the telencephalon. This connection may contribute, directly or indirectly, to object processing, visual attention and decision making.

One example of top-down modulation was found in the study by Ruhl and Dicke (2012). Neurons of the tectum responded to prey-like objects and were inhibited in their spike-rate when objects were presented in the surrounding receptive field of a neuron. After lesioning the dorsal thalamus, such an inhibition was lacking and it was suggested that the dorsal thalamus acts as a top-down modulatory station for visual tectal neurons (Ruhl & Dicke, 2012). In the thalamus, several types of projection neurons have also been described (Roth *et al.*, 2003; Skorina *et al.*, 2016). However, neurons from the dorsal area of the thalamus do not project in any large quantities to the tectum (Roth *et al.*, 2003).

1.4 Midbrain microcircuitry and visual processing

1.4.1 Structure of the tectum

The discrimination of objects in a visual field, such as prey from non-prey, requires an evolved central nervous system, that for example requires specialized neuronal networks and sophisticated physiological mechanisms. Behavioural patterns that are dynamic and adaptive in order to respond to the constantly changing environment seem to represent a key trait. As already described, the main visuomotor integration centre of amphibians is the tectum, the dorsal part of the mesencephalon. In a transversal view of the tectum, alternating layers of neuropil and neurons are apparent. In amphibians, the neurons of the tectum tend to be located more closely to the ventricle. Anatomically, the tectum of frogs is organized into nine layers (Potter, 1969). A majority of tectal neurons are local interneurons and approximately 5 % are projection neurons (Dicke & Roth, 2009). Layer 1 is closest to the ventricle and it consists of ependymal glial cells. These cells have long processes extending up to the tectal surface. The periventricular grey matter comprises the layers 2, 4 and 6, which are divided by the two deep fibre layers 3 and 5. These fibres are mainly unmyelinated and consist largely of non-retinal afferents and efferents. Layer 6 is the most superficial cellular layer, even though some migrated neurons are found in the superficial fibre layers. Layer 7 contains the bulk of efferent fibres, while layer 8 contains only very few scattered and loosely arranged neurons embedded in a network of dendrites and afferent fibres. Layer 9, which is the most superficial layer, barely contains any neurons. Most retinal afferents are found in layer 9. Layer 8 and 9 are subdivided into seven laminae, namely A to G (Dicke & Roth, 2007). Neurons are found mainly in lamina C and E, whereas laminae B, D, F and G contain the majority of myelinated and unmyelinated fibres (Roth, 1987). Using labelling techniques, neurons of the amphibian tectum have been sorted into types according to their morphology, arborization and projection pattern (Antal *et al.*, 1986; Lazar, 1988; Dicke & Roth, 1996; Roth *et al.*, 1999).

1.4.2 Neuronal types of frogs

The optic tecum of frogs is layered structure, with ependymal cells being close to the ventricle. Within the different layers of the tectum, certain types of neurons can be described in regard to the structure and response characteristics. The following classifications follow general anatomical findings (Antal *et al.*, 1986; Lazar, 1988; Dicke & Roth, 1996)

- Type-1 neurons are large and their pear- or pyramidal-shaped somata are situated mainly in layer 6. Some migrated neurons of type-1 are found in layers 7 or 8. Their dendritic tree is candelabrum-shaped and extends mainly into lamina A. Their axons descend contralaterally along the tectobulbospinal tract to the medulla oblongata.
- Type-2 neurons have both ascending and descending projections. They possess small, spindle-shaped somata located superficially in layer 7. Commonly, they have two thick dendrites, which originate directly at the soma and branch into thick secondary dendrites. The dendritic tree regularly extends to the tectal surface.
- Type-3 neurons have similar projection patterns as type-2 neurons. Their somata are pear- or pyramidal-shaped. They are located closely to the periventricular grey (layer 2 and 4). Their dendritic tree is wide and arborizes within lamina C or D.
- Type-4 neurons also have pear-shaped somata. They are frequently found in deep cellular layers. Typically, they have slender dendritic trees, which arborize up to lamina C. Their axonal projections descend ipsilaterally to the ventrolateral part of the rostral medulla oblongata. Some axons ascend to the ipsilateral thalamus.
- Type-5 neurons are situated within the deeper part of the periventricular grey. The dendritic tree is flat and often T-shaped; it extends to the efferent fibre layer 7. Type-5 neurons have descending axons, which are part of the ipsilateral tectobulbospinal tract.
- Interneurons also have pear-shaped somata. Typically, they possess slender dendritic trees with a highly variable arborization inside different laminae of the tectum. Commonly, interneurons are found as migrated neurons in a superficial position above layer 6.

The layering of salamanders differs to that of frogs in such that the number layers is inverted. Layer 1 is the superficial layer and layer 9 is the layer with ependymal cells bordering the ventricle (Roth *et al.*, 1999).

1.5 Object discrimination during vision

In the classical view of the past time, amphibian vision has been regarded as a simple reflex, i.e., the frog stereotypically reacts to a prey stimulus with a snapping behaviour (Larsen & Guthrie, 1975; Thexton *et al.*, 1977). Several studies clearly showed that amphibians are not only capable of discriminating objects from each other but are also able to react dynamically to certain stimuli or learn from experiences (Schuelert & Dicke, 2005; Jenkin & Laberge, 2010; Dicke *et al.*, 2011). As previously described, the tectum receives major afferents from both the retina and other brain areas such as the diencephalon. The visual afferents are retinotopically organized (Scalia & Fite, 1974). The tectum is the main visuomotor-integration centre, where visual information is represented via population coding of neurons (an der Heiden & Roth, 1987). The modulation of these neurons by feedback-loops and top down modulation seems to represent a sort of attentional system in amphibians (Ruhl & Dicke, 2012). It is mainly achieved via inhibitory pathways, e.g., an inhibitory projection of the pretectum (Ingle, 1973b; Luksch & Roth, 1996). Another example is a tecto-isthmo-tectal connection, which enhances calcium influx at optic nerve terminals and thus is involved in the processing of visual information (Dudkin & Gruberg, 2003).

Within the tradition of ethological research, the feeding behaviour of amphibians has been extensively studied in neuroscience. This behaviour is mainly visually guided (see chapter 1.2.1) and thus an ideal behavioural pattern to study vision.

In short, the feeding behaviour is induced by the movement of a potential prey in the visual field of the animal. This induces vigilance, which can be observed by a slight raising of the head of an amphibian. Subsequently, the animal will orient itself toward the potential prey, either by turning its body or head. Amphibians employ several strategies to hunt; they slowly approach a prey, wait until a prey approaches (e.g., ambush feeders) or reduce the distance to the prey with great speed (hunters). Individuals may employ different strategies depending on the prey, environment, experience or motivation (Ingle, 1975; Luthardt & Roth, 1979; Kostyk & Grobstein, 1982; Masino & Grobstein, 1989).

Object processing in amphibians was studied in detail by presenting two different prey objects at the same time and observing the behaviour of the individual (Ingle, 1973a). The underlying idea is that the animal is able to choose between two options and choose a potential prey, which will maximise its gain (Feger, 1978). The object itself is analysed with regard to its features such as shape, size, colour, texture, orientation and/or speed

(Schuelert & Dicke, 2005). Studies of the neuronal responses to visual stimulation of the retina and tectum clearly show that neurons in the tectum code these specific features of objects. In addition, modulatory top-down influences play an important role in object discrimination. Experience and motivation contribute to the processing of the perceived object; projections from more rostrally located brain areas to the tectum may represent the basis of such a modulation (Luthardt & Roth, 1979; Glagow & Ewert, 1997; McConville *et al.*, 2006). Schuelert and Dicke (2002) confronted salamanders simultaneously with two objects. The objects differing in size, shape, velocity or texture were presented in the centre of the visual field and the orienting reaction of the salamander was recorded. Behaviourally, salamanders responded best to large and fast objects and a preference list of these objects was created (Schuelert & Dicke, 2005). In a follow-up experiment (Schuelert & Dicke, 2005), the membrane responses of tectal neurons were extracellularly recorded during presentation of the same objects. In general, highly preferred objects commonly elicited a higher spike-response as objects with low-preference. However, some exceptions were observed, such as rectangles, which are behaviourally not highly preferred, they elicited a high spike rate due to the high contrast of the object. The lower preference of that object in the behavioural experiment is a clear indicator of a top-down modulation. In the study by Schuelert and Dicke (2005), two objects were also presented to the salamander and the membrane responses of tectal neurons were recorded. One object was presented inside and another one outside the receptive field (RF) of the recorded neuron. Neurons responded with a lower spike-rate to the object inside the RF, when another object was present outside the RF, i.e., within the surround of the RF. The strength of such an inhibition correlated with the behavioural preference of the object. When a low-preferred object was presented in the surround, only a slight inhibition was observed. However, the presentation of a highly preferred object in the surround of the RF led to a strong inhibition of responses to the presented object inside the RF. This phenomenon was termed the 'inhibitory effect'. Ruhl and Dicke (2012) aimed to investigate the circuitry of this effect. After lesioning the dorsal thalamus, salamanders were not able to select an object during presentation of two objects. Furthermore, during extracellular recording of lesioned animals, the inhibitory effect was no longer present and tectal neurons were disinhibited in their spike charges (Ruhl & Dicke, 2012). This study suggest that the dorsal thalamus serves as an important modulatory relay in object discrimination and visual processing. A subsequent study investigated the influence of the striatum in object discrimination, because the striatum is a potential candidate involved

in the tectum-thalamus-telencephalon feedback loop. The striatum seems not to contribute with a direct inhibitory feedback projection to tectal processing. The striatum is a multisensory integration area, which generates behavioural patterns that influence motor areas in the medulla oblongata (Ruhl *et al.*, 2016). A similar functional connectivity is likewise present in other vertebrates. The lamprey *(Lampetra fluviatilis)* has been frequently used as a model animal, because its central nervous system can also be seen as a prototype for other vertebrates (Grillner, 2003). Lamprey brains are homologous to those of amphibians and many parallels exist in anatomical and functional aspects. In lampreys, excitatory inputs from the eyes to the tectum are commonly found (Kardamakis *et al.*, 2015) as well as γ-aminobutyric acid (GABA) releasing projections to the optic tectum are present. Using tracer studies, strong inputs to the optic tectum originate from the caudoventral part of the medial pallium, the ventral and dorsal thalamus and the nucleus of the posterior commissure, the torus semicircularis and the nucleus isthmi (Robertson *et al.*, 2006). The authors of the latter study conclude that forebrain input may play a similar role in lamprey as in mammals. Studies in mammals and other vertebrates also investigated the role of GABA and its involvement in circuits between the diencephalon and mesencephalon. The authors conclude that local circuits of neurons in interaction with other brain areas may mediate behaviours such as saccadic eye movement and decision making (Meredith & Ramoa, 1998; Isa & Hall, 2009; Phongphanphanee *et al.*, 2014).

1.6 Neurotransmitters and receptors in the amphibian brain involved in vision

In all vertebrate brains, synapses serve as a transmitting and communicating zone between two or more neurons. Synapses are points of contact between cells and form the most basic unit of a neuronal network: a presynaptic cell, a synapse and a postsynaptic cell (Dale, 1935). Two types of synapses are known: electrical and chemical synapses. Electrical synapses employ gap-junction channels to directly link the pre-synaptic and post-synaptic cell. Gap-junction channels are a low-resistance connection, which allows electrical current to freely flow between two neurons (Bennett, 1997). This enables almost instantaneous transmission of information across cells depending on additional conditions such as pH-value, presence of calcium (Ca^{2+}) or voltage present across the membrane. Electrical synapses are commonly found in amphibians as well, usually in structures where a very fast connection between neurons is required. Electrical synapses are found in the retina (Akopian, 2000) or between the segments of developing motor neurons (Roberts & Perrins, 1995). The other type of synapses are chemical synapses. An action potential occurring in the pre-synaptic cell initiates the release of neurotransmitters into the synaptic cleft. Neurotransmitters are stored in specialized zones of the axon, termed active zones, and are discharged by exocytosis. An action potential within the pre-synaptic neuron leads to an increase of intracellular Ca^{+2} concentration (Cornell-Bell *et al.*, 1990). This in turn causes the fusing of the presynaptic membrane with the synaptic cleft. Neurotransmitters interact with specific receptors controlling the opening of ion channels in the postsynaptic cell either directly or indirectly. Ionotropic receptors such as the nicotinic actetyl-choline receptor gate the opening of ion channels directly (Unwin, 1993). After binding with their specific neurotransmitter, receptors undergo a conformational change which opens an ion channel. Ionotropic receptors act within a few milliseconds and result in very fast response times. Such synaptic connections are found in neuronal circuits which mediate rapid behaviour. The other type of receptors are metabotropic receptors, which indirectly influence ion-channels in the postsynaptic neuron. Commonly, the interaction between neurotransmitter and receptor stimulate the production of second messengers within the intracellular medium. A large portion of second messengers activate protein kinases, often phosphorylating ion channels, which leads to their opening or closing. Metabotropic receptors produce slower responses, which can last from seconds to minutes. Furthermore, the involvement of an activated second messenger system may lead to

induction of gene expression and long-term physiological and morphological changes in a cell. Metabotropic receptors are usually found in pathways modulating behaviour and are critical in reinforcing pathways during learning (Kandel, 2013). Cellular membranes have the capability to produce an electric potential, because of the isolating properties of the membrane and the unequal distribution of ions. Specific membrane proteins are responsible for keeping a stable potential over time. Therefore, in order to understand the function of specific receptors in the brain, a short explanation of membrane properties and the methods to investigate those will follow in this chapter.

Action potentials are generated through depolarization, which is caused by opening of voltage-gated ion channels. This is especially important during whole-cell recordings, because the potential recorded between the recording and reference electrode is the sum of all ion channels in the cell (Numberger & Draguhn, 1996).

Typically, the flow of current across ion channels is measured in terms of conductance, expressed in Siemens, and this value gives the inverse of resistance. This unit is used because opened ion channels usually have a constant conductance and are therefore following Ohm's law, i.e. the relationship between current and voltage is linear. A typical method in investigating the activity of a neuron channel is plotting current against voltage at the tip of an electrode. Depending on the intra- and extracellular concentrations of ions, a channel has a certain reversal potential, at which the net flow of ions changes directions. Thus, the measurement of membrane characteristics serves an important method in the characterization of the physiological properties of a neuron. Indirectly, properties of the local networks and microcircuits are investigated by studying the properties of membranes.

Information about microscopic single-channel currents using opening probability for voltage-gated channels explains membrane reactions regarding currents. The current-dependency of the opening probability of a neuron is measured with the following method: A neuron is clamped at a sufficiently negative holding-potential, so that all channels are set to an activatable state. Then, a short spike of positive potential is applied to the electrode, which leads to an opening of a subset of ion channels. The amplitude of the voltage is directly proportional to the opening probability of the ion channel and therefore also directly proportional to the applied positive voltage. When repeated for different positive voltages, the resulting current will suddenly change direction. This can be displayed in a characteristic current-voltage-graph. The linear shape of this graph is

explained because the driving force of the sodium-selective ion-channel will decrease near the sodium-equilibrium potential. Then it will reverse when the applied voltage is above it. Typically, the voltage is given as a characteristic for a neuron, in which exactly half of the channels are open. This value is expressed in a fitted curve, calculated by normalizing the amplitude to their maximal value. A curve is fitted using a Boltzmann-Function and the slope of this curve gives the relationship between conductivity and voltage of a given neuron (Standen *et al.*, 1987; Hille, 2001).

1.6.1 The cholinergic neurotransmitter system in amphibians

The principal cholinergic neurotransmitter in the amphibian brain as well as in other vertebrates is acetylcholine. It plays a role in the visual system, because the nucleus isthmi comprises a large number of cholinergic neurons (Ricciuti & Gruberg, 1985; Wallace *et al.*, 1990). Acetylcholine is the major neurotransmitter in neuromuscular junctions. Two classes of receptors are known to exist: nicotinic receptors, which are ionotropic receptors with mainly two subtypes, and the muscarinic receptor class, which are a group of metabotropic receptors classified as M_1-M_5. Neurons possessing acetylcholine are also found in the tegmentum, in salamanders in the tectum and in addition, in the diencephalon and forebrain (Puelles *et al.*, 1996). Cholinergic neurons in the striatopallidum of amphibians are often co-localized with other neurotransmitters or neuropeptides such as glutamate, GABA, dopamine or substance P (Reiner *et al.*, 1998; Muhlenbrock-Lenter *et al.*, 2005). However, these cholinergic neurons are not densely packed in nuclei but rather scattered inside the striatopallidum.

1.6.2 The GABAergic system in amphibians

The most important inhibitory neurotransmitter in the adult amphibian brain is GABA. It is found throughout the central nervous system. GABA plays a critical role during development and it is present in projection neurons of the medulla oblongata. GABAergic projection neurons of the salamander *Plethodon jordani* from the medulla were stained using immunoreactive techniques in order to understand the distribution of such neurons (Landwehr & Dicke, 2005). GABA immunoreactive neurons were found scattered among all layers of the optic tectum of the salamander *Triturus cristatus* and *Pleurodeles waltl*, with most of the GABA positive neurons found in the fibre layers of the tectum, suggesting the role of GABA-positive interneurons (Franzoni & Morino, 1989; Naujoks-Manteuffel & Niemann, 1994).

In *Plethodon jordani* and *Hydromantes italicus*, GABA-immunoreactive neurons are present in approximately 30 % of neurons of the tectum opticum. A majority of neurons with GABA-immunoreactivity were found in layer 8, followed by layer 6. GABA was commonly co-localized with glutamate-immunoreactivity (Wallstein & Dicke, 1996). For the midbrain of amphibians, the presence of GABAergic neurons was investigated using immunoreactive techniques. In *Rana catesbeiana* and *Xenopus laevis,* GABA immunoreactive somatas were found throughout all cellular layers of the tectum. Dense population of GABA-immunoreactive neurons were found in layers 2, 4 and 6 (Hollis & Boyd, 2005). When estimating population size of GABA-immunoreactive neurons, nearly a third of all neurons were found to be positive for GABA immunoreactivity (Antal, 1991). Using such techniques, some aspects of microcircuitry are revealed as well. For example, in *Bufo marinus* nearly 57% of retinal projections terminate on GABA-immunoreactive neurons (Gabriel & Straznicky, 1995). Furthermore, neurons that constitute a part of retinotectal projections do not have close synaptic connections with neurons from the isthmotectal system (Rybicka & Udin, 1994). GABA was found co-localized with neuropeptide Y in approximately half of the cases in layer 6 of the tectum of *Rana esculenta* (Kozicz & Lazar, 2001).

These findings may be due to the fact that glutamate may serve as a precursor to GABA. The receptor for GABA is a ligand-gated ion channel, which is composed of five closely related subunits that possess four transmembrane α-helixes (Olsen & Sieghart, 2009; Zhu *et al.*, 2018). GABA-receptors are conserved within vertebrates and are genetically closely related to the receptors for acetylcholine and glycine (Schofield *et al.*, 1987). Receptors for GABA typically are sensitive for Cl^- and are thus essential in neuronal inhibition. Typically, the resting potential of a neurons is between – 40 mV and – 65mV and slightly more positive than the equilibrium potential of chlorine ions (E_{CL^-} -70 mV). As a result, the opening of chloride channels leads to a positive, outward current of the cell. When observing an inhibitory postsynaptic potential (IPSP), this positive outward current is associated with an influx of chloride ions into the cell toward its electrochemical gradient. Therefore, the net negative charge inside of the neuron increases and leads to a hyperpolarization of the membrane. GABA-receptors in a cell do not only contribute to the occurrence of IPSP. The inhibitory effect of GABA-receptors is also present during excitatory postsynaptic potential (EPSP). When GABA-receptors are open and an influx of chloride ions occurs, the increased conductance of the membrane is comparable to a

short-circuiting of the membrane-model. This effect leads to a decreased magnitude of EPSPs (Schofield *et al.*, 1987; Kandel, 2013).

1.6.3 The glutamatergic system in amphibians

Like in most vertebrates, the main excitatory neurotransmitter in the central nervous system of adult amphibians is L-glutamate, which is abundant in all brain parts and localized in projection neurons as well as in local interneurons. Excitatory potentials are mediated by glutamate-gated channels, which are permeable to both Na^+ and K^+. It is of note that the permeability for the two ions is almost equal. This latter fact results in an reversal potential for current flow at 0 mV (Thoreson & Bryson, 2004). Two receptors for glutamate are known in vertebrates and are categorized in two groups. Firstly, an ionotropic glutamate receptor exists, which is a direct channel and is always excitatory. Secondly a metabotropic glutamate receptor exists, which functions inhibitory or excitatory. Ionotropic glutamate receptors are grouped into three subtypes, named after their respective agonists: α-amino-3-hydroxy-5-methyl-4-isoxazolepropionic acid (AMPA-receptors), Kainate-receptors and *N*-Methyl-D-aspartic acid (NMDA-receptors). Furthermore, AMPA and kainate receptors are often referred to as non-NMDA-receptors, because they are not affected by the presence of NMDA. In amphibians, glutamate and glutamate receptors are widely found in excitatory connections. For example, retinal ganglion cells are mainly glutamatergic. Hickmott and Constantine-Paton (1993) investigated the response patterns of tectal neurons in amphibians and found that in an *in vitro* slice-preparation both non-NMDA and NMDA receptors mediate polysynaptic responses, whereas functional NMDA receptors are not responsible for the bulk of normal excitatory activity (Hickmott & Constantine-Paton, 1993). Glutamate is used as the chief neurotransmitter of retinal ganglion cells projecting to the tectum. Using retrograde labelling technique showed that 88 % or retinal axon terminals of the optic tectum were immunoreactive to glutamate(Gabriel *et al.*, 1992; Gabriel & Straznicky, 1995).

Glutamate is also used as a neurotransmitter in the telencephalon of amphibians, where it is found co-localized in neurons with other neurotransmitters and neuropeptides such as GABA, acetylcholine, dopamine, substance P and others (Muhlenbrock-Lenter *et al.*, 2005). Glutamate receptors are also found outside of the central nervous system of amphibians. For example, using immunoreactive-methods Glutamate-positive cells were found in the vestibular organ of salamanders (Panzanelli *et al.*, 1991). For motor signal transmission in the brainstem of amphibians, both NMDA and non-NDMA glutamate

receptors are vital; for example, the application of a rhythmic spike-train to trigeminal and hypoglossal nerves critically affects the respiratory motor output (Kottick *et al.*, 2013).

1.7 Aims

The present work aimed to investigate the functional connectivity between the thalamus and the optic tectum and the role of it in inhibition of tectal neurons observed during paired presentation of two prey like objects. When an object is presented inside the receptive field and another one outside the receptive field of a neuron, an inhibition is observed when compared to the single presentation of the object inside the receptive field. This inhibition depends on certain characteristics of the object in the surround (see chapter 1.3). Using lesion studies, Ruhl and Dicke (2012) found that the dorsal thalamus plays a critical role in object discrimination during perception and selection of a prey. After lesioning the dorsal thalamus, the inhibition effect described above is no longer present. It is assumed that this phenomenon comprises a case of attentional selection involving a feedback-loop. However, it is not yet fully understood how this feedback-loop works on a neuronal and microcircuit level. The present thesis will pursue two main avenues of investigation: the electrophysiological characterization and the pharmacological characterization of tectal inhibition involving the thalamus.

The inhibitory influence of the thalamus will be electrophysiologically characterized by thalamic stimulation. Membrane potentials from neurons in the optic tectum were recorded using whole-brain preparations from *Bombina orientalis.* During recording, the brain was either stimulated at the optic nerve (ON STIM), the dorsal thalamus (TH STIM) or at both sites simultaneously. Stimulation at the stump of the optic nerve served as a simulation of the excitatory inputs from retinal ganglion cells (Scalia & Fite, 1974; Roth *et al.*, 2003). Thalamic stimulation represented the top-down modulation during object processing such as in the paired object presentation described above. The thalamus is comprised of several nuclei, therefore, it will be stimulated at various sites and the membrane responses will be compared. These experiments are conducted under the assumption that a stimulation of the optic nerve leads to a glutamatergic response of retinal ganglion cells (Dicke & Roth, 2007). This thesis hypothesizes that mainly low-latency monosynaptic responses are expected as a response. The response latency and the general membrane response characteristics and how they correlate with the neuron type will be investigated. A further hypothesis is, that stimulation of the thalamus leads either to excitation or inhibition, depending on which circuit within the thalamus was activated.

The pharmacological aim of the present work was to investigate the role of GABA in tectal inhibition involving the thalamus. A novel semi-intact brain preparation was created in the present thesis, which keeps the forebrain and the connective fibres between forebrain and midbrain intact and at the same time allows patch-clamp recording of neurons in the tectum. This preparation will be used for applications of antagonists of NDMA and non-NMDA glutamate receptors during the recording of tectal neurons. Labelling studies investigated receptor distribution of the amphibian optic tectum showing both glutamate and GABA receptors are present on tectal neurons and involved in visual processing. The hypothesis states that excitatory responses after ON STIM will ablate after applying NMDA-antagonists antagonists while will be present after application of AMPA-antagonist antagonists.

The approach using the semi-intact brain preparation will also be used for the characterization of GABAergic projections originating from the thalamus. The same stimulation regime will be used as described above, while applying a GABA antagonist. It its therefore hypothesised that inhibition by thalamic inhibition should be reversibly supressed using this regime.

The present thesis will investigate the microcircuitry of the tecto-thalamic connections using a novel experimental approach of a semi-intact brain preparation coupled with an in-vitro patch-clamp analysis. The amphibian animal model is a suitable instance to study the inhibitory effect during object processing and will help to better understand the functioning of neuronal networks and their role in behaviour in amphibians and further forms a groundwork for the condition in other vertebrates.

2. Material and methods

2.1 Animals

All experiments of the present work were conducted with the fire-bellied toad *Bombina orientalis*, which were first described by Boulenger (Boulenger, 1890). It belongs to the family *Bombinatoridae* and is a mostly aquatic toad with a warty skin. *Bombina* is known by its usually bright and colourful belly, and the secretion of the skin glands are highly toxic in some species. *Bombina* prefers cold, fast streams and naturally occurs in southwest Asia. When disturbed, the toad displays a reflex, in which it turns on its back in order to expose the coloured belly that indicates threat. For a long time, toads have been a classic amphibian studied in physiology and neuroscience. The toads used in the present thesis were either purchased from a local animal trader ("Zoo am Hulsberg") or they were offspring of these bred in the animal facility. The snout-vent-length of toads investigated ranged from 3.2 cm to 5.5 cm; both male (n = 47) and female (n= 36) toads were investigated. The gender of the animal was determined after anaesthesia has been performed. The ventral skin was opened by a cut from the cloaca to the area above the heart. The organs were checked for parasites, and the gender was identified by the presence of ovaries or testicles. The animals were sacrificed and all experiments conducted in accordance with the EU Guideline 2010/63 and the German animal welfare act (TSchG).

Figure 1. A group of individuals of the species Bombina orientalis kept in a glass box. *The box is placed in a climate-controlled room of the lab in the Brain Research Institute, Bremen, Germany. Semiaquatic living conditions were provided. The ground consisted of gravel; the environment was enriched by plants as well as by larger stones, clay pots and slate plates to offer climbing and hiding opportunities. Access to fresh water was likewise present. Picture: Barbara Klazura; used with permission.*

The individuals were housed in glass boxes sized 55 cm x 35 cm x 30 cm in groups from 8 to 12 individuals. This ensured a safe cohabitation and limited conflicts between individuals during feeding. The boxes were illuminated in a 12:12 light: dark cycle throughout the year. The boxes were kept in a climate room at a room temperature of 23 °C and 45 % humidity. The glass boxes were lined with small-scale gravel and several pieces of damp peat in order to guarantee a moist environment throughout the day. Larger stones, clay pots and plants were added to enrich the environment (*Figure 1*). Furthermore, each box contained two water containers, which were accessible via clay plates. The animals were fed twice a week with crickets (*Gryllus bimaculatus*) from the institute's own breeding stock. Once a month, the animals were additional fed with fruit flies (*Drosophila melanogaster*), which were also bred in the institute.

2.2 Brain Preparation

One day prior to experimentation, the toad was transferred from the glass box into a small plastic box bedded by a wet paper towel. After transport from the animal facility to the laboratory the toad was deeply anesthetized with 1% Tricaine methanesulfonate (Sigma-Aldrich, Munich, Germany) diluted in tap water in a glass cuvette. The cuvette was placed in a darkened chamber in order to reduce stress for the animal. After approximately 10 minutes, deep anaesthesia was verified by checking the leg retraction reflex. The animal was sacrified by decapitation. The decapitated head was fixed on a sylgard-plate, and the skin and mucosal tissue was removed using forceps. Contact of brain tissue with skin glands or mucosal tissue needs to be avoided, because the glands and mucosal tissue of amphibians contain several proteolytic enzymes. Subsequently, the head was transferred to a second dish and submersed in ice-cold Ringer solution. The Ringer solution is based on the composition used by Straka and Dieringer (1993) and consisted of the following substances: D(+)Glucose monohydrate (Sigma Chemical, St. Louis, USA) 11mM; potassium chloride (KCl; AppliChem, Darmstadt, Germany) 2 mM; magnesium chloride ($MgCl_2$; VWR, Leuven, Belgium) 0.5 mM; sodium chloride (NaCl; AppliChem, Darmstadt, Germany) 75 mM; sodium bicarbonate ($NaHCO_3$; AppliChem, Darmstadt, Germany) 25 mM; calcium chloride ($CaCl_2$; AppliChem, Darmstadt, Germany) 2 mM; sucrose (Sigma-Aldrich, Taufkirchen, Germany) 29 mM. The chemicals were dissolved in 2 L distilled water and exposed to carbogen (95 % O_2, 5% CO_2) (Linde; Bremen, Germany) until a pH value of 7.25-7.3 was reached. The osmolarity of the solution was regularly monitored with an osmometer (Osmometer 800cl, Slamed, Frankfurt, Germany) and adjusted, if necessary, to 240 mosmol/kg (Straka & Dieringer, 1993).

A binocular (8x magnification) was used for the observation during extraction of the brain. Ocular scissors with a narrow blade were used to open the connective tissue between the ventral plate of the skull and the first vertebrate. Scissors were inserted into the brain cavity for cutting the skull. Two cuts were made from caudal to rostral at the left and right edge of the ventral skull overlying the brain. Then, the ventral skull overlying the vertebrates were likewise cut, and the bone above the brain and the rostral spinal cord was removed. The roots of the cranial and cervical spinal nerves and major blood vessels were cut. After that, the brain could be easily displaced from the dorsal skull and transferred into a smaller dish filled with ice-cold Ringer solution. The dura mater

covering the brain was removed by the use of two very fine forceps in order to allow a better diffusion of Ringer solution into the brain.

In the experiments using intracellular recordings, a whole-brain preparation was used. For patch-clamp recordings, the brain was further manipulated. A semi-intact brain preparation with an exposed transverse edge along the caudal bulb of the tectum was produced. This preparation leaves intact the tectal projection neurons and their ascending tracts and enables the study of the physiology of these neurons by patch-clamp recording. In order to create a flat, exposed plane in the caudal tectum, using fine ocular scissors the roof of the tectum was initially opened on one lateral side and a cut was made to the other side. The most caudal part of the tectum together with the tegmentum, cerebellum and medulla oblongata was removed (Figure 2). The preparation was stored at 4 °C in Ringer solution and was used for electrophysiology for maximally four days. After recording sessions, the brain was stored in glass beakers with oxygenated Ringer's solution at 4°C. The solution was changed on a daily basis and oxygenated.

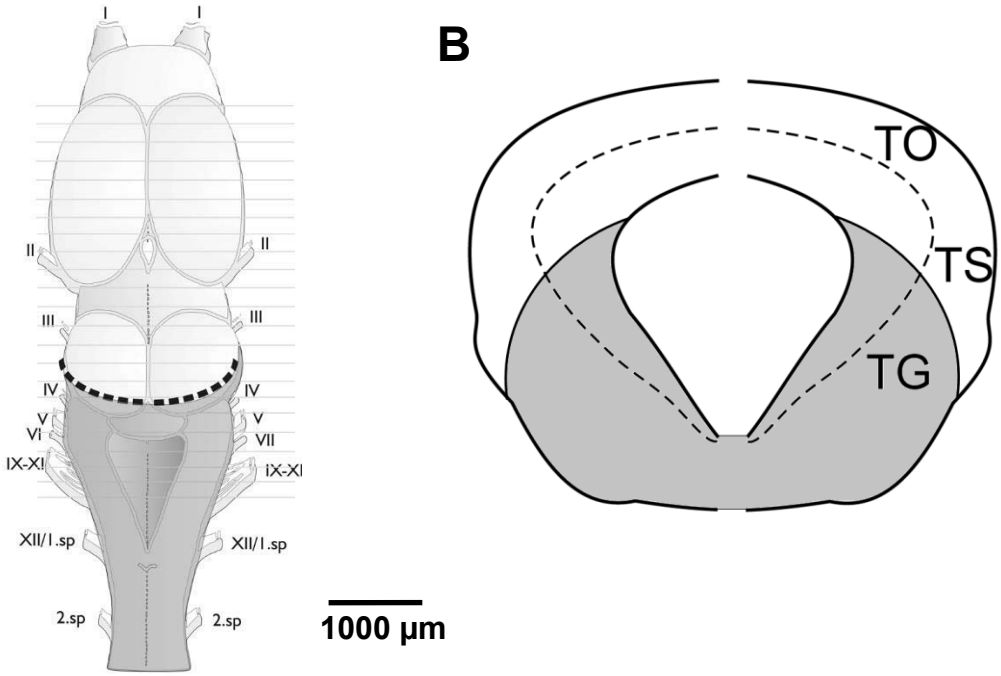

Figure 2. Schematic representation of the semi-intact brain preparation. *Dark grey areas were removed during preparation.* ***A*** *Dorsal view of the brain of Bombina orientalis. The black dotted line indicates the cut for the removal of the dark grey area comprising the very caudal tectum, the cerebellum, the caudal brainstem, and spinal cord. Tectal neurons were recorded and labelled by introducing the electrode through this cut of tectal layers. Roman numerals indicate cranial (I –XII) nerves; 1.sp first and 2.sp second spinal nerve.* ***B*** *Transverse view of the midbrain of Bombina orientalis at the level of the cut in the caudal tectum. TO optic tectum, TS Torus semicircularis, TG tegmentum*

2.3 Electrophysiology

2.3.1 Whole-brain intracellular electrophysiology

In order to perform *in vitro* whole-brain recordings on tectal neurons, micropipettes for high-impedance recordings were manufactured from borosilicate-glass capillaries (0.86x1.5x100mm; GB150F-10, Science Products, Hofheim) and pulled in a horizontal electrode-puller (P-87, Flaming Brown, Sutter Instrument Company, Novato) and stored for up to 48 hours in a dust-free environment. The ends of the capillaries were blunted using a Bunsen burner. This simplified backfilling and handling of the electrodes and minimized damage to the rubber gaskets of the electrode assembly. The micropipettes were backfilled with 2M potassium-acetate, which resulted in a resistance ranging from 60 to 200 MΩ measured in Ringer solution. A reference electrode was constructed using a circular silver-silver-chloride (Ag-AgCl) wire that was fixed (around the prepared brain) in the floor of the recording chamber and connected to the recording instrument. Ringer solution continuously passed (20ml/min) through the recording chamber using an overflow system, in which excess liquid led away into a discard tube system. Electrodes were positioned and manipulated using micromanipulators (Narishige, Olympus, Tokyo, Japan) and were slowly placed above and advanced into the brain. Six areas of the tectal surface were defined to assign roughly in which region of the tectum a neuron was recorded and/or labelled. Two lines in the rostrocaudal axis and one in the mediolateral axis, equidistant to each other, divided the tectal area (*Figure 3*). This division was used as a guide in order to ensure comparable number of recordings in each of the areas. The signal was amplified by a Cyto 791 unit (World Precision Instruments, Friedberg), digitized via an CED micro 1401 mkii apparatus (Cambridge Electronic Design Milton) and monitored and stored for off-line analysis on a commercial PC. For single-neuron tracing, a 4% solution of biocytin (Sigma) was dissolved in 0.3 M potassium-chloride solution and backfilled into a micropipette. Tectal projection neurons were recorded at single or double stimulation. Two stimulation electrodes, namely, one suction electrode with the stump of the cut optic nerve and one bipolar electrode in the dorsal thalamus, and three experimental conditions were used. In the study on the influence of the thalamus during simulated object processing, these conditions were tested in a pseudo-randomized order (Table 1). The stimulation in each condition consisted of a single pulse, which was delivered every two seconds. The three conditions formed a block, which was repeated several times per neuron.

Table 1. Two sites of stimulation using single or double stimulation

	Optic nerve electrode	Thalamus electrode
Optic nerve stimulation ON STIM	Single Pulses	-
Thalamic stimulation TH STIM	-	Single Pulses
Double stimulation DUAL STIM	Single Pulses	Single Pulses

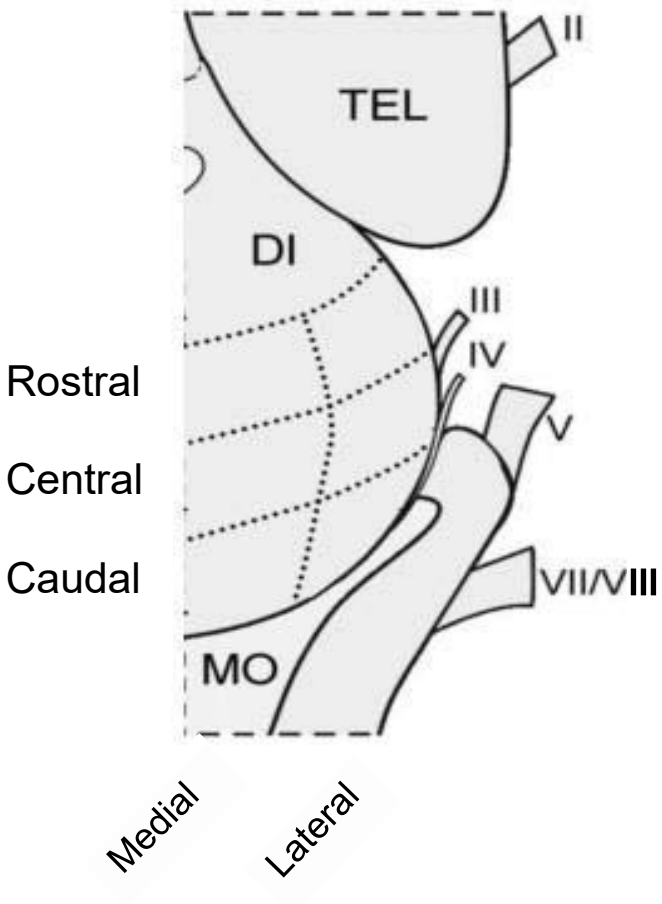

Figure 3. Subdivisions of the tectum*. Areas divided by stippled lines are roughly similar in size. A longitudinal medial and lateral zone and three horizontal zones in the rostral, central and caudal tectum form six subdivisions in the tectum. Tel telencephalon, Di diencephalon. MO medulla oblongata, cranial nerves II-V and cranial nerve VII/VIII*

2.3.2 Patch-clamp electrophysiology

For patch clamp recording, a new brain preparation as described above was created in order to have better access to the tectal layers (Figure *2*). The semi-intact brain preparation was transferred into a recording chamber, where it was fixed with a U-shaped steel weight. Thinly coated wires aligned parallel to the U-shaped weight ensured a stable recording position (Custom-made, Polytetrafluoroethylene 75 µm diameter wires). Like in the intracellular recordings, the brain was perfused with fresh Ringer's solution, which was continuously provided at a rate of 2 ml/min. The Ringer's solution was cooled using a long silicone tubing-system, which was led through a polystyrene box containing ice. The length of the tube and the rate of flow was calculated to ensure a stable temperature of 16 °C (± 1 °C) inside the recording chamber. An electric grounded pump (Masterflex L/S, Gelsenkirchen, Germany) controlled the flow of Ringer's solution. An overflow system was used to ensure a homogenous mix of Ringer's solution and pharmaceutical agents. The recording electrode was grounded via a chlorinated silver wire, which was shielded by a barrier of solid agar-agar dissolved and heated in a 2 M NaCl solution.

Recording was conducted using borosilicate-glass capillaries (GB150F-10, Science Products, Hofheim, Germany) The electrodes were manufactured in a horizontal micropipette puller (P-87, Flaming/Brown, Sutter Instruments, Novato, USA). The resulting tip resistance was 14 MΩ (± 1 MΩ). The tip diameter ranged between 3-5 µm (Sutter Instruments Company, 2008). A recording solution was backfilled prior to the experiments using a solution developed by Yang and Feng (2007, 2009). The solution contained the following buffers and salts: K-gluconate 110 mM; KCl 10 mM; $CaCl_2$ 0.1 mM; $MgCl_2$ 1 mM; HEPES (Sigma-Aldrich, Munich, Germany) 10 mM; EGTA (Sigma-Aldrich, Munich, Germany) 5mM; NaGTP (Sigma-Aldrich, Munich, Germany) 0.3 mM; MgATP (Sigma-Aldrich, Munich, Germany) 3 mM (adapted after (Yang & Feng, 2007; Yang *et al.*, 2009). The ideal osmolarity was empirically derived and regularly checked for each new preparation. If the osmolarity was above or below 280 - 300 mosmol/kg, it was adjusted by adding very small doses of NaCl. The stimulation electrodes were manufactured in the same way as the recording electrodes and filled with the same solution. The current for stimulation was generated using an isolated stimulus generator (WPI Isostim A320, Sarasota, USA). The stimulation amplitude was adjusted to be above the spiking threshold

and ranged from 1 mA to 10 mA. The square pulse used for stimulation lasted 700 µs. An electronic servo-driven micromanipulator ensured a high precision when approaching somata for recording (LM I; Luigs &Neumann, Ratingen, Germany). The position of the electrode and the neuron were monitored using an optical microscope (BX50WI, Olympus, Hamburg Germany). The entire set-up was placed on a vibration-dampening workbench (Newport, Irvine, USA) that was located inside a faraday cage; the latter was grounded. An isolated air-system with a three-way valve was attached to the recording electrode. This system allowed to exert a positive or negative pressure to the tip of the recording electrode. During initial recording, a positive pressure was applied to keep the electrode clear of particles. When approaching a cell, the pressure was reduced, and the tip was gently brought in contact with the cell. Subsequently, a slight negative pressure was applied to the electrode. This led to the spontaneous formation of a gigaseal. In the gigaseal state a series of negative pressure was applied, which induced the rupture of the plasma membrane. Neurons were then recorded in a whole-cell state.

Two different experiments were conducted using the preparation described above. In an initial experiment, the optic nerve was stimulated via an electrode that was manufactured in the same way as the recording electrodes. The optic nerve was stimulated using a built-in DC-converter, which was included in the sampling unit (CED Mikro 1401 mkii, (Cambridge Electronic Design Milton). Square pulses of 700 µs were applied that varied in voltage from 1 V to 5 V. The final voltage for stimulation was empirically determined to be just above the threshold for the release of a postsynaptic response. Neurons were patched in a whole-cell state and the stimulation of the optic nerve was performed for 5 minutes. Responses were recorded and taken as control. After recording in this control condition the neuron was stimulated in three different ways. These states occurred in a pseudo-randomized fashion and each in a rhythm of 0.5 Hertz:

a) A current in addition to the holding current was applied for 0.5 s stepwise increasing from -10 mV, -5mV, 0mV, +5mV, +10mV, +15mV. +20mV.
b) The stimulation electrode of the optic nerve was activated as described above.
c) No manipulation and stimulation was applied to the neuron.

In a second experiment, after five minutes of control condition, pharmaceutical agents were washed in using a three-way valve system. The solution with the pharmaceutical agents was completely diffused in the recording chamber after approximately one minute. After further five minutes, regular flow of Ringer's solution was performed again by the

use of the three-way valve system. Neurons were recorded during application of agents and after wash-out for further 10 minutes or as long as the connection remained stable. In order to characterize glutamate receptors, two pharmaceutical agents were chosen. For the characterization of GABAergic receptors, a single pharmaceutical agent was chosen.

A potent, selective and competitive AMPA-Agonist (NBQX, Bio-Techne GmbH, Wiesbaden-Nordenstadt) was diluted in Ringers solution in a concentration of 10 µM. DL-AP5 (Bio-Techne GmbH, Wiesbaden-Nordenstadt) was used as a competitive NDMA antagonist in a concentration of 100 µM diluted in Ringers solution. As a GABA antagonist, SR-95531 or Gabazine (Sigma-Aldrich, Munich, Germany) was used in two concentrations. 0,1 µM Gabazine and 10 µM Gabazine were dissolved in Ringers solution and kept frozen.

2.3.3 Labelling of neurons

As previously described, a number of neurons were labelled with biocytin and subsequently stained. For subsequent labelling of neurons, micropipettes were backfilled with a 4 % solution of biocytin (Sigma, St. Louis, USA) dissolved in 0.3 M potassium chloride, which resulted in an impedance between 150 and 250 MΩ. After recording, the biocytin-containing electrode was kept in the neuron for 10 minutes, during which a pulsing voltage of 5 V with a frequency of 1 Hz was applied. Then, brains were fixed overnight in phosphate buffer containing 2 % glutaraldehyde and 2 % paraformaldehyde. Coronal sections of 40 µm were cut on a vibratome (Leica VT 1000S, Wetzlar, Germany). Biocytin-labelled neurons were visualized by means of an avidin-biotin-HRP complex (Vector Standard Kit; Vector Laboratories, Burlingame, CA) using diaminobenzidine (DAB, Sigma) as chromogen and a heavy-metal intensification. The sections were then lightly counterstained with Cresyl violet, which enabled differentiation between somata and fibre layers of the tissue. Stained neurons were dark brown or black, and their dendritic trees and axons were traceable over several sections of the brain. Biocytin-labelled neurons were identified, and photographs were taken under a light microscope (Axioskop, Zeiss, Jena, Germany). For reconstruction of the morphology of neurons the software Fiji (Modified after ImageJ, Wayne Rasband, NIH) was used (Schindelin *et al.*, 2012).

2.4 Data Processing

The sampling rate of the analogue data was set to 50 kHz, which allowed the system a high-temporal resolution of fast-acting synaptic activities. The raw data was analysed using search algorithms in Signal 4.05 (Cambridge Electronic Design Milton) and was then processed further by the use of a built-in feature of Signal 4.05. An algorithm, the so-called "cursor"-function searched for a peak within the waveform. It was applied to each waveform, and a processing sweep across one waveform in a 2-second chunk was performed as follows: First, an average potential was determined using all data points from the 500 ms immediately prior to stimulation, a second post-stimulus average potential was calculated the same way, following 100 ms after the onset of the stimulation pulse. Amplitudes were calculated from the difference between the pre-stimulus average voltage of the recorded neuron and the voltage at a certain time point, calculated with the search algorithm. Latencies were determined using the difference between the onset of the stimulation artefact and the sampled data point (Figure 4). Using the data points 500 ms immediately prior to stimulation, the standard deviation of data points was calculated. Onset describes the time when the fall of the slope starts, and the signal crosses the threshold of the standard deviation given by the first 500 ms. The minimum value is the time when the minimal voltage is reached, and the recovery value (Recovery) is the time when the membrane potential returns to the lower boundary baseline potential, also defined by the mean and its corresponding standard deviation. Furthermore, the minimal value of the inhibition and the rebound of the inhibition were calculated as the difference between the mean value and the minimal value, or the recovery value (Figure 4). The characteristics of EPSPs were calculated in a similar fashion. The stimulation artefact was used as a guideline and the mean value 500 ms prior to stimulation was calculated along with the corresponding standard deviation. Latencies were defined as the time difference between the stimulus artefact and the points of interest. The steepest point of the EPSP and the maximum value give the time when the potential reaches the point of the steepest rise of the slope and the maximal voltage, respectively. The afterhyperpolarization is defined by the time between the occurrence of the maximum voltage and the most negative voltage (Figure 5).

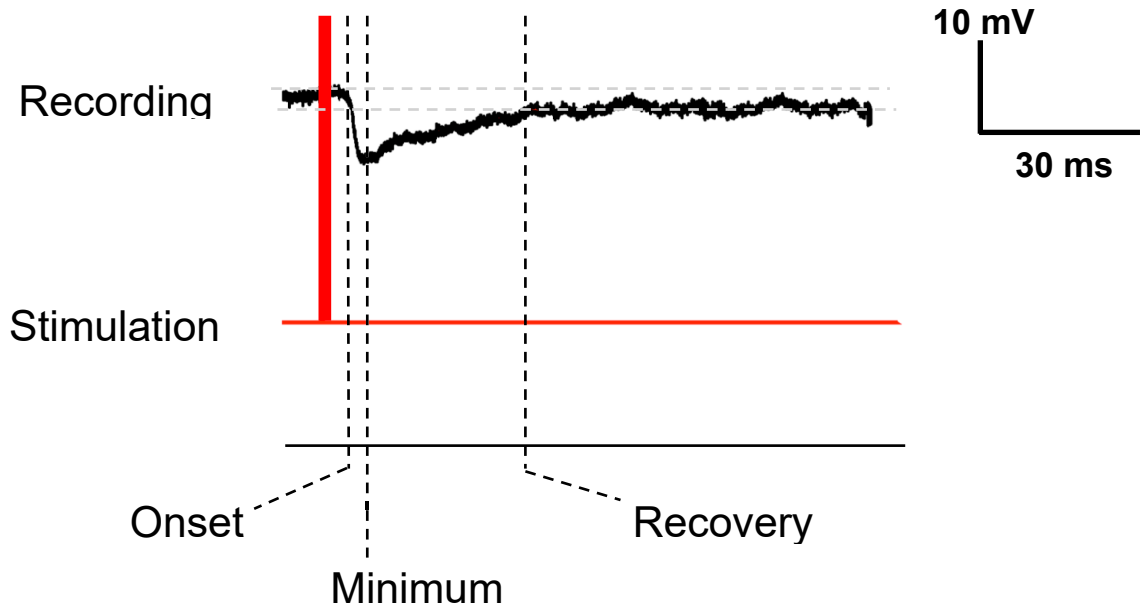

Figure 4 Characterization of a representative IPSP after stimulation. *The black trace is the membrane potential recorded from a tectal cell. The vertical red bar indicates the stimulation artefact. Stimulation was applied to the optic nerve stump. The latencies are defined as the time difference between the vertical red bar and the dashed vertical lines. Onset describes the time when the fall of the slope starts. The minimum value is the time when the minimal voltage is reached, and the recovery value (Recovery) is the time when the membrane potential returns to the lower boundary baseline potential (dashed lower grey line above the trace of the membrane potential). The two dashed horizontal lines give value of the standard-deviation (SD).*

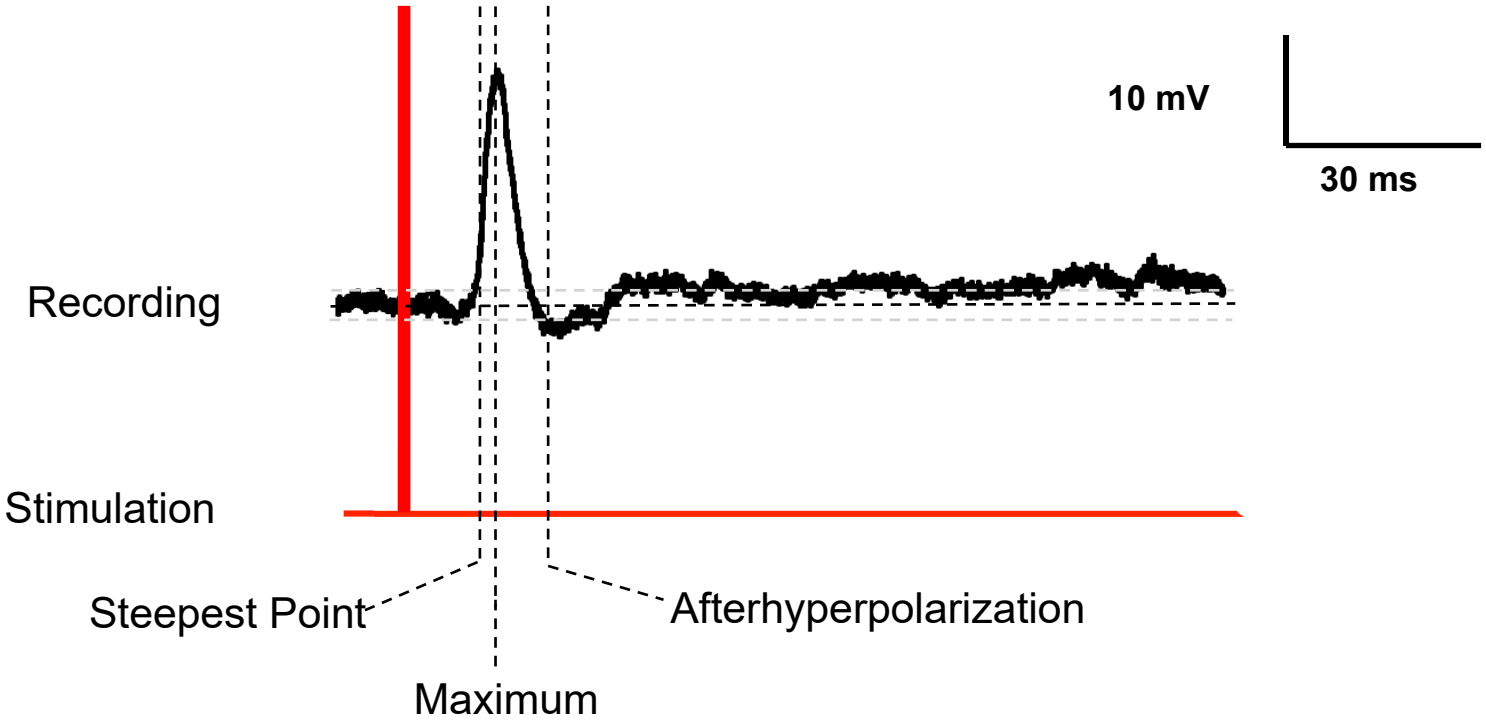

Figure 5 Characterization of a representative EPSP after stimulation. *The black trace is the membrane potential recorded from the optic tectum. Vertical red bar indicates the stimulation artefact. Stimulation was applied to the optic nerve. The latencies are defined as the time difference between the vertical red bar and the dashed black vertical lines. The steepest point and the maximum give the time when the potential reaches the point of the steepest rise of the slope and the maximal voltage, respectively. The afterhyperpolarization is defined by the time when after occurrence of the maximum the most negative voltage is reached. The dashed black horizontal line gives the mean voltage, the grey horizontal dashed lines give the upper and lower standard deviation (SD).*

2.5 Statistical analysis

Data was analysed using Graphpad prism V6 (GraphPad Software Inc, La Jolla, USA). The amplitude and latency of each of the EPSPs were tested for normality by the Kolmogorov-Smirnov test with Dallal-Wilkinson-Lilliefor for P value. Normally distributed data was analysed by one-way ANOVA with post-hoc Tukey's multiple comparison tests. Nonparametric data was analysed using the Mann-Whitney-U-test. Statistical significance was assumed at $p < 0.05$. Datasets that were incomplete or contained heavy artefacts, such as high-amplitude low frequency oscillations, strong 50 Hertz oscillations or high frequency noise were excluded from statistical analyses. A cause for exclusion was given when less than four responses in one or more states of stimulation occurred. Furthermore, recordings containing signals from multiple neurons were also excluded from analyses. Multi-neuron recordings were identified when two different action potentials with an amplitude difference of more than 10mV were observed.

3. Results

3.1 Biocytin labelling

In this work, two categories of experiments were conducted. The first category of experiments were single cell recordings on whole brain preparations of *Bombina orientalis*. The second category were patch-clamp recordings on semi-intact brain preparations of *Bombina orientalis*. In total, 83 animals were sacrificed for intracellular and patch clamp recordings and 370 separate neurons were recorded. For patch-clamp experiments, 115 individual neuronal recordings were made.

An average 5 individual neurons were recorded from each animal and 25 neurons were labelled with biocytin. Of those 12 were successfully labelled, which resulted in a labelling success rate of 48 %. For representation of labelled and reconstructed neurons see Figure 7, Figure 8, Figure 9 and Figure 10. In general, most successful recordings were performed after short, intermittent "tickling" of the electrode tip. This is a feature of the Cyto 791 unit (World Precision Instruments, Friedberg), in which high-amplitude, high frequency electrical oscillations were applied to the electrode. This causes the electrode to vibrate very slightly in the horizontal direction. It has been assumed that this mechanical motion causes debris and cellular material, which has accumulated on the tip of the electrode, to disengage from the opening of the electrode. It can be observed that the electrode resistance decreases approximately 10-20 MΩ after several short instances of "tickling". Therefore, it is assumed, that the electrode only interacts occasionally with a neuron, which leads to an electrical connection in which spiking can be observed. However, these strong oscillations of the electrode seem to facilitate "breaching" or "tearing" of the membrane. Commonly, a very high frequency (>20 Hz) spiking behaviour with a gradually decreasing amplitude can be observed when making connection with a neuron. Usually, the neuron fades to silence after approximately 60 seconds. Very stable recordings with a neuron are rare when using high-impedance glass electrodes *in vitro* with brain preparations of *Bombina orientalis.* The most common case are unstable recordings, in which a neuron can be recorded for several minutes, after which spike-amplitude becomes sub-threshold. Subsequently, four representative labelled neurons will be described in detail.

The neuron reconstructed in Figure 7 C was located within the central optic tectum, about 75 µm from the medial line. The somata was pear shaped, with a wide dendritic tree. The somata itself was located within the upper layers of layer 6 of the optic tectum. Dendrites

were clearly identifiable by their receding thickness. The axon of the neuron was projecting ventrally towards layer 5. However, the projection target of that neuron was not identifiable. Several spines on the dendritic tree were also reconstructed, especially towards the medial part of the dendritic tree. Thin dendrites were reconstructed spreading laterally and medial within layer 7. The bulk of the dendritic tree was located within layer 8 G to D, with some branches of the dendritic tree reaching layer 8 A (Figure 7 B & C). The neuron responded with short latency excitation (4,2 ms) with an amplitude of 7,1 mV to ON stimulation. The neuron did not respond to TH STIM. After stimulation of both the ON and the TH, the neuron responded with EPSPs with an average latency of 4,4 ms and an amplitude of 6,1 mV (Figure 7 D). The neuron can be categorized as a TO1 (Type 1) neuron.

The neuron reconstructed in Figure 8 was located within the rostral optic tectum, half way between the medial line and the lateral border of the tectal bulb. The dendritic tree ascends narrowly, branching after several micrometres into several thinner secondary dendritic branches, immediately above layer 7. The somata itself is located within the upper part of layer 6. Small dendritic branches either terminate within laminae F or in some cases ascend to lamina D. No spines were found within this neuron and no axon could be reconstructed (Figure 8 C). Membrane responses to ON stim were excitatory, with an average latency EPSP of 3,3 ms and an amplitude of 15 mV. The membrane responded with IPSP towards TH stimulation, with an average inhibitory amplitude of -7 mV. The neuron responded with excitation to DUAL stim, with an average latency of 12 ms with an amplitude of 14,7 mV (Figure 8 D). The neuron can be most likely classified as an TO1 (Type 1) neuron.

The neuron described and reconstructed in Figure 9 was located within the rostral part of the tectal bulb. It was located very laterally when viewed from a coronal section. The somata was located within layer 7. The shape of the somata is not clearly discernible, since two adjacent somata were stained in the course of this recording. The dendritic tree was very wide and candelabra shaped, with dendritic branches reaching up to lamina A. No axon was stained for this neuron (see Figure 9). Interestingly, this neuron responded with inhibition to both ON stim and TH stim as well as to DUAL stim an average latency to the onset of ON stim in 20,1 ms, an average latency to TH stim of 22,6 ms and an average latency of 19,4 ms to DUAL stim. IPSP amplitudes for ON stim were recorded as -3,8 mV, -3.8 mV for TH STIM and as -3,5 mV for DUAL stim. Due to the location of the soma,

classification of this neuronal type was not possible, also due to the reason that no axon could be reconstructed. Since the dendritic tree is very wide (more than 70 μm), the most likely type for this neuron is TO2 (type 2).

The neuron described in Figure 10 presents as a very atypical neuron, possessing a small and rounded somata, located high within layer 7, bordering on layer 8. This neuron possesses a rounded dendritic tree, with branches forming connection both within the layer and along the dorsoventral axis. Some small dendritic branches reach lamina A. A suspected axon projects ventrally, reaching through layer 6, where it was so longer able to be reconstructed (Figure 10 C). The neuron responded with ISPS to both ON STIM and TH STIM as well as DUAL STIM. After ON STIM the neuron responded with an average onset latency of 26,2 ms and an amplitude of – 3 mV. After DUAL STIM the membrane responded within 25,8 ms and an amplitude of –2,2 mV. Using the DUAL STIM experimental condition, an onset latency of 25,9 ms with an amplitude of – 2,8 mV was recorded. Due to its unusual dendritic tree configuration, the neuron is difficult to categorize. Most likely, the neuron can be identified as an interneuron.

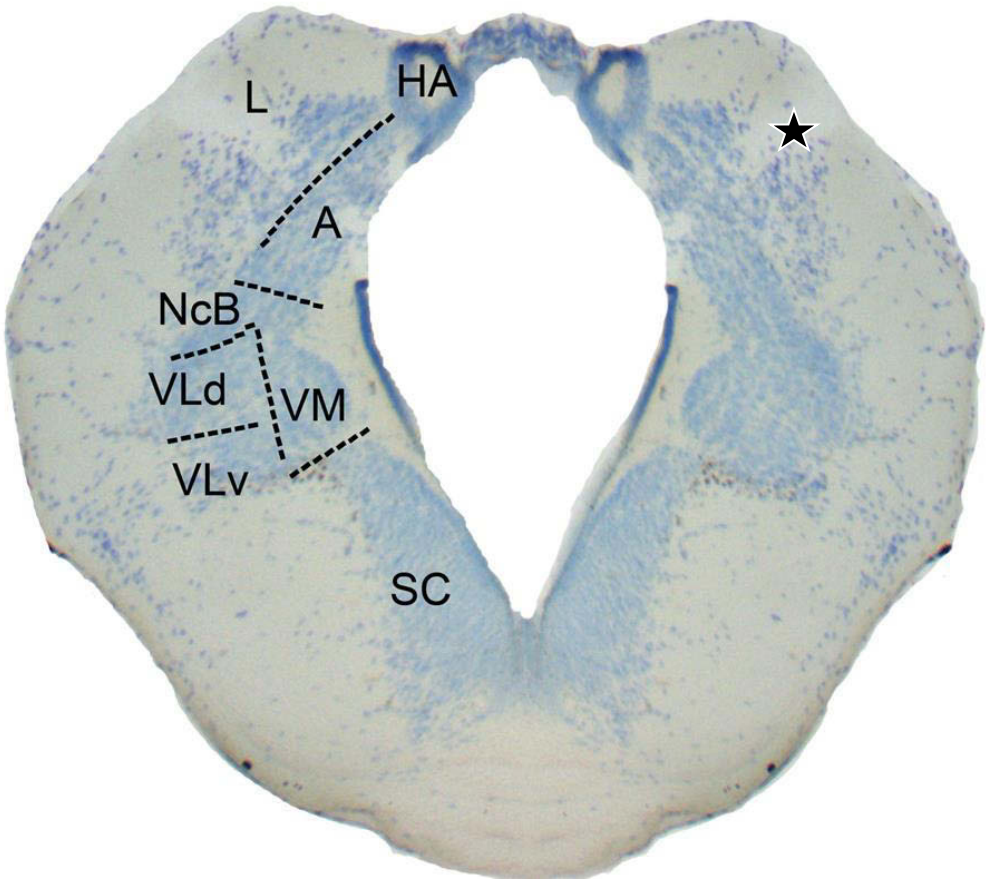

Figure 6 Representative histological damage after stimulation within the thalamus at various depths. *Abbreviations: A: anterior dorsal nucleus, HA: Habenula, L: lateral dorsal nucleus, NcB: Nucles of Bellonci, SC: suprachiasmatic nucleus, VLd: dorsal portion of the ventrolateral nucleus, VLv: ventral portion of the ventrolateral nucleus, VM: ventromedial nucleus. Asterisks indicates a faint track marks produced by the stimulation electrode.*

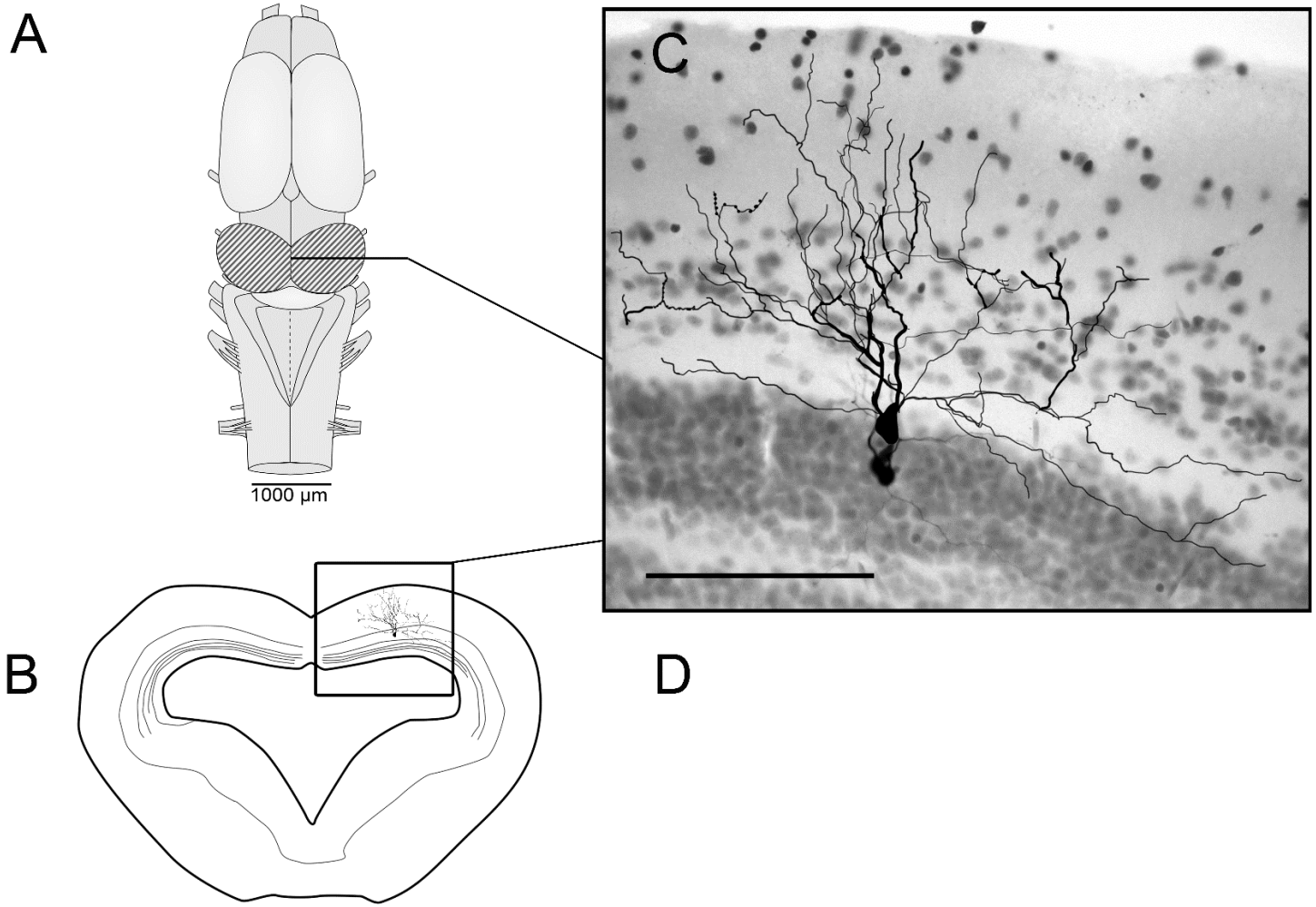

Figure 7 Tectal neuron labelled with biocytin and subsequently reconstructed. ***A*** *Schematic overview of the soma position within the dorsoventral axis.* ***B*** *Schematic coronal view of the tectum.* ***C*** *Reconstructed neuron and surrounding tissue. Scale bar 100 µm .*

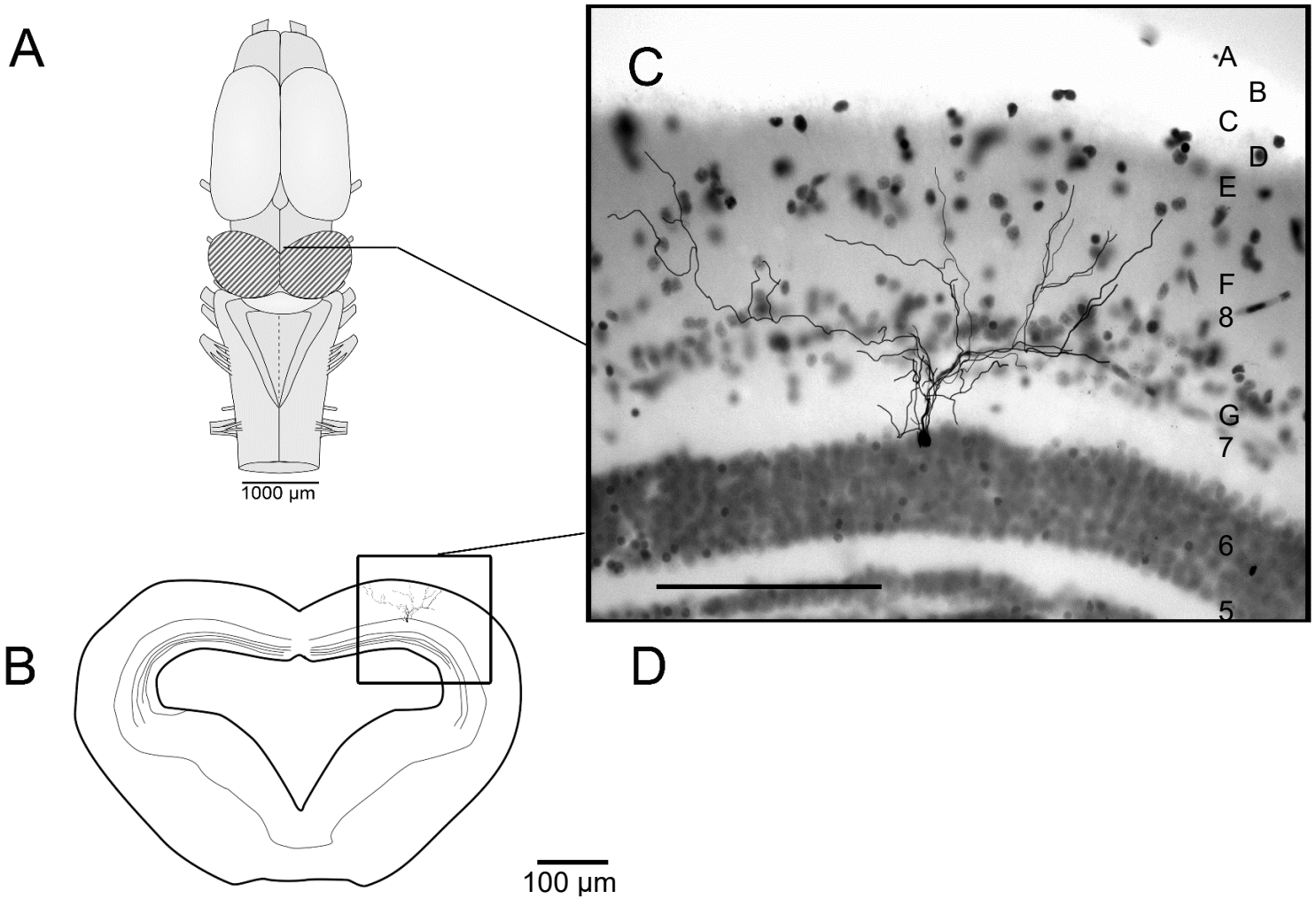

Figure 8 Tectal neuron labelled with biocytin and subsequently reconstructed. ***A*** *Schematic overview of the soma position within the dorsoventral axis.* ***B*** *Schematic coronal view of the tectum.* ***C*** *Reconstructed neuron and surrounding tissue. Scale bar 100 µm.*

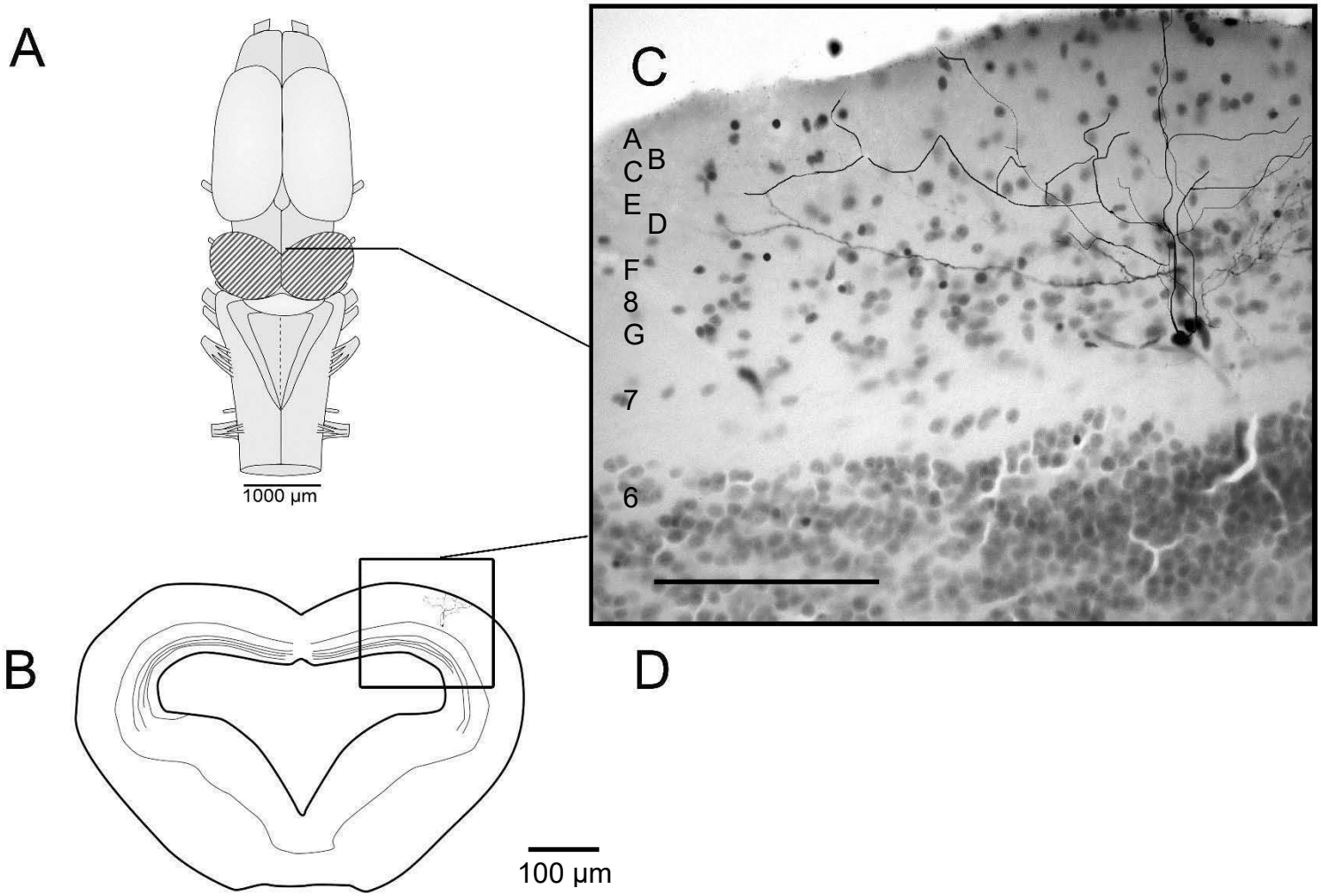

Figure 9 Tectal neuron labelled with biocytin and subsequently reconstructed. A *Schematic overview of the soma position within the dorsoventral axis.* ***B*** *Schematic coronal view of the tectum.* ***C*** *Reconstructed neuron and surrounding tissue. Scale bar 100 µm.*

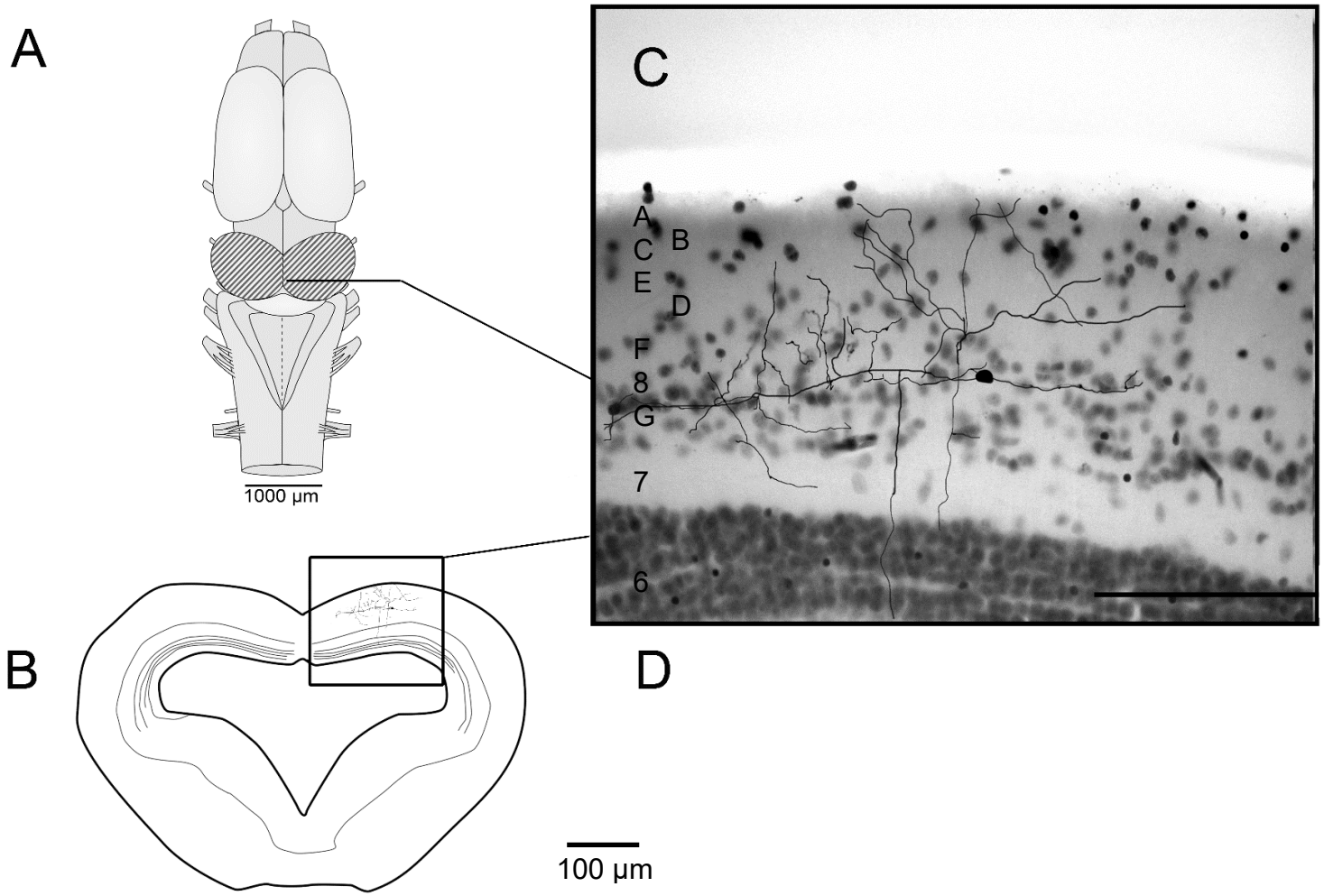

Figure 10 Tectal neuron labelled with biocytin and subsequently reconstructed. A *Schematic overview of the soma position within the dorsoventral axis.* ***B*** *Schematic coronal view of the tectum.* ***C*** *Reconstructed neuron and surrounding tissue. Scale bar 100 µm.*

3.2 Tecto-thalamic interaction and response properties to stimulation

In the following section, the results for membrane responses after stimulation of the optic nerve (ON), thalamus (TH) and both simultaneously will be described (DUAL STIM) (see also chapter 2.31). A total of 34 whole-brain preparations of *Bombina orientalis* were analysed in this configuration and tested for tecto-thalamic interactions. In *post-hoc* histological investigations, only slight lesioning was detectable in the thalamus and the optic tectum, even though large sections of the dura and pia mater were removed prior to recording. Similarly, after *post-hoc* sectioning, no large lesioning occurred due to the described experimental protocols. Only faint tracks created by the electrode were visible (Figure 6). Recorded neurons in the upper layers of the optic tectum readily responded to stimulation of the contralateral optic nerve. Low-latency, high-amplitude single-spike impulses usually yielded the highest response rate. Stimulation of the contralateral optic nerve did not decrease the recording quality over time. Approximately 7 % (n= 25) of recorded neurons were spontaneously active. On average 3,1 full experimental cycles were performed with neurons responding in sufficiently high quality. The highest number of neurons were recorded in medial areas of the optic tectum, even though the number of experimental tracks was distributed equally among all areas, the tectal bulb.

The proportion between EPSP to IPSP to TH stim was not equally distributed across the tectal bulb. As described in Material and Methods 2.3.1 and Figure 3, the tectal bulb was divided into six equally sized areas. Recordings were divided equally across all areas. The highest percentage of EPSP were found within the medial-central area of the tectum, with 36 % of all recorded PSP being EPSP. A high percentage of recorded PSP were excitatory within the rostral section of the tectum. 33 % EPSP within the medial-rostral area of the tectum and 29 % EPSP within the lateral-medial area of the tectum were recorded. A low number of PSP were found within the caudal area of the tectum, with 4 % of all PSP being EPSP in the medial-caudal area of the tectum and 15 % of all PSP being EPSP in the lateral-caudal area of the tectum (Figure 11).

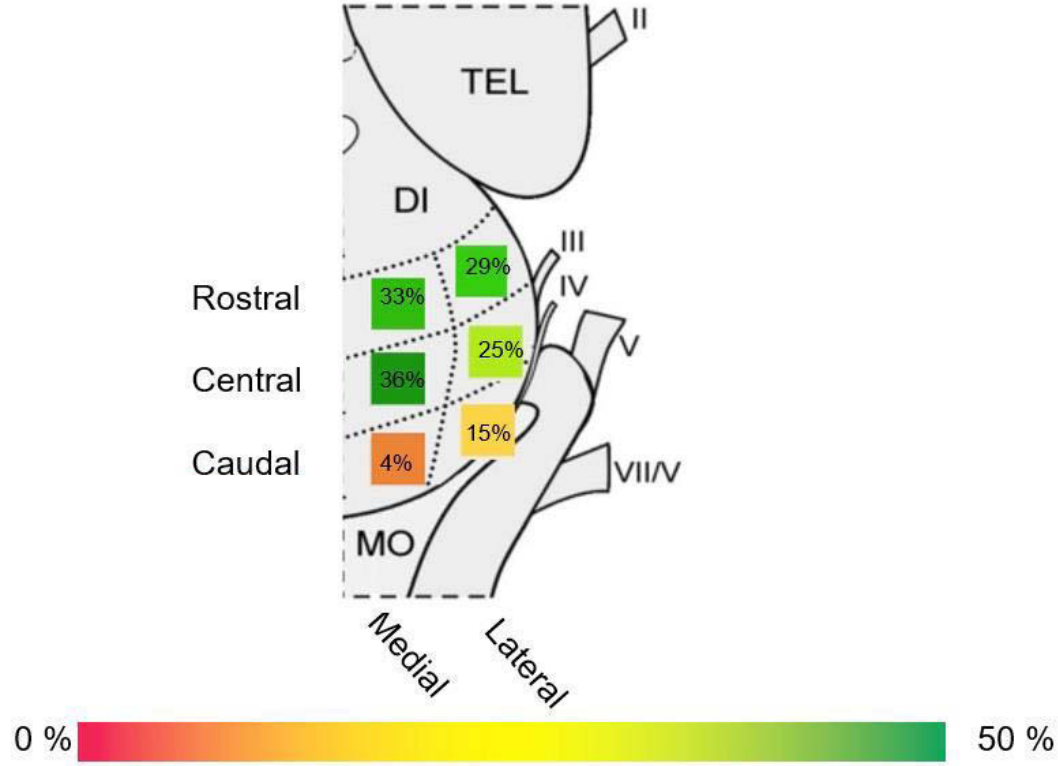

Figure 11 Percentage of EPSP after TH STIM across differing areas of the surface of the optic tectum. *Colour scale gradient from 0% to 50 % EPSP incidence.*

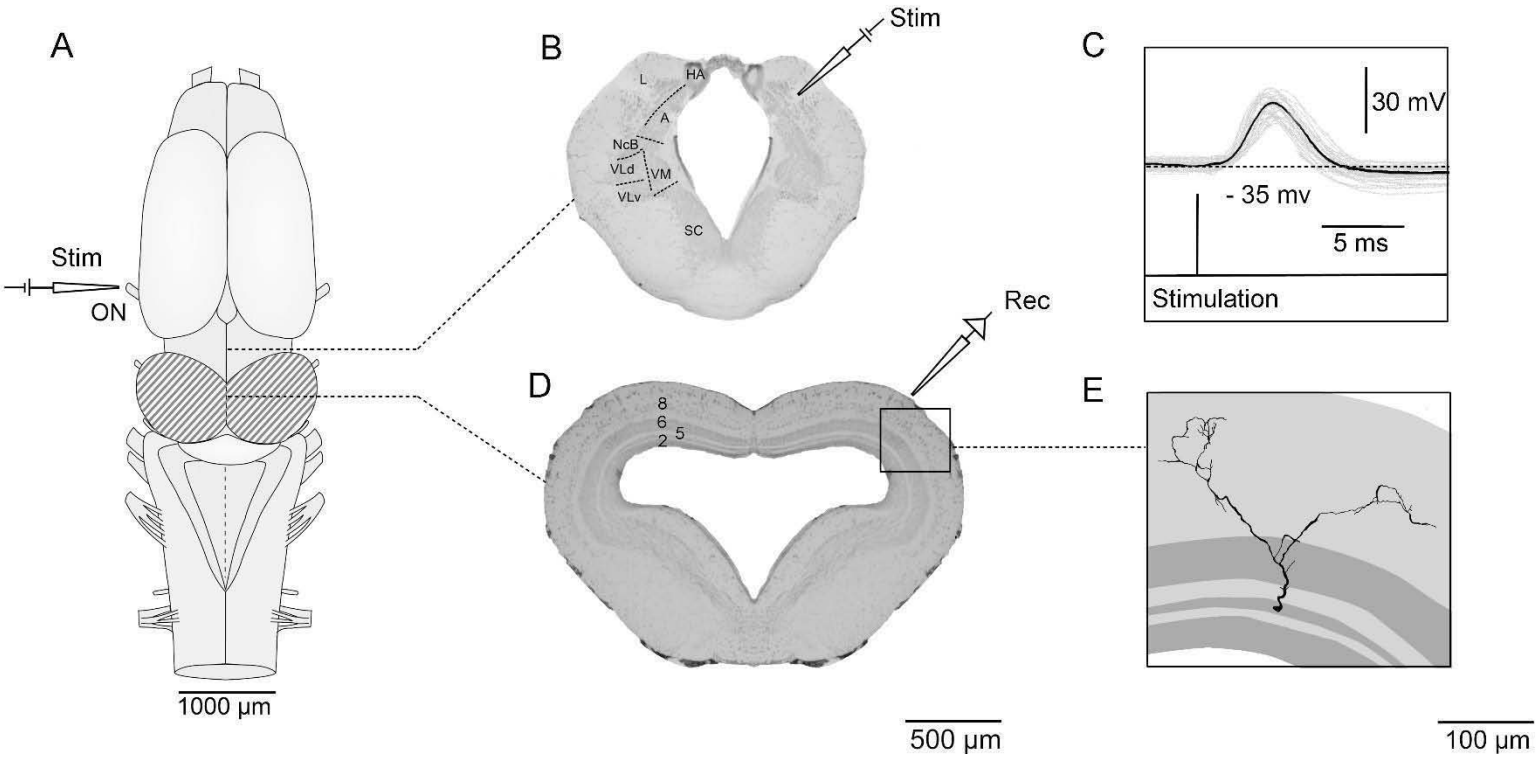

Figure 12 Experimental setup with double stimulation conditions A *Schematic illustration of dorsal view from an in vitro brain-preparation of Bombina orientalis used to investigate synaptic responses of tectal neurons to stimulation of the optic nerve and dorsal thalamus. Dashed area indicates the optic tectum.* ***B & D*** *Microphotographs of transverse sections from the medial diencephalon (B) and the medial tectum (D) in Bombina orientalis. Cellular layers, in which neurons were recorded are indicated via numbers. Dashed lines indicate the borders in nuclei of the thalamus* ***C*** *Representative reconstructions of tectal type 1 neuron, intracellularly labelled with biocytin.* ***E*** *Representative intracellular recording of a tectal neuron in response to contralateral stimulation of the optic nerve. Abbreviations: Rec: intracellular recording electrode; Stim: extracellular stimulation electrode, HA: Habenula; L: lateral dorsal thalamic nucleus; A: anterior dorsal thalamic nucleus; NcB: nucleus of Bellonci; VLd: dorsal portion of the ventrolateral nucleus; VLv: ventral portion of the ventrolateral nucleus; VM ventromedial thalamic nucleus; SC, suprachiasmatic nucleus*

3.2.1 Response characteristics of tectal neurons to stimulation of the optic nerve and the Thalamus

3.2.1.1 Excitatory evoked responses

Neurons readily and commonly responded with depolarization or action potential to stimulation of both the optic nerve (ON STIM) and the thalamus (TH STIM). Both transient depolarization of the membrane (EPSP) and action potentials were observed (See Table 1). In total 16 neurons (n = 21 for DUAL STIM) were analysed according to their average amplitude and latencies. The distributions within excitatory responses were all not normally distributed, and the Mann-Whitney-U-Test was used to test for statistical differences.

The point on a fitted curve between spike threshold and the peak of the action potential was defined as the steepest point (see also chapter 2.4 and Figure 5). Neurons responding to TH STIM were recorded having the highest amplitude steepest point (14,71 ± 4,82 mV), followed by responses to DUAL STIM (12,98 ± 4,19 mV) and ON STIM (10,77 ± 4,73 mV). However, no statistical differences were found (ON vs. TH p = 0,28; ON vs. DUAL p = 0,89, TH vs DUAL p = 0,79; Mann-Whitney-U test).

Similarly, very slight numeric differences were found in the afterhyperpolarization curves. The highest afterhyperpolarization amplitude was found in neurons responding to ON STIM (-3,99 ± 0,64 mV), followed by the afterhyperpolarization of neurons responding to DUAL STIM with an afterhyperpolarization of (3,25 ± 0,31 mV). Lastly, neurons responding to TH STIM have the lowest amplitude afterhyperpolarization (3,21 ± 0,6 mV). Comparing the amplitudes of the afterhyperpolarization, no statistical differences were found (ON vs. TH p = 0,33, ON vs. DUAL p = 0,42, TH vs DUAL p = 0,44, Mann-Whitney-U test).

The amplitude to the peak of EPSP and action potentials (highest point) showed the largest differences. Neurons were responding to ON STIM with the highest amplitude (32,42 ± 2,29 mV), followed by neurons responding to thalamic stimulation (TH STIM) (28,26 ± 6,89 mV) with neurons responding to a dual stimulation (DUAL STIM) 18.6 (± 3.67) mV. (ON vs. TH p = 0,68; ON vs. DUAL p = 0,21, TH vs DUAL p = 0,33; Mann-Whitney-U test). See also *Table 2. General overview of EPSP and action potential membrane responses in optic tectum neurons* and supplementary Figure 31.

.

Table 2. General overview of EPSP and action potential membrane responses in optic tectum neurons

A. ON stim			
	Steepest point	Peak	AHP
Number of neurons	16	16	16
Mean (± Std. Error) [mV]	10.77 (± 4.73)	32.42 (± 2.29)	-3.99 (± 0.64)
Latency (± Std. Error) (ms)	8.48 (± 1.62)	10.61 (± 2.29)	37.95 (± 8.16)
B. TH stim			
	Steepest Point	Peak	AHP
Number of neurons	16	16	16
Mean (± Std. Error) [mV]	14.71 (± 4.82)	28.26 (± 6.89)	-3.21 (± 0.6)
Latency (± Std. Error) (ms)	18.28 (± 1.65)	21.82 (± 1.68)	83.78 (± 8.05)
C. DUAL stim			
	Steepest Point	Peak	AHP
Number of neurons	21	21	21
Mean (± Std. Error) [mV]	12.98 (± 4.19)	18.6 (± 3.67)	-3.25 (± 0.31)
Latency (± Std. Error) (ms)	15.55 (± 1.81)	17.5 (± 2.19)	62.18 (± 8.27)

Abbreviations: IPSP: inhibitory postsynaptic potential ON: optic nerve TH: thalamus DUAL: simultaneous stimulation of the optic nerve and thalamus, AHP: afterhyperpolarization

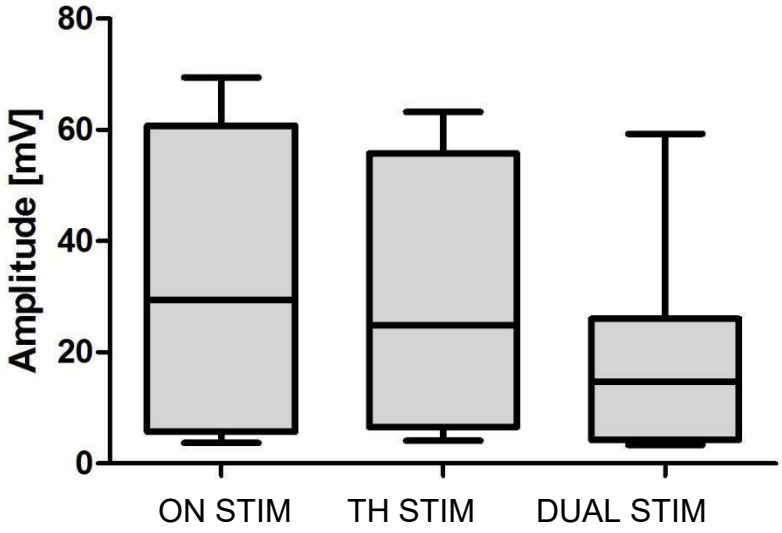

Figure 13 Average EPSP amplitudes during stimulation of the optic nerve (ON STIM), the thalamus (TH STIM) and both simultaneously (DUAL STIM). *Middle black bar represents the average, while the grey box represents 50% of datapoints, black whiskers represent the distance to the highest and lowest recorded values. n = 16 ($n_{DUAL\ STIM}$ = 21)*

In total 16 neurons (21 for DUAL STIM) were analysed regarding their EPSP latencies. Three points within the EPSP were characterized, the steepest point during the rise of the EPSP, the maximal amplitude and the afterhyperpolarization (See chapter 2.3 and Figure 5). Average latencies for the steepest point of neurons responding to ON STIM (n = 16) were measured as 8.48

for TH STIM. Statistically, a significant difference was found between the ON STIM condition and the DUAL STIM condition (ON vs. TH p = 0,07; ON vs. DUAL p = 0,012, TH vs DUAL p = 0,12; Mann-Whitney-U test). The average latencies until the peak of the EPSP were as follows; neurons that were stimulated with the ON condition

ms. Statistically significant differences were found between the ON STIM and the DUAL STIM condition and the ON STIM and the TH STIM condition (ON vs. TH p = 0,013 ON vs. DUAL p = 0,012, TH vs DUAL p = 0,12; Mann-Whitney-U test). Due to the low amplitudes, the latencies of the afterhyperpolarization had much higher latencies compared to the other points of the EPSP analysed above. Furthermore, the lowest point of the afterhyperpolarization had a much higher variance than the other aspects of the EPSP. A

latency of 37.95 (± 8.16) ms to the afterhyperpolarization was recorded for neurons responding to the ON STIM. Neurons responding to the TH STIM had a latency to the afterhyperpolarization of 83.78 (± 8.05) ms, while neurons responding to the DUAL STIM condition had a latency of 62.18 (± 8.27) ms. No statistically significant difference was found within these three distributions (ON vs. TH p = 0,06; ON vs. DUAL p = 0,16, TH vs DUAL p = 0,4; Mann-Whitney-U test, see also Table 2). Several representative EPSP of tectal neurons during different experimental conditions and recording techniques can be seen in Figure 14.

The shape of the distribution of EPSP will be described now, since statistical testing for normal distribution showed that response latencies are not normally distributed. No EPSP were observed with an amplitude below 3 ms. Note: Due to the binning method used in Figure 15 the lowest possible bin includes all EPSP with a latency from 0 ms to 3 ms. The distribution of the ON STIM condition is compact with a low variance. Most EPSP recorded are low latency and all are below 10 ms. TH STIM condition EPSP are more widely distributed with a high variance. However, no EPSP were recorded with a latency below 10 ms. Within the DUAL STIM condition, the highest variance in latency was recorded, both very short and very long latencies were observed within this experimental condition (See Figure 15 and Figure 16).

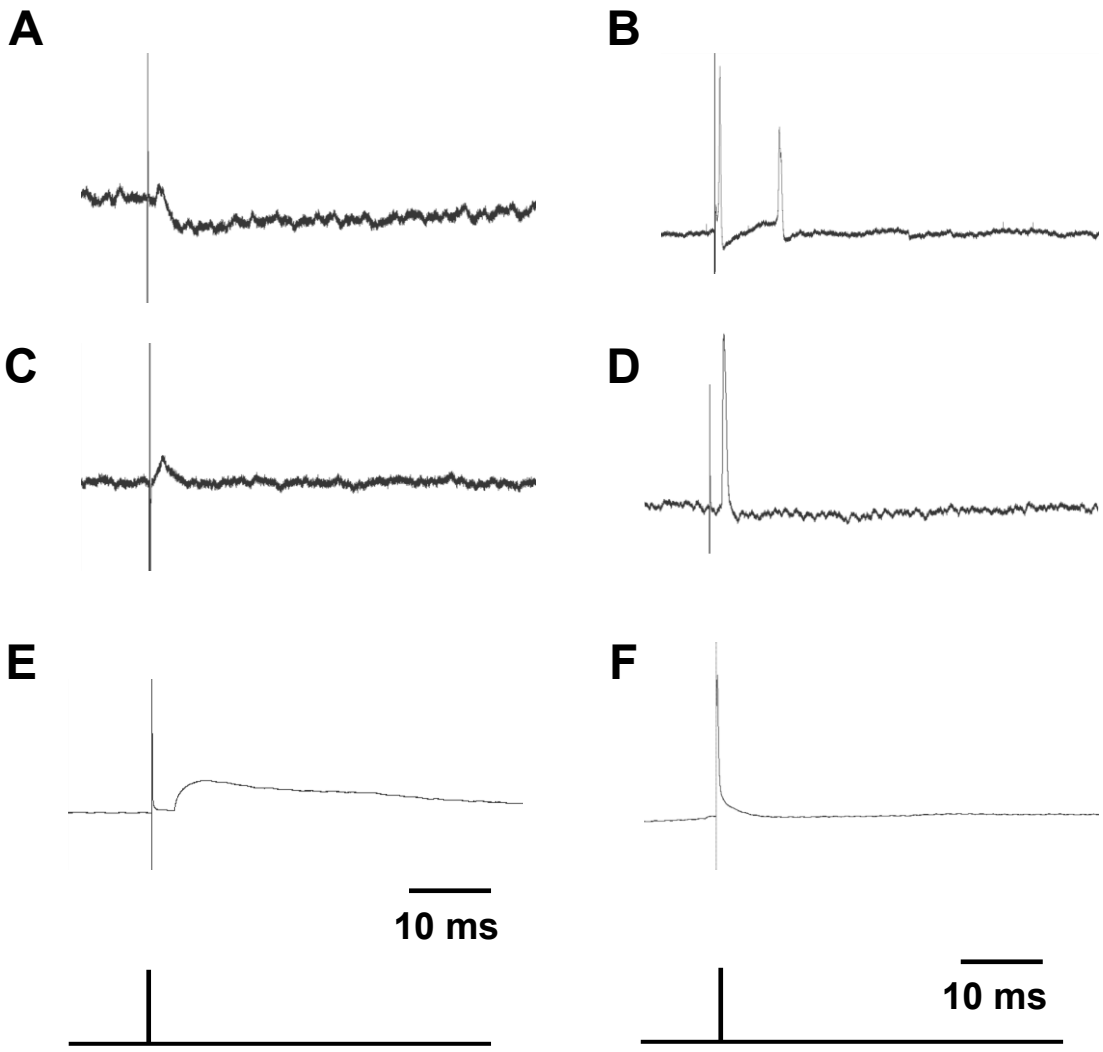

Figure 14 Representative traces of EPSP of neurons from the optic tectum. *The black traces are voltages of the membrane in mV. Voltage scaling varies.* ***A.*** *EPSP after stimulation of ON* ***B.*** *AP after stimulation of the ON* ***C.*** *EPSP after stimulation of the TH* ***D****. AP after stimulation of the ON TH,* ***E.*** *EPSP in patch-clamp current-clamp after stimulation of the ON STIM* ***F.*** *EPSP in patch-clamp current-clamp after stimulation of the ON*

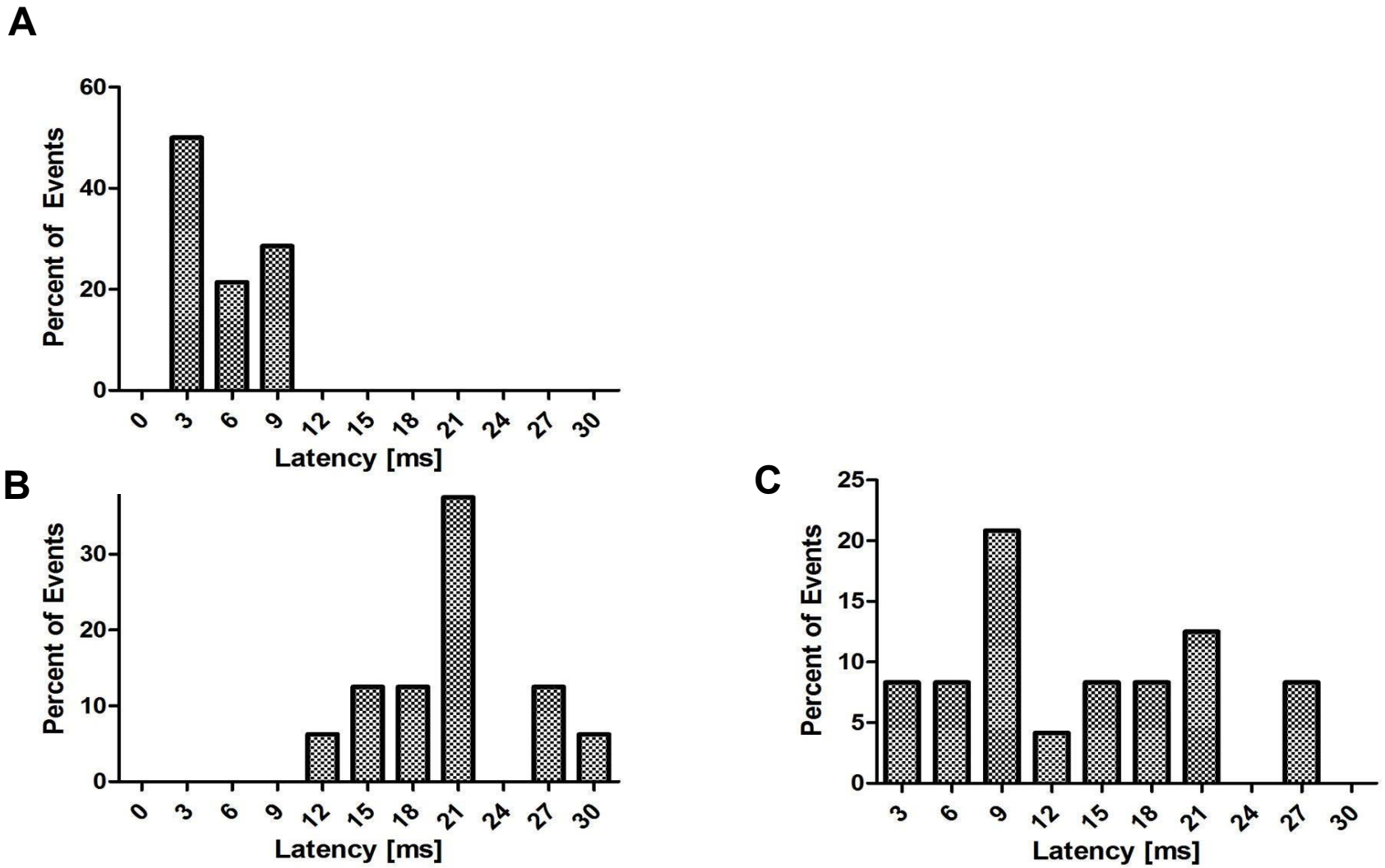

Figure 15 Latency distribution histograms in EPSP. *PSP with latencies above 30 ms were not considered.* ***A*** *Histogram of latencies after ON STIM.* ***B*** *Histogram of latencies after TH STIM.* ***C*** *Histogram of latencies after DUAL STIM. The distribution was calculated via binning of the respective 2 ms intervals. Starting from 0 to 2 ms, 2 to 4 ms and so forth.*

Within a secondary analysis, only EPSP with an amplitude higher than 20 mV were investigated. A total of 9 neurons were included in this analysis. The average latency of an EPSP within the ON STIM condition was 6,01 (± 1,93) mV. The average latency of an EPSP within the DUAL STIM condition was 16 (± 9,78) mV. Using the Mann-Whitney-U-Test a statistically significant difference was found between those two conditions (p = 0,029, see Figure 16 A). It was also possible to visually distinguish the two experimental conditions, as visualized for an representative traces from one neuron, where an action potential was delayed by applying the DUAL STIM condition (Figure 16 B). The probability of appearance of these action potentials will be described in detail in chapter 3.2.3.

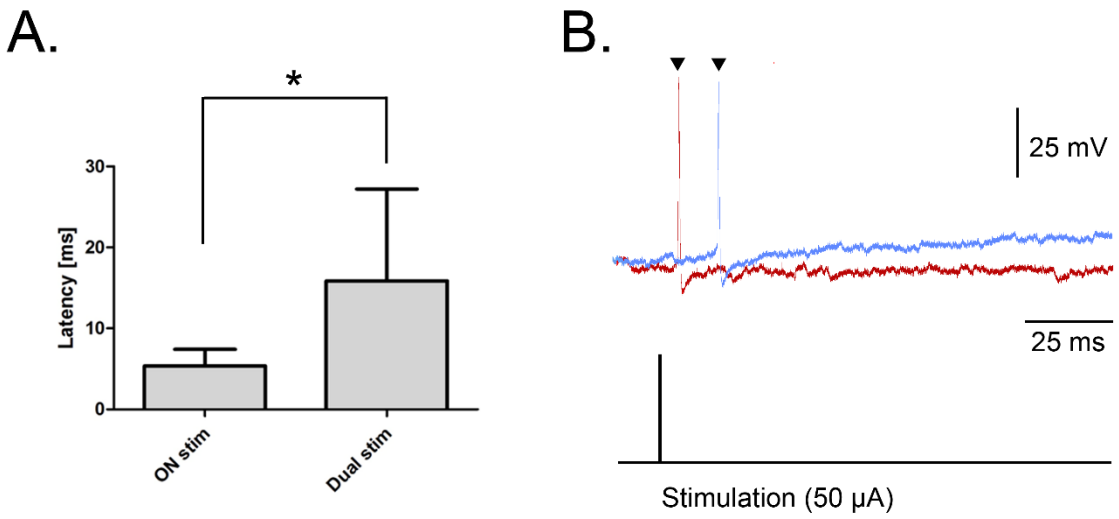

Figure 16 Action potentials are delayed at DUAL stimulation. A. *Average latency of action potentials after stimulation. Only neurons were included that responded to both ON stim and DUAL stim with an action potential larger than 20 mV. Error bars represent standard error. * p > 0,05. B. Representative trace of a recorded tectal projection neuron. black triangles represent peak excitation. notice the difference between the two peaks. Red: ON STIM. Blue: DUAL STIM*

3.2.1.2 Inhibitory evoked responses to optic nerve and thalamic stimulation

Neurons commonly responded with inhibition, signified as transient depolarization to stimulation of either the optic nerve or the thalamus. Inhibitory postsynaptic events (IPSP) were analysed using principles described in in chapter 2.3 and Figure 4. In general, a total of 24 neurons were analysed for their membrane responses to ON stim. The same holds true for TH STIM (n = 23) and DUAL STIM (n = 22). Some neurons had to be rejected for analysis based on recording artefacts. For representative traces of IPSP during various experimental conditions see Figure 17. On average, neurons depolarized with an amplitude of -3,75 (± 0,41) mV with a latency 32,3 (± 3,2) ms after ON STIM. The average onset of the IPSPs after ON stim was determined to be 19,3 (± 1,9) ms. The amplitude of the IPSP after TH STIM was calculated to be an average of 5,9 (± 0,6) mV with an average latency of 41,94 (± 3,7) ms. An average onset for TH STIM of 17,35 (± 1,68) ms was calculated. DUAL STIM neurons had an average amplitude -5,8 (± 0,5) ms after 36.64 (± 3.41) ms, with an average onset 16.1 (± 3.41) ms. The time until the membrane potential recovered to the baseline potential (Recovery) differed strongly. This value was also highly variable. Neurons in the ON stim condition recovered their membrane potential on average after 63.97 (± 5.03) ms. Neurons stimulated in the TH stim recovered their membrane potential on average after 107.6 (± 22.63) ms. Neurons as a part of the DUAL stim condition recovered their membrane potential on average after 80 (± 49,14) ms (Table 3, *Figure* 17). No statistical differences were found between the three experimental conditions (Minimal value amplitude: ON vs. TH p = 0;91 ON vs. DUAL p = 0,82 TH vs DUAL p = 0,88 Minimal value latency: ON vs. TH p = 0,59 ON vs. DUAL p = 0,81 TH vs DUAL p = 0,78 Onset latency: ON vs. TH p = 0;68 ON vs. DUAL p = 0,85 TH vs DUAL p = 0,86 Mann-Whitney-U test).

Table 3. General overview of average IPSPs recorded in neurons both stimulated at the ON and the TH

IPSP ON stim			
	Minimal value	Onset of IPSP	Recovery
Number of Cells	24	24	24
Mean (± Std. Error) [mV]	-3.75 (± 0.41)		
Latency (± Std. Error) (ms)	32.32 (± 3.2)	19.34 (± 1.92)	63.97 (± 5.03)
IPSP TH stim			
	Minimal value	Onset of IPSP	Recovery
Number of Cells	23	23	23
Mean (± Std. Error) [mV]	-5.91 (± 0.55)		
Latency (± Std. Error) (ms)	41.94 (± 3.70)	17,35 (± 1,68)	107.6 (± 22.63)
IPSP DUAL stim			
	Minimal value	Onset of IPSP	Recovery
Number of Cells	22	22	22
Mean (± Std. Error) [mV]	-5.82 (± 0.53)		
Latency (± Std. Error) (ms)	36.64 (± 3.41)	16.1 (± 3.41)	80 (± 49.14)

Abbreviations: IPSP: inhibitory postsynaptic potential ON: optic nerve TH: thalamus DUAL: simultaneous stimulation of the optic nerve and thalamus

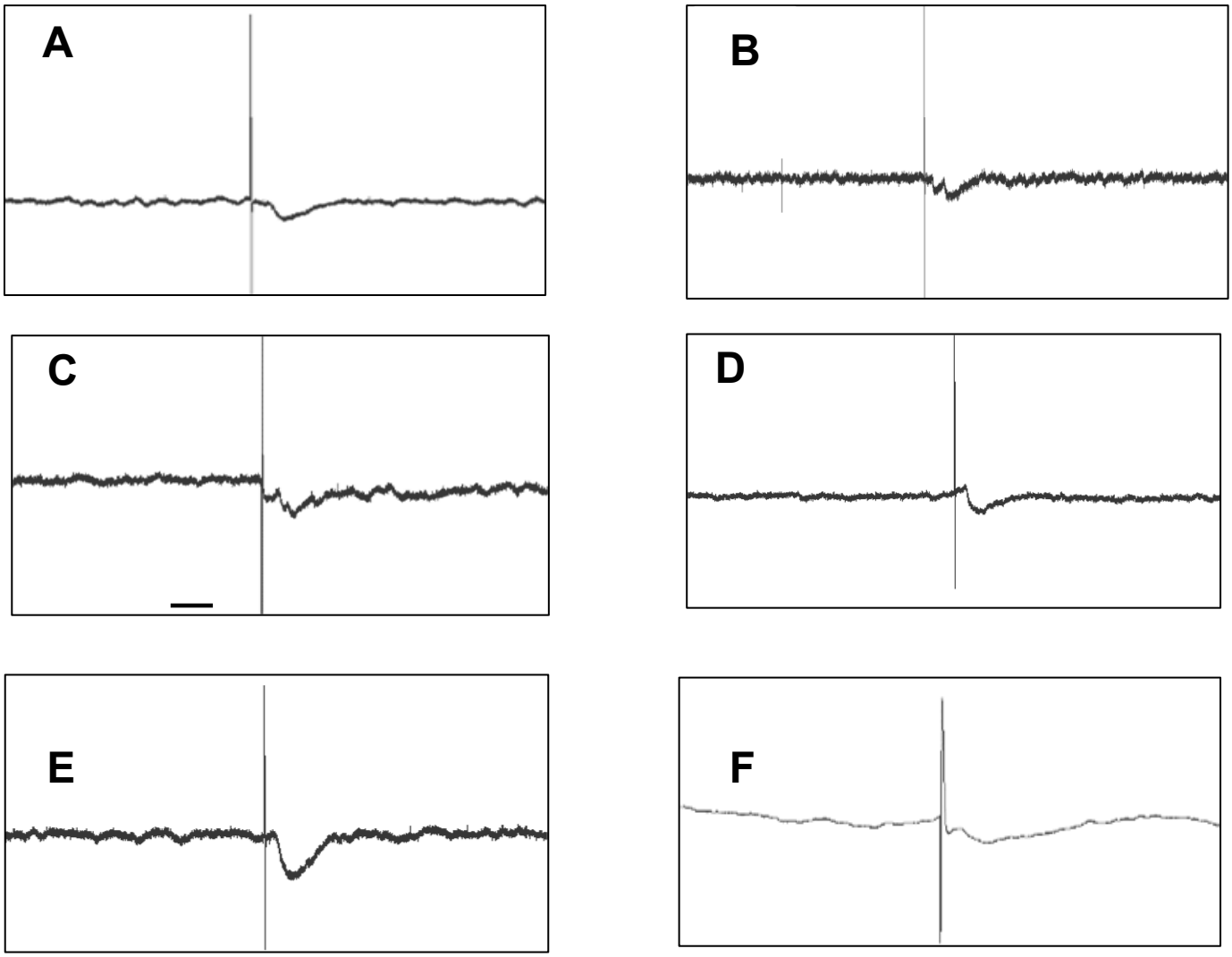

F*igure 17 Representative traces of IPSP of neurons from the optic tectum.* *The black traces are showing voltages in mV. Voltage (y-axis) scaling varies.* ***A, B, C*** *IPSP after stimulation of ipsilateral TH,* ***B*** *IPSP after stimulation of the ipsilateral dorsal thalamus,* ***C, E*** *IPSP after stimulation of the ipsilateral optic nerve,* ***F*** *Current-Clamp patch-clamp voltage trace after stimulation of the ipsilateral thalamus*

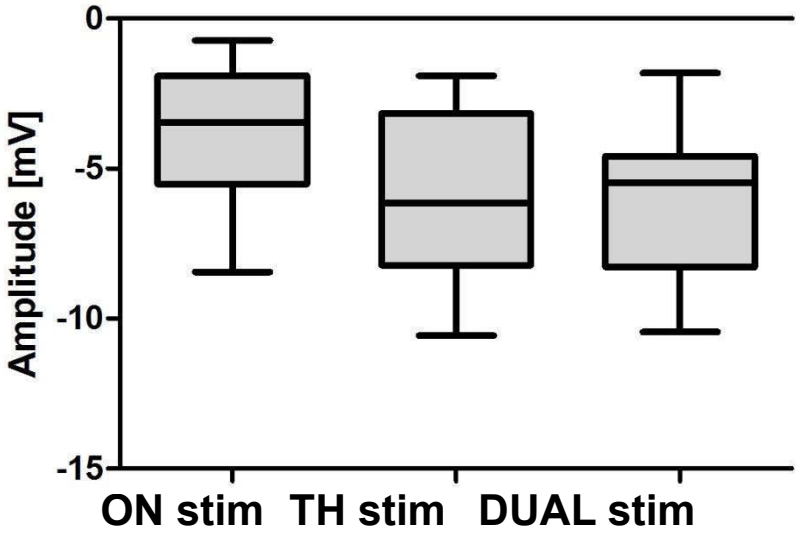

Figure 18 Average IPSP amplitudes during stimulation of the optic nerve (ON STIM), the thalamus (TH STIM) and both simultaneously (DUAL STIM). *Middle black bar represents the average, while the grey box represents 50% of datapoints, black whiskers represent the distance to the highest and lowest recorded values. n = 16 ($n_{DUAL\ STIM}$ = 21)*

Using the same experimental conditions as described in chapter 2.3.1, neurons were also stimulated repeatedly within a short burst. Five shocks were delivered within this condition using a frequency of 100 Hz. Within this experiment, the shape of IPSP did not differ from single stimulations. Latencies of IPSP did not change after repetitive stimulation. However, in some cases spontaneous IPSPs were observed for approximately 500 ms after repetitive stimulation (Figure A). In some cases, with each shock of repetitive stimulation the amplitude of the IPSP increased (Figure B).

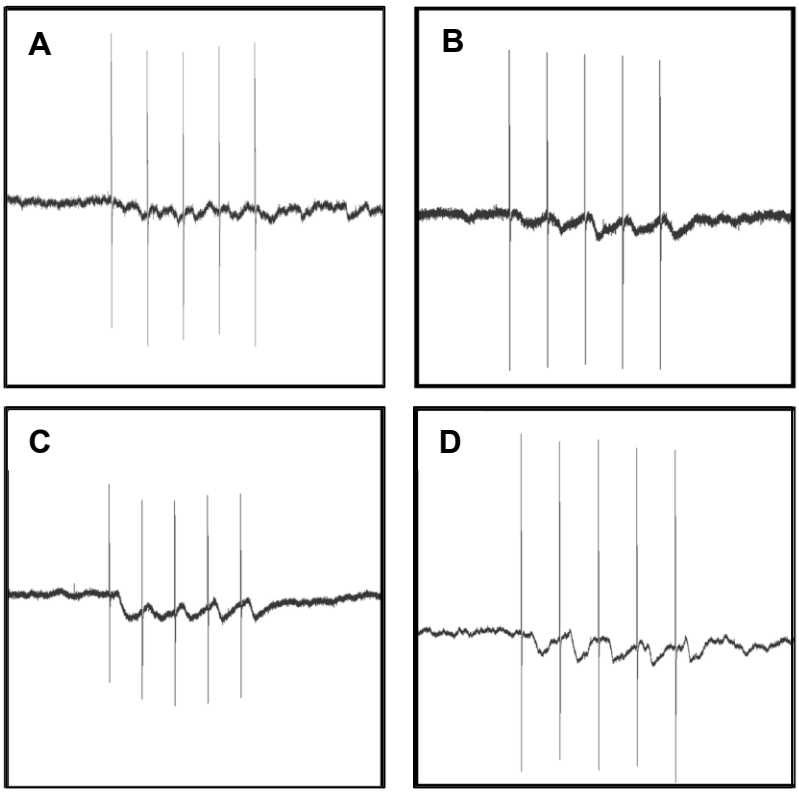

Figure 19 Membrane potential of optic tectum neurons after multiple repetitive stimulations A & B *representative traces after repetitive stimulation of the TH* ***C & D*** *representative traces after repetitive stimulation of the ON*

3.2.2 Thalamic stimulation in various areas

In order to investigate the differing roles of the nuclei of the thalamus, the stimulation electrode has been inserted at various depths along the ventrodorsal-axis of the brain at the thalamus. The stimulation electrode was inserted at an angle and inserted up to the ventricle (See Figure 6). The experiments were conducted using the same experimental routine described in chapter 2.3.1. In total, 40 neurons of the optic tectum were recorded using this experimental regime. Those neurons were recorded from 13 different animals. Only neurons with evoked responses above 5 mV above the baseline were considered. In total, 16 neurons were recorded where the TH was stimulated at a depth from 0 to 50 µm. The lowest latency recorded was 8 ms (6 % of total EPSP) and the highest latency was 28 ms (18 % of total EPSP). The average response was 22 ms (See Figure 21A). A total of 16 neurons were recorded where the TH was stimulated at a depth between 50 to 300 µm. The lowest latency recorded within this group was 12 ms and the longest latency was 32 ms. On average the recorded latency for the group between 50 to 300 µm was 19 ms (See Figure 21 B). At a depth above 300 µm a total of 8 neurons were recorded. The lowest recorded latency within this group was 12 ms and the highest latency 36 ms. The average latency was 21 ms (Figure 21 C). Within this context, only the latencies of EPSP were analysed.

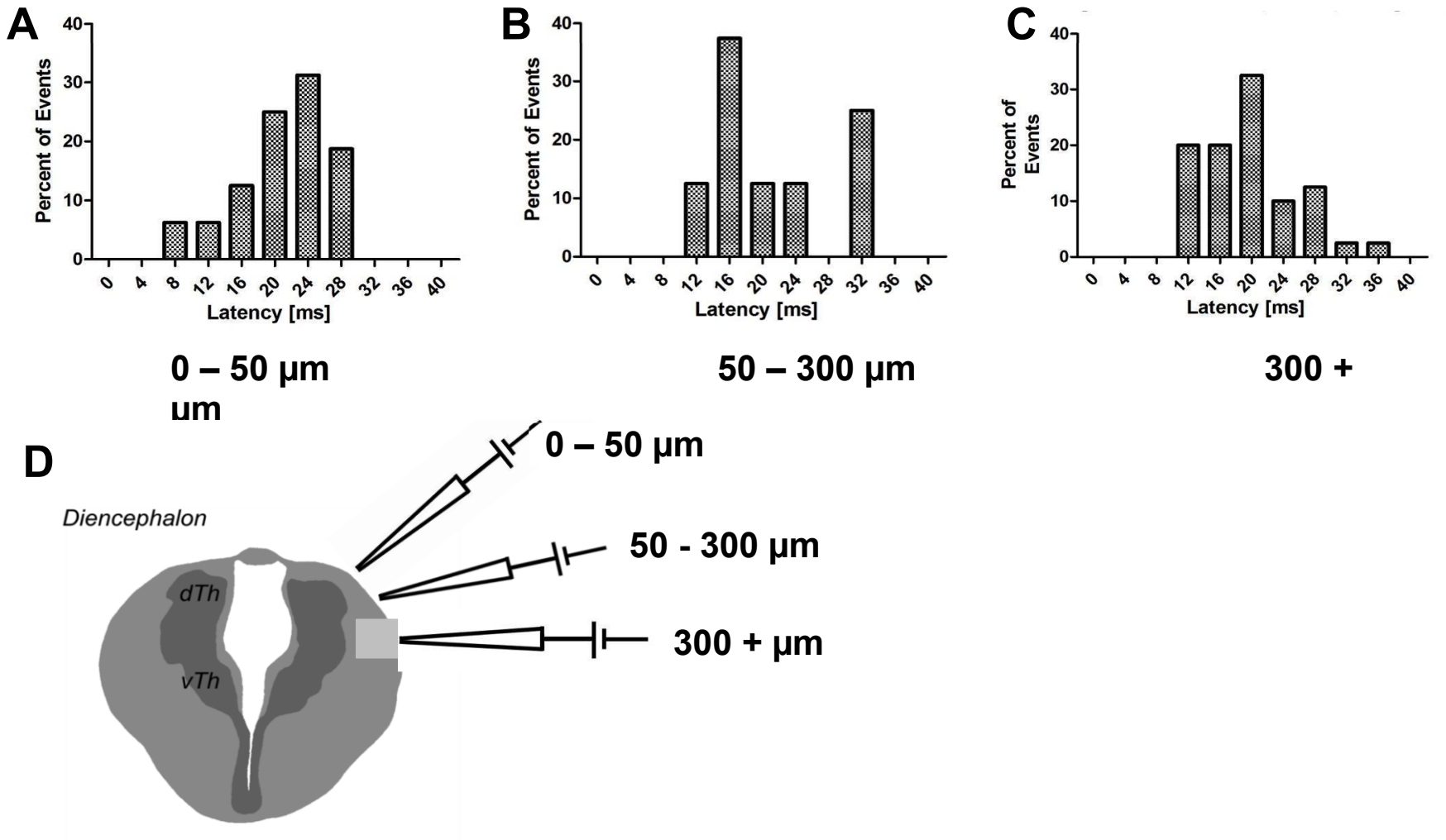

Figure 20 Membrane responses of tectal neurons to thalamic stimulation at various areas. A to C *Bars are percentages of total recorded latencies within each group. The distribution was calculated via binning of the respective 2 ms intervals. Starting from 0 to 4 ms, 4 to ms and so forth.* ***D*** *Schematic drawing of experimental configuration. Abbreviations: dTh: dorsal thalamus, vTh: ventral thalamus.*

3.2.3 Action potential probability to stimulation of the optic nerve and thalamus

Within this chapter, the different probabilities to elicit an action potential after ON STIM, TH STIM and DUAL STIM will be described. In order to do this, the ratio between stimulation trials that failed to elicit an action potential and trials that elicited an action potential was calculated. Taking the average across all cells, a probability to generate potential after stimulation was calculated. The results show that neurons readily respond with action potentials to stimulation after optic nerve stimulation (79,2 ± 7,2 %). A slight decrease in probability of action potentials was observed after several minutes of recording. However, this effect was not significant, when neurons that were completely detached from the electrode were considered. Neurons also readily and consistently respond to TH STIM, however, at a lower rate (72,5 ± 7,1 %). No statistical difference was found between the two experimental conditions. When applying a DUAL STIM statistically significantly lower probability to elicit an action potential was observed (58,4 ± 8,9 %). The DUAL STIM condition also significantly differed from the TH STIM condition (see Figure 21).

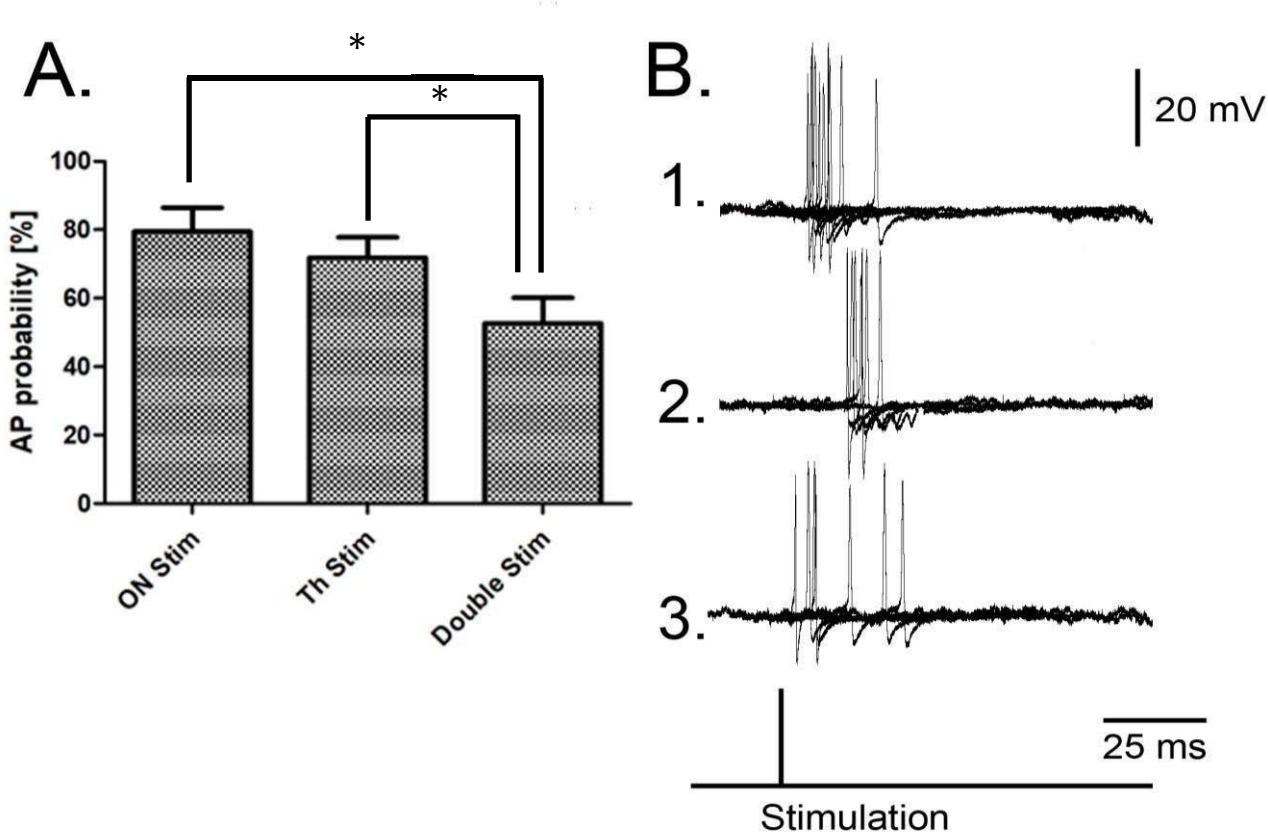

Figure 21 Thalamic stimulation modulates the probability to elicit an action potential*. Thalamic stimulation reduces probability to elicit an action potential after stimulation of the optic nerve.* ***A****. Probability to evoke an action potential in tectal neurons within of one experimental set. 100% represents that all instances stimulatory instances of a recorded neuron that evoked an action potential. Error bars represent standard error.* ***B****. Representative traces evoked action potentials of a tectal projection neuron in an overlay view (n = 8). Traces after 1. ON STIM 2. TH STIM and 3. DUAL STIM. Stimulation artefact removed for better visibility.*

3.3 Pharmacological characterization of tectal neurons responding to stimulation of the optic nerve and the thalamus

To further understand the synaptic properties of the visual system, pharmacological experiments using patch-clamp methods were utilized (See also chapter 2.3.2). Whole-cell patch-clamp recording allowed the investigation of ascending visual connections in combination with the application of reversible pharmacological agents. Receptor properties of tectal neurons were characterized during membrane response to optic nerve stimulation (ON STIM) and thalamic stimulation (TH STIM). In total 150 neurons were recorded. 3 of those neurons were labelled with biocytin and subsequently reconstructed.

3.3.1 Glutamate receptors in tectal neurons responding to optic nerve stimulation

In Bombina, the interconnection between retinal ganglion cells and tectal neurons and the dynamics involved in EPSP are mainly mediated by the neurotransmitter glutamate (see chapter 1.4.3). Retinal ganglion cells terminate in the superficial layers of the tectum, where the dendrites of tectal projection neurons were located. The newly developed semi-intact brain preparation used to investigate synaptic dynamics of retinal ganglion cell projection to tectal projection neurons was applied for this experiment (see chapter 2.2).

The semi-intact preparation allowed for simple identification of tectal structures (Figure 22 A & B). Even though the semi-intact tectal bulb was several hundred micrometres thick, neurons could be easily identified. After approaching the neurons and establishing a gigaseal, neurons were visibly attached to the electrode (Figure 22 C & D). All neurons were characterized for their membrane properties. In order to do this, a transient current was applied for 0,5 s. Three positive currents (0,1 pA, 0,2 pA, 0,3 pA) and three negative currents (-0,1 pA, -0,2 pA, - 0,3 pA) were applied and the membrane response observed (Figure 23 A). Positive currents could be used to estimate a firing threshold for each neuron, while negative currents were used to estimate the capacitance properties of the neuron. This relationship was mapped for a representative neuron (Figure 23). Tectal neurons have mostly linear relationships between applied current and spike frequency. Neurons were recorded using a whole-cell current-clamp mode. A clamping voltage was set below a spiking threshold, which rested usually between -35 mV and -45 mV .

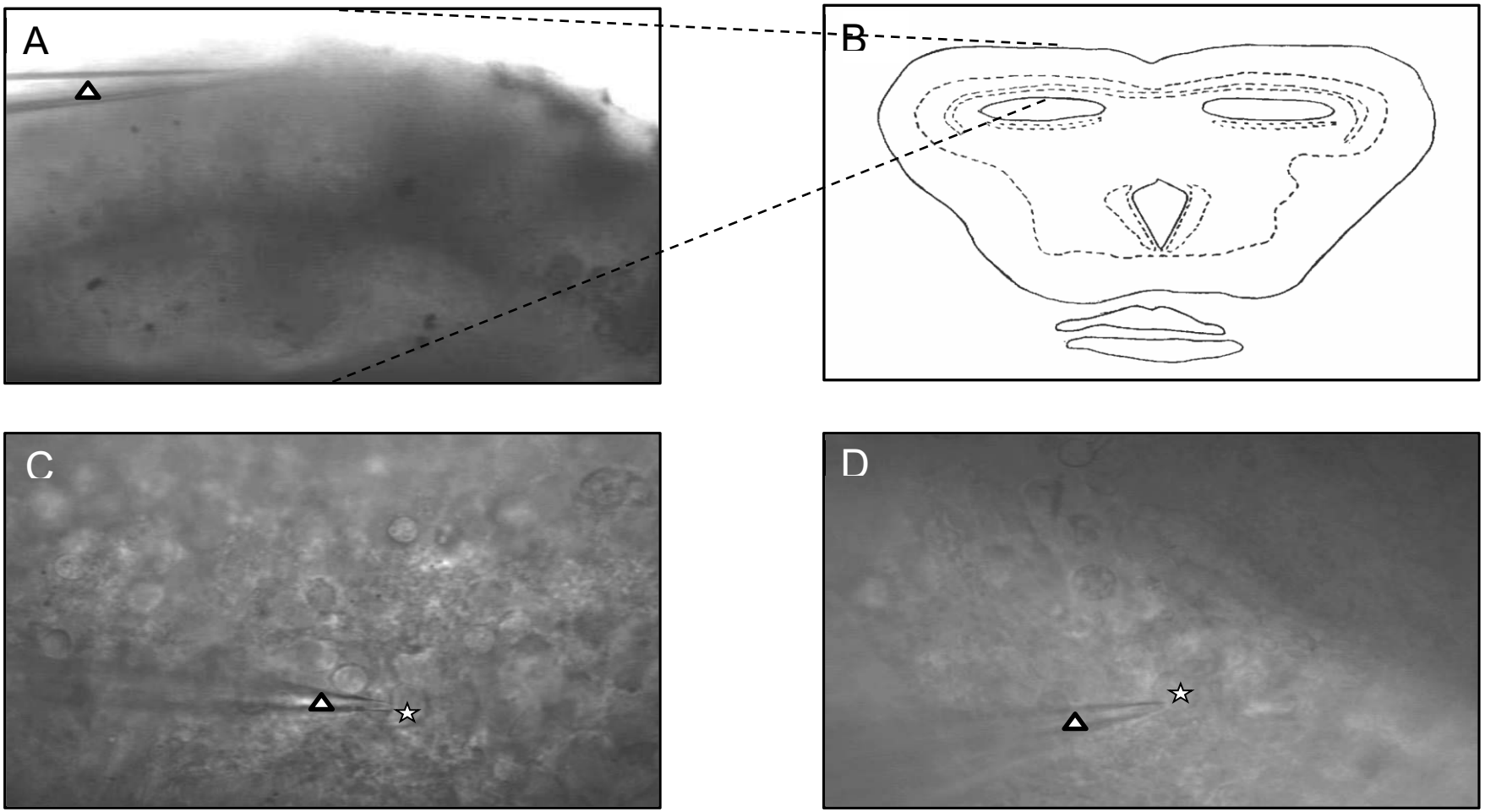

Figure 22 Representative optical microscope images and schematic drawing (Modified after U. Dicke) of patch-clamp recordings. A *overview of semi-intact brain preparation, visible is the part of the dorsal bulb of the optic tectum.* ***B*** *Schematic drawing of a coronal slice of the midbrain.* ***C & D*** *Close up images of recording situation. White asterisks represent recorded neurons and white triangles the patch-clamp micropipette*

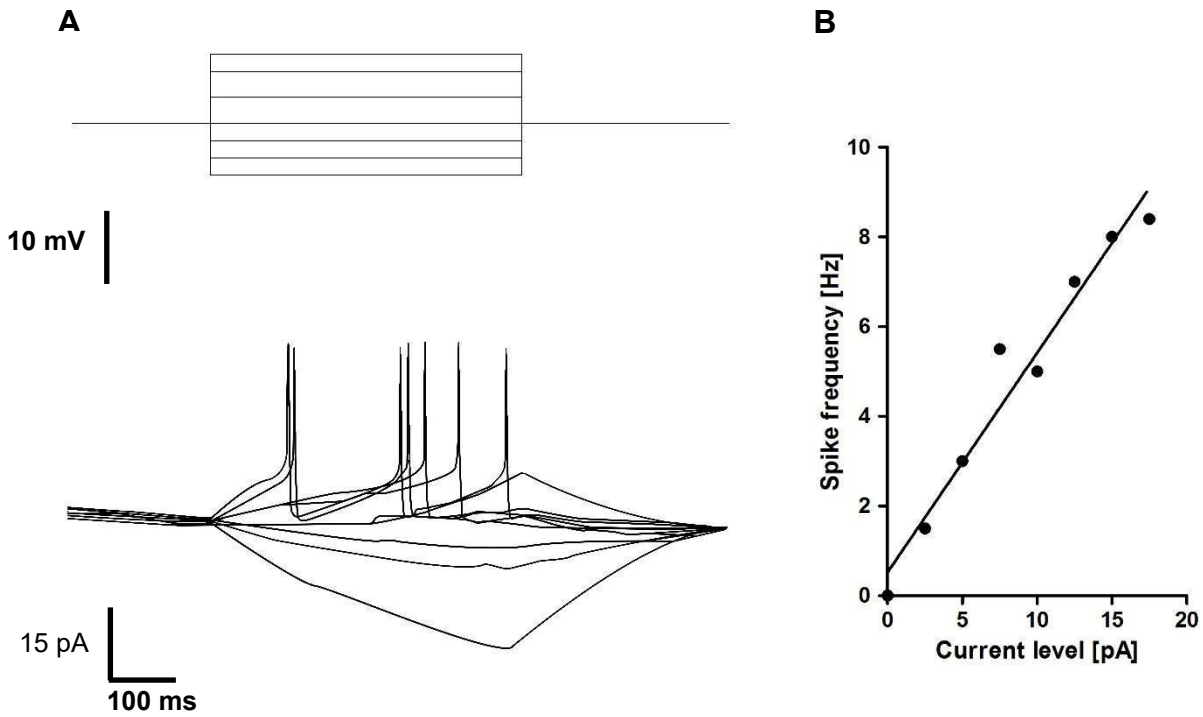

Figure 23 Characterization of tectal neurons to membrane to current application A. *Representative ramp-function of a tectal projection neuron. Applied voltage above, with corresponding current of the neuron below.* ***B.*** *Spike-rate voltage relationship for tectal projection neurons.*

In total, 25 neurons were characterized in their responses to ON STIM and treated with a potent, selective and competitive AMPA-Agonist (NBQX, Bio-Techne GmbH, Wiesbaden-Nordenstadt). Furthermore, 25 neurons were characterized in the same way and treated with a potent, selective NMDA antagonist (DL-AP5, Bio-Techne GmbH, Wiesbaden-Nordenstadt). Two recorded neurons were labelled with biocytin and subsequently reconstructed. A bath application was chosen using an intraindividual experimental regime, where the same neuron and its membrane response was used as a control after wash-in of the pharmaceutical agent. Subsequent wash-out confirmed the reversibility of the pharmaceutical agents. Tectal projection neurons were selected visually, possessing a large axon hillock. Secondarily, they were confirmed by low-latency response to stimulation of the optic nerve. Most neurons responded with excitation to ON STIM (86 %). Rarely, neurons did not respond with excitation to ON STIM (14 %). On average within this group, the tectal projection neurons had a response latency of 4,4 ms (±0.9 ms). After initial recording of responses to single and multiple stimulations, the pharmaceutical agent was washed in. After treatment with NBQX, no apparent change in amplitude could be observed. On average, the amplitude to peak excitation increased by 1,2 % from 5,2 mV to 5,26 mV. After washing out the pharmaceutical agent for 10 minutes, a decrease from the average response amplitude of 5,26 mV to 2,99 mV was observed. Statistical testing revealed no significant change from control to wash-in condition, and no statistically significant change from wash-in to wash-out condition ($p_1 = 0,89$; $p_2 = 0,26$, see Figure 24).

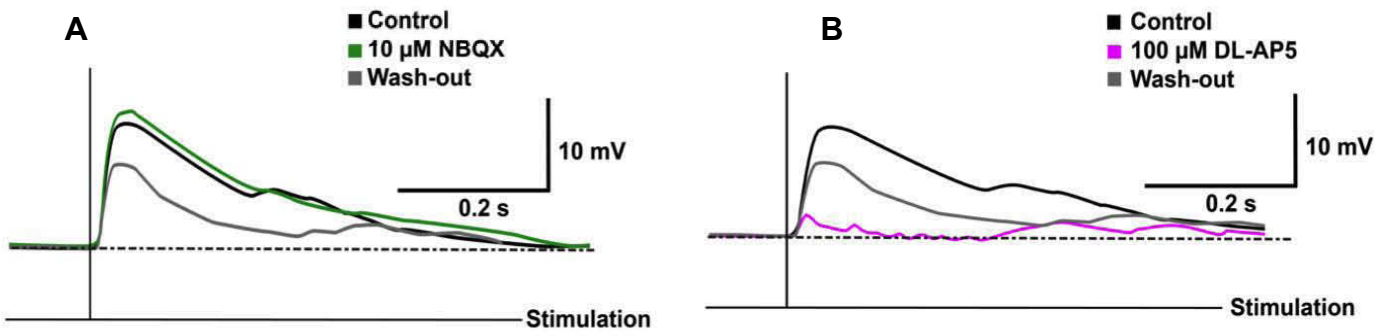

Figure 24 Averaged EPSP after ON stim and application of pharmacological agents. ***A*** *Application of 10 µM NBQX after 5 min of pre-wash (control), perfusion with Ringer's solution and 10 µM NBQX for 20 minutes and a wash out phase of 15 minutes,* ***B*** *Application of 100 µM DL-AP5 after 5 min of pre-wash (control), perfusion with Ringer's solution and 10 µM DL-AP5 for 20 minutes and a wash out phase of 15 minutes*

Almost no change in latency was detected after the application of 10 µM NBQX and after 15 minutes of wash-out (see Figure 24 A). During the control condition, an average maximal amplitude of 13,1 mV was measured. After application of 10 µM NBQX an average amplitude of 12,2 mV above the baseline was recorded. After 15 minutes of wash-

see Figure 24 A). Evoked EPSP responses

for three different neurons were also averaged and 100 µM of DL-AP5, a potent antagonist NMDA was applied. The latency of those evoked responses was very similar in the three experimental conditions, between 3 ms and 5 ms (see Figure 24 B). During the pre-wash control condition, an amplitude above the baseline of 12,8 mV was calculated. After application of DL-AP5 to the bath solution most of the evoked potentials were no longer discernible or visually confirmable. On average, an amplitude of 0,8 mV was calculated. After 15 minutes of wash-out, the average amplitude increased to 8,8 mV. The general shape of all evoked EPSP stayed roughly similar, except after application of DL-AP5, where in most cases no clear evoked EPSP was visible. During the whole experimental regimes, neurons readily responded with action potentials to electrode current. In order to understand the changes in evoked EPSP amplitudes to stimulation of the optic nerve and application of NBQX and DL-AP5, the relative amplitude of those potentials was investigated. EPSP during the pre-wash control condition were and set as 100%. EPSPs belonging to other experimental conditions were matched to the control condition within the individual recording session. Relatively, the normalized EPSP amplitude changed to

thin 10 minutes application of 100µM DL-AP5. On average, the normalized EPSP amplitude

were tested for statistically significant differences using the Mann-Whitney-U-test. A statistically significant difference was found between the control (pre-wash) condition and application of 100µM DL-AP5 ($p < 0{,}001$). See also Figure 25.

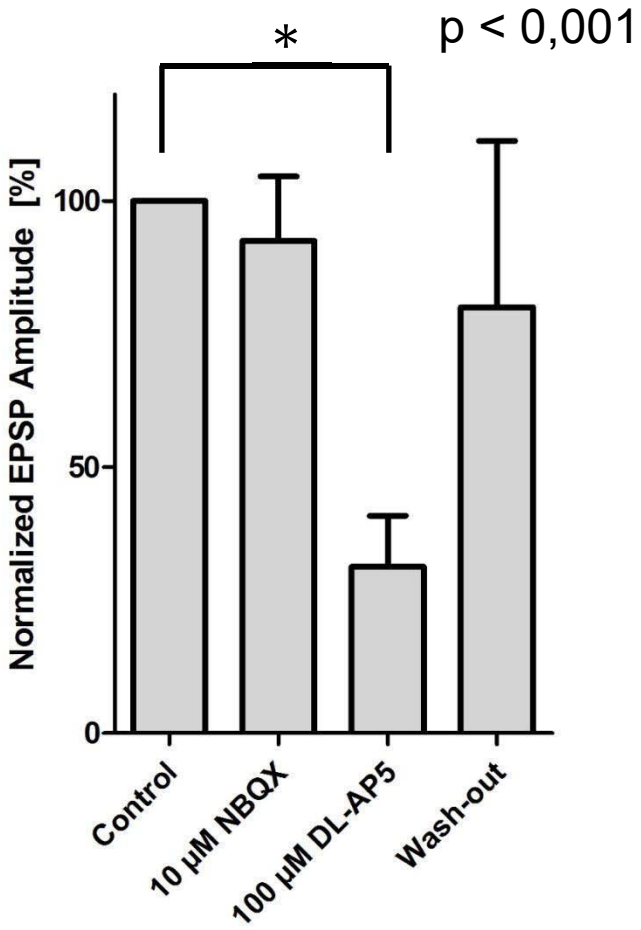

Figure 25 Changes in normalized EPSP after application of 10 µM NBQX and 100 µM DL-AP. *EPSP values normalized after the average amplitude of EPSP within the control condition.*

3.3.2 GABA receptors in tectal neurons responding to thalamic stimulation

With the newly developed semi-intact brain preparation it was possible to stimulate the thalamus and record membrane responses of tectal neurons, as described in chapter 3.2.1.2. During whole-cell patch clamp recording, neurons of the optic tectum commonly

The IPSP recorded within this configuration did not differ in amplitude and temporal characteristics from neurons recorded in whole brain recordings. Representative IPSP can be seen in Figure 26. IPSP after TH STIM did almost ablate after application of 10 µM Gabazine, with only very shallow IPSP still visible

er 30 minutes wash out phase, IPSP almost fully recovered to a shape before wash-

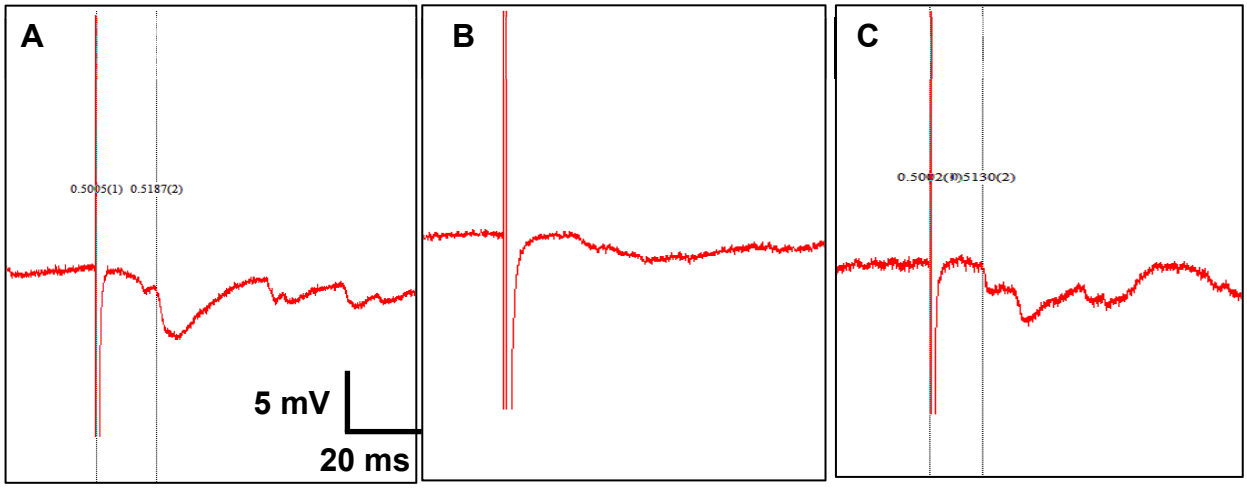

Figure 26 Representative inhibition to TH stim during patch clamp recording and blockage of inhibition by application of Gabazine. A *Control condition 5 min pre wash.* ***B*** *Stimulation of the thalamus after 10 min of bath application of 0,1 µM Gabazine.* ***C*** *Wash-out phase, 10 minutes after the end of Gabazine application Waveform average (n = 5) Response onset: 18 ms*

IPSPs were normalised to the average amplitude before wash-in of pharmacological agents. On average, the membrane potential was clamped at a subthreshold potential of -55 mV for neurons (n = 19) responding with IPSP to TH STIM. The average onset latency was 23 ms with an average amplitude of -2 mV. IPSP are highly variable in their shape. Some IPSP reach their minimal potential very quickly, while some neurons have a slow decrease in their membrane potential. In some cases, 'double inhibitions' could be observed, where two IPSP are overlaid in a fast succession. Long term patch-clamp recording of neurons proved very stable, with only 7% of recordings not completing the full experimental regime. The experimental regime as described in the chapter 2.3.2 was repeated each 60 s. The experiment was performed for 30 minutes. After 10 minutes into the experiment, Gabazine (SR-95531, Sigma-Aldrich, Munich, Germany) was washed into the bath solution. After 10 minutes elapsed after the start of the experiment, the application of Gabazine was stopped and bath application without pharmaceutical agents was applied to the bath solution. Two different concentration of Gabazine were applied, once 0,1 µM and 10 µM. After 10 minutes of bath application of 0,1 µM of Gabazine, IPSP minimal value increased from 9,2 mV to 3,1 mV. Within 30 minutes, after washing out Gabazine from the bath solution, the minimal value increased to 12,5 mV (Figure 27). Gabazine (10 µM) was applied using the same regime. IPSP amplitude increased from a value of -9,9 mV to -0,3 mV within 10 minutes of bath application. After 30 minutes wash-out the amplitude of the IPSP recovered to -10,7 mV. Temporal characteristics of those IPSP did not change with the application of both concentrations of Gabazine (Figure 27 A). The amplitude of IPSP was normalized to the average amplitude pre-wash. Application of 0,1 µM Gabazine lead to a decrease to 8 (± 1,8) %. This change was confirmed as statistically significant, using the Mann-Whitney-U-test ($p < 0,05$). The application of 10

μM Gabazine lead to a decrease of normalized IPSP amplitude to 0,1 (± 1,5) %. This change was also statistically significant (Mann-Whitney-U-test, $p < 0{,}001$). See also Figure 28 B.

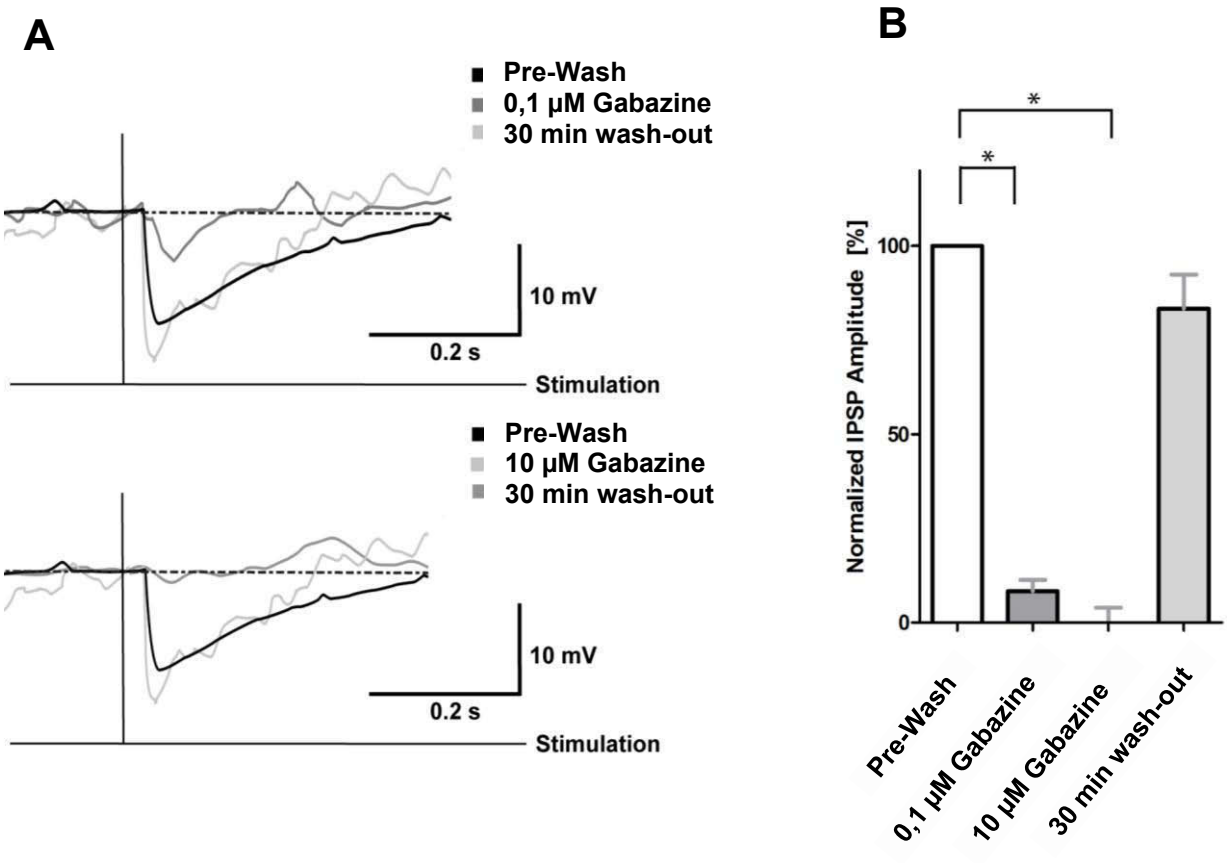

Figure 27 Characterization of inhibitory postsynaptic potentials after thalamic stimulation. A *Representative IPSP after application of 0,1 µM Gabazine and 10 µM Gabazine.* ***B.*** *IPSP values normalized after the average amplitude of IPSP within the control condition. Asterisks indicate statistical significance p < 0,05*

Each experimental regime consisted of several repeats of TH STIM, a probability to elicit an ISPSP could be calculated, from the ratio between recorded IPSP and stimulations of the TH. Pre-wash in of 100 µM Gabazine resulted in an probability to elicit an ISPS after TH stim between 47 % and 66 %. After application of 100 µM Gabazine a drop in IPSP probability was observed and after 16 minutes, no IPSP were observed. After wash-out, within 2 minutes, an increase of IPSP probability was observed, however with a high variability. After 30 minutes, a probability of 54 % was observed (See Figure 29).

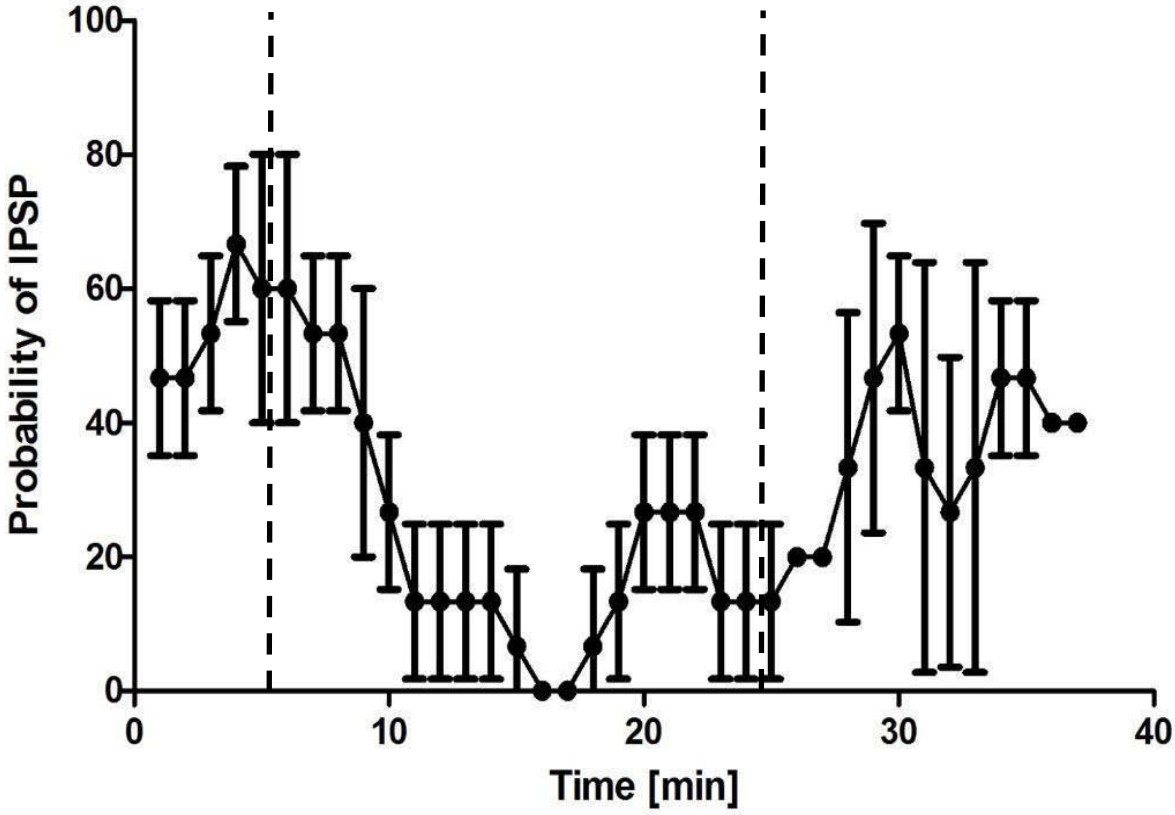

Figure 28 Probability for tectal neurons to elicit IPSPs during thalamic stimulation and 100 µM application of Gabazine. *Percentage calculated as recorded IPSPs per minute divided by number of stimulations per minute. Dashed lines signal application of 100 µM Gabazine and beginning of wash-out phase. Error bards indicate SE.*

4. Discussion

4.1 Structure and function of biocytin labelled neurons in the optic tectum

One of the aims of this thesis was to investigate the response characteristics of projection neurons (PN) in the optic tectum of *Bombina orientalis*. The challenge in this context has proven to be the identification of PN. PN are described by Antal (1986), Matsumoto and colleagues (1986) and Roth and colleagues (1999). From a total of 370 recorded neurons, 25 were attempted to be labelled with biocytin. 12 neurons were successfully labelled using the avidin-biotin reaction. Labelled somata of the neuros were well visible under light microscopy, however the dendritic tree and axons were not always fully visible (See Figure 8). Using stacking and reconstruction techniques, a total of 9 neurons were reconstructed and partially matched to the neuronal types as described by Roth and colleagues (1999). This may be due to two factors: either a blockage of the electrode tip stemming from organic hydrophobic molecules or due to general tissue degradation after labelling. Recorded neurons were suspected to be PN when they showed very short latency responses to ON STIM. It can be assumed that those neurons are all visual neurons, i.e. neurons included in the processing of visual information.

Based on anatomical studies (Roth *et al.*, 1999), the distance between the stump of the ON and the TH was found to be no less than 2 mm and no more than 4 mm, regardless of the size of the animal. The optic nerve, which is largely made up of unmyelinated fibres, was shown to have a conduction velocity between 0.2 and 2 m/s, which corresponds to the latencies found in other amphibians (Dunlop & Beazley, 1987). Tectal PN were labelled using a 4 % Biocytin solution which was added to the recording electrode. Labelling was consistent, despite not every attempted labelling resulting in a fully labelled neuron. However, after reconstruction most axons from PN were clearly visible. Reconstructed neurons were used to identify tectal PN. The question which this thesis will discuss is, how the response latency and the general membrane response characteristics correlate with the neuron type (See also Figure 7, Figure 8, Figure 9, Figure 10).

Excitatory responses to thalamic stimulation were not equally distributed across the surface of the optic tectum, when viewed as a grid, subdivided into 6 distinct areas. A majority of excitatory responses were found within the central-medial area. A gradient is present, with a clear decrease of excitatory responses from rostral to caudal (see Figure 11). There may be the possibility of retrograde, dendritic depolarization occurring from the current which is applied at the diencephalon. In some cases, the stimulation electrode

was located within 0,5 mm of the recording electrode. However, membrane depolarization would be recorded as very-low latency EPSP, usually with latencies within the 1 ms range (Satou & Ewert, 1984). Those events were very rare and were mostly correlated with neurons that were spontaneously active during recording. Descending PN have been studied and categorized. Roth and colleagues (2003) found and described three types of descending neuron types (TH4, TH5 - TH5.4), whose axons terminate within the optic tectum. The neuronal types described all terminated within the ipsilateral hemisphere of the somata. A large subgroup of the descending PN, such as TH4.1, are located within the central dorsal nucleus of the thalamus, having axonal projections to the medial pretectum. Furthermore, TH5.4 neurons, which are neurons whose projections exclusively descending, have axonal terminals within the medial tectum (Roth *et al.*, 2003).

Retinotopic maps have been described for mammals (Gias *et al.*, 2005) as well as amphibians (Montgomery & Fite, 1989), where it is presented along the surface of the optic tectum. Montgomery and Fite (1989) described a retinotopic map of R*ana pipiens* using retrograde horseradish-peroxidase-labelling (HRP) of neurons. They found that the first terminals of the projections from retinal ganglion cells to be the suprachiasmatic nucleus and the preoptic nucleus, following bands arranged along the rostro-caudal axis (Montgomery & Fite, 1989). It may be possible that a similar stratification is present in neurons descending from the thalamus. Those findings may be playing a role in the unequal distribution to excitation found when stimulating the TH.

4.2 Membrane responses of tectal projection neurons

4.2.1 Response characteristics of membranes of tectal projection neurons to optic nerve stimulation

EPSPs were measured in optic tectum neurons by using both described stimulation conditions. Statistically, in every experimental condition, no normal distribution in terms of amplitude was found. This is due to the fact that, within the EPSP group, stereotypical action potentials are present, whose amplitude is strongly conserved along most neurons. In addition, as described in the Material and Methods section (See 2.4 Data Processing), there was a cut-off applied to EPSP below 5 mV. These factors may compound finding a possible tuning curve to certain stimuli using this method.

Of a total of 16 evaluated neurons, a mean peak amplitude of 32,42 (± 2,29) mV was recorded with a clear AHP of -3,99 (± 0,64) mV which is due to the inclusion of action potentials into the analysis (Figure 13; Table 2). Results for stimulation of the thalamus were very similar and showed no statistical difference. In parallel to that, no statistical difference was found within the two other groups (See supplementary Figure 31). This is somewhat to be expected though, since neurons typically respond with stereotypical responses, depending on the activation pattern. However, the general distribution of amplitudes after DUAL STIM suggests slight inhibition, since EPSPs are governed by multiple axon terminals over the entire dendritic tree (Maturana, 1959). Furthermore, either local interneurons modulating neuronal excitation or projecting GABAergic interneurons may be involved (Roth *et al.*, 1999; Ruhl & Dicke, 2012). Those modulations can act as a general downregulation of excitatory activity within the optic tectum. A clearer image emerges when comparing the action potentials amplitude during ON STIM condition and during DUAL STIM condition. Almost no change either in the average amplitude and distribution was detected (see supplementary Figure 31), which is expected due to the stereotypical nature of action potentials.

Tectal PN readily responded to stimulation with low-latency excitation between 3 and 10 ms (Figure 15). Retinal ganglion cells project across the optic chiasm to the upper layers of the optic tectum. Axons found within this nerve-bundle were both myelinated and unmyelinated (Maturana, 1959), which in part may account for the variance in response latencies found. Response latencies of 3 to 10 ms were found to be consistent with those found in salamanders (Roth *et al.*, 1999) and other amphibians (Finkenstädt & Ewert, 1983). Those projections were found to be mainly glutamatergic (Hickmott &

Constantine-Paton, 1993). Most neurons responding with excitation were found to be retinal PN. Low-latency excitation has been previously correlated with visual processing in amphibians (Schuelert & Dicke, 2005). However, multiple spikes have been rarely observed. Since in the present *in vitro* brain preparation stimulated the whole optic nerve with a high voltage for a very short time, it can be assumed that only transient excitation is achieved. Furthermore, horizontal inhibition via interneurons may explain this phenomenon (Gale & Murphy, 2016). Using similar recording techniques, Matsumoto (1980) found two distinct groups of response types of latency in tectal neurons and using labelling techniques with Procion Yellow correlated the recordings with the morphological types. Matusmoto and Bando concluded that excitatory long latency responses were mainly produced by large neurons with narrow dendritic trees (V-Type), which closely relates to what Roth (1987) described as tectal PN (Matsumoto & Bando, 1980). Additionally, Matsumoto and Bando described a very similar distribution of membrane responses as described in this thesis, showing a distinct distribution of short latency responses and another distribution of long latency response. The characteristics of excitation described in this thesis in tectal PN are consistent with those of recordings in other amphibians (Roth *et al.*, 1999) and other vertebrates (Kardamakis *et al.*, 2015).

4.2.2 Response characteristics of membranes of tectal projection neurons to thalamic stimulation

In this thesis, the ipsilateral TH was stimulated using a bipolar stimulation electrode. The dorsal part of the TH was targeted in order to gain an understanding of the functional characteristics of tecto-thalamic interactions during visual processing. Tectal PN responded with both excitatory and inhibitory postsynaptic potentials. A majority of responses observed were inhibitory (76 %) (Figure 11). Inhibition of tectal neurons were mainly as expected and in the introduction of this thesis. Following the hypothesis of an attentional system suggested by Ruhl and Dicke (2012), using inhibition and disinhibition of tectal neurons modulated by projecting neurons of the thalamus, such a result is consistent with the hypothesis.

Furthermore, some responses were not monosynaptic, but rather oligosynpatic. This suggests a more modulatory system controlling spiking activity throughout the tectum. Using Biocytin labelling techniques, Roth and Grunwald (2000) characterized five classes of thalamic neurons. Of those classes TH1, TH2 and TH3 both were innervated visual afferents and had axons projecting to the optic tectum. Interestingly, TH1, TH2 and TH3

neurons are predominately located further in the ventral part of the TH. Moreover, projections from the dorsal part of the TH were reported to be very sparse (Wiggers, 1999). Since the stimulation electrode used in this thesis had a diameter of approximately 500 µm, it can be assumed that all classes of neurons were depolarized by the voltage used to stimulate in this thesis. Himstedt and colleagues (1987) characterized thalamic neurons and their response properties, finding oligosynaptic excitatory responses to visual stimuli, further supporting the idea of the thalamus serving as a controlling and modulatory gateway in an ascending visual pathway.

4.2.3 Response characteristics of membranes during simultaneous stimulation of the optic nerve and the thalamus

In the previously described experiments, tectal PN responses were recorded after simultaneously stimulating the ON and the TH. The tectum is strongly innervated with glutamatergic fibres both projecting from retinal ganglion cells and other brain areas among that TH (Roth *et al.*, 2003). The TH receives excitatory afferents from retinal ganglion cells and responds with long-latency spikes to stimulation of the ON (Roth *et al.*, 2003; Dicke & Roth, 2007). Lesion studies in amphibians (Ruhl & Dicke, 2012) suggested the presence of a feedback loop between the optic tectum and the TH, which is part of the visual system and plays a key role in guiding attention. The authors observed a disinhibition of tectal PN after lesioning the dorsal TH during a two-alternative visual task. Furthermore, the authors concluded that the role of the TH as a key part in a tecto-thalamic feedback loop and is centrally involved in guiding attention during a behavioural task. They suggest that during visual processing, tectal PN representing non-salient are inhibited while neurons representing salient information are disinhibited (Ruhl & Dicke, 2012). The attentional system in amphibians is furthermore modulated by the striatum located in the pallium. In this system, the TH works as a centrally located relay in the bottom-up processing of visual information. They suggest the TH uses both information from the striatum, retinal ganglion cells to either inhibit or disinhibit neurons located in the tectum (Ruhl *et al.*, 2016).

When comparing responses of tectal PN to ON stimulation and simultaneous stimulation of the ON and TH, two clear differences were found in this thesis: a) action potentials were delayed in average of 10.5 ms after simultaneous stimulation and b) action potentials were less likely to occur after stimulation. When comparing response characteristics of membrane responses within the TH and optic tectum, we propose that these connections

are not monosynaptic but rather di- or oligosynaptic (Matsumoto & Bando, 1980; Roth *et al.*, 2003; Laberge *et al.*, 2008). The findings therefore suggest that neurons from the TH, possibly being relayed from local interneurons within the TH to thalamic PN and then to interneurons within the optic tectum, ultimately inhibiting a certain population of tectal neurons. Visa versa, the same connection may enhance spiking activity within the optic tectum, thus, guiding attention. This connection is coupled within a feedback-loop, since a majority of tectal PN have axons terminating within the TH. In mammals, similarly the superior colliculus relays information via the inferior pulvinar nuclei mainly to dorsal telencephalic areas (Kaas & Lyon, 2007). This suggests that thalamic neurons mainly innervate tectal interneurons, which in turn inhibit local tectal PN. Thalamic neurons were found to be both glutamatergic and GABAergic (Landwehr & Dicke, 2005), which would explain observing both inhibition and excitation after stimulating the TH thalamus.

4.2.4 High-latency EPSP responses of tectal neurons

During intracellular and patch clamp recordings, high-latency EPSP responses in optic tectum neurons have been recorded. However, only in very rare cases, EPSP with higher latency than 15 ms have been observed recordings (Figure 18 A). Those events, with higher latency than 30 ms have been excluded form analysis, since it cannot be assumed that those events are correlated and caused by electrical stimulation. When conducting intracellular recordings, a majority of high-latency EPSP have been found when stimulating the TH (See Figure 18). In parallel to that, when recording after DUAL STIM, a larger portion of recorded EPSP can be considered high latency (Latencies < 15 ms) (See Figure 18 B & C). These findings are supported by the fact, that action potentials are temporally delayed during DUAL STIM (See Figure 16 A).

4.2.5 Inhibitory membrane responses of tectal neurons

A large percentage of postsynaptic events recorded within the experiments conducted in this thesis were IPSP. They were both recorded during intracellular recording and during semi-intact patch-clamp recording (See Results 3.2.1.2 and Results 3.3.1). IPSP were usually recorded as short dips in membrane potential, quickly recovering to a baseline membrane potential (See Figure 17). Those connections had amplitudes between -1 mV to -10 mV. Interestingly, direct correlation between stimulation amplitude and amplitude of IPSP was found. As described by Roth (1999), in some cases neurons were found that displayed either "double-dips" in inhibition or inhibition followed by excitation (See supplementary Figure 30). Those finding, being difficult to quantify, clearly suggest systematic processes and visual processing systems being activated by stimulation of the TH. Those short inhibitions may be a signpost to local inhibition as a signpost to visual object processing as described by Ruhl & Dicke (2013). No clear and statistically significant differences were found within differing depths of stimulation of the TH (See Figure 18). Those findings were unexcepted, since no direct monosynaptic projections from the dorsal TH were found (Roth *et al.*, 2003) and studies by Ruhl (2013) clearly showed that the dorsal TH, which is within the first 50 µm of the tectum, is essential to the inhibitory phenomenon found in amphibians during visual object processing. Those findings give no clear cue, whether the source of tectal inhibition stems either from pretectal neurons (Ewert, 1968) or from local interneurons within the optic tectum (an der Heiden & Roth, 1987).

4.3 Evaluation of the novel semi-intact approach to patch-clamp electrophysiology

In the present thesis, a novel method was used to approach patch-clamp electrophysiology. Traditionally, patch-clamp electrophysiology has been conducted in slice-preparations (Edwards *et al.*, 1989; Hamodi & Pratt, 2014). Whole-brain preparations were not feasible for the microscopy used during the experimentation. Furthermore, since the diameter of patch-clamp micropipettes is several times larger than the somata of neurons, it has been historically difficult to approach neurons located in deeper layers of the tectum. The aim of this thesis is to investigate functional connection between the tectum and brain areas, which are relatively far away, the classical approach using coronal or horizontal slices was not satisfactory. The preparation used in this thesis is being referred to as 'semi-intact slice preparation', since all brain areas located rostrally to the tectum are left intact, yet the tectum is an approachable with micropipettes as a slice. This preparation made it possible to record from tectal neurons within several layers during one experimental session. The tissue remained heathy and stable under cooled conditions and neurons were recordable for several days after the brain preparation. All histological processes are also possible with this type of preparation. In total, 12 neurons were labelled with biocytin and their dendritic trees reconstructed (See Results 3.1 and Figure 7, Figure 8, Figure 9 and Figure 10). The neurons are identifiable by their neuron type as described by Roth (1999). However, the dendritic trees are not large as neurons labelled under whole brain conditions. This may be due to the fact, that some portion of the dendritic tree is always damaged during the slice preparation process. Likewise, cells are may be further damaged after slice preparation, leading to fraying and degeneration of the dendritic tree. Furthermore, no axons have been reconstructed using this technique. Due to the nature of this technique, only axons projecting rostrally are possible to label. No axons were identifiable in neurons recorded in semi-intact slice preparation and labelled with biocytin, which may be due to the difficulty of tissue handling during the recording session, which led to tissue degradation.

Within the literature, the presence of a topographic map in the optic tectum of frogs is discussed (Gaze, 1958; Montgomery & Fite, 1989). It has been a long established and successful way of understanding animal vision. The role of the NMDA receptor in amphibians has been investigated, for example an in vivo study by Cline and colleagues (1987) who showed through chronic application of an NMDA inhibitor (APV) during

development, that no discernible organization and pattern in the tectum was established. Introduction to NMDA essentially eliminates the postsynaptic response recorded in the tectum (Cline *et al.*, 1987; Debski *et al.*, 1991).

4.4 Microcircuitry of the optic tectum

4.4.1 Glutamatergic projection from the retina to the optic tectum

As previously described the most common response of tectal neurons to stimulation of the optic nerve is an EPSP. Since retinal ganglion cells project to the roof of the midbrain, such results are expected. Biocytin labelling revealed that both projection neurons and interneurons may respond with EPSP to optic nerve stimulation (See Figure 7, Figure 8, Figure 9 and Figure 10). Since both latencies are likely monosynaptic, this suggest that retinal ganglion cells form synaptic connection with both tectal projection neurons (Type 1 – 5) and interneurons. In Rana, Hickmott and Constantin-Paton (1993) found polysynaptic responses of tectal cells to optic nerve stimulation. The highest latency found during whole-brain recording after ON STIM was 9 ms (See Figure 13). This EPSP may be likely disynaptic or polysynaptic. GABA may also be an transmitter of retinal ganglion cells, this may explain IPSP found in some cases of ON STIM and only about a third of measured responses after ON STIM were EPSP (See Figure 11). Application of an NMDA-receptor antagonist (DL-AP5) revealed that projections by the fibres of the retinal ganglion cells are mainly glutamatergic. These results have been confirmed ablation of EPSP after bath application.

4.4.2 GABAergic interneurons within the optic tectum

It can be concluded that tectal PN receive oligosynaptic excitatory and inhibitory input from the dorsal TH. The dorsal TH acts as a mediator or gateway for object-directed attentional-like behaviour in amphibians. The basic anatomical organization of all vertebrates brains are very similar, even though a myriad of sensory adaptations and specific function of sensory organs and behaviour is known. The findings show a feedback-loop, which modulates spiking activity of visual neurons. When comparing this to other vertebrates such as mammals (Basso & Wurtz, 1997) or lampreys (Robertson *et al.*, 2006), the same basic mechanism has been described. Such as systems serve as a basic attentional circuit, inhibiting objects which are of low interest to the animal and enhancing the representation objects with high behavioural relevance. Coincidently, those neurons give output information to motor centres. Since amphibians are a basal group within the vertebrates, it may be assumed that such systems were retained throughout the evolution of vertebrates. In rodents and zebrafish, competitive inhibition in the colliculus with strongly connected GABAergic neurons has long been investigated

(Barker & Baier, 2013). Therefore, amphibians serve as excellent model-systems for feedback mechanisms in visual attention among other generic neuronal mechanism.

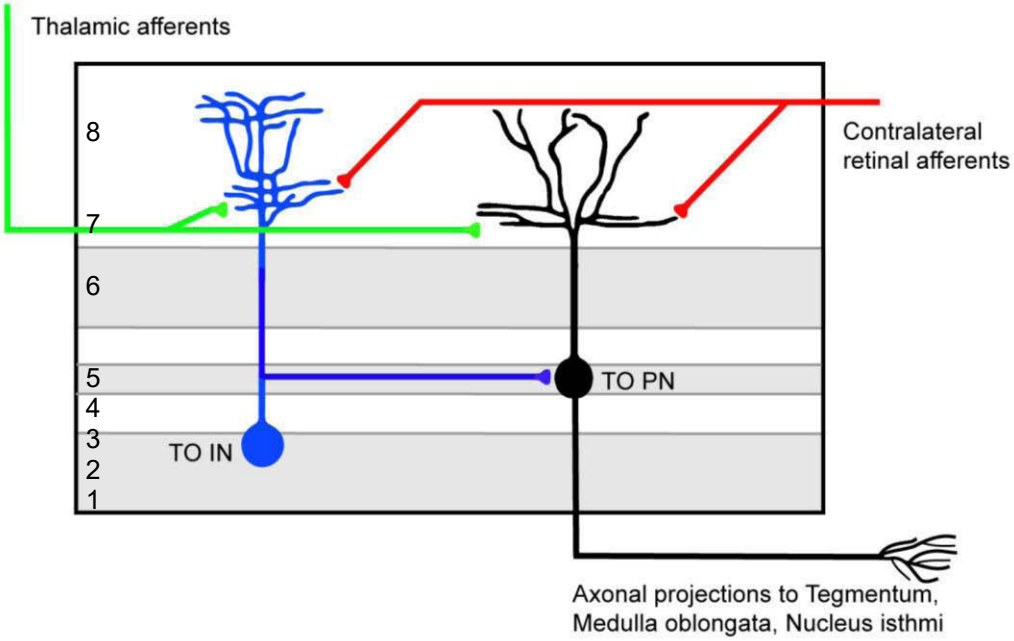

Figure 29 Proposed midbrain microcircuitry governing the disinhibition phenomenon found during amphibian object discrimination. *Grey areas are cellular layers, while white areas are neuropil. Red and Green are excitatory, blue are inhibitory connections. optic tectum IN: tectal interneuron, optic tectum PN: tectal projection neuron (type 1-5). Different types of tectal projection neurons are condensed for sake of clarity.*

4.4.3 Comparison between other vertebrates and amphibians of the optic tectum

The optic tectum in all vertebrates is involved in orienting behaviour and gaze movements (Dean *et al.*, 1989; Moschovakis *et al.*, 1996; Basso & Wurtz, 1997), in addition to integration of different sensory modalities, e.g. vision, auditory and electroreception (Bodznick, 1990; Wallace *et al.*, 1996; Meredith & Ramoa, 1998). Multisensory integration has been shown to be based on a set of empirical principles and is constrained within the spatial and temporal dimensions (Stein & Stanford, 2008). In particular, when extracellularly recording optic tectum neurons, their spike-rate increases with congruent cues, stemming from both spatial and temporal dimensions. In contrast, the spike-rate of those neurons decreases the more disparate the spatial and temporal cues were presented (Meredith *et al.*, 1987; Meredith & Stein, 1996; Kadunce *et al.*, 1997; Recanzone,

2003). Using conceptual and computational models in regard to multisensory integration, the existence of an inhibitory mechanism in regard to these findings has been independently proposed (Rowland *et al.*, 2007; Alvarado *et al.*, 2008; Ursino *et al.*, 2009).

In lampreys, the existence of a motoric map within the optic tectum has been demonstrated. Saitoh and colleagues (2007) used site specific stimulation within a deep layer of the optic tectum and observed head gaze shifts of a specific amplitude and direction, corresponding to this stimulation (Saitoh *et al.*, 2007). In lampreys, deep layer neurons within the optic tectum receive monosynaptic excitatory input from both sensory afferent pathways present. Those projecting output neurons also receive disynaptic inhibition which is triggered by the same afferent system. As a result of this, if two signals are originating from the same area, no inhibition is triggered. However, signals from the surrounding area trigger only inhibition within those neurons (Kardamakis *et al.*, 2015). These findings closely resemble the findings of those in amphibians, corresponding to the highly conserved organization of the optic tectum (Nieuwenhuys *et al.*, 2014; Asteriti *et al.*, 2015).

4.4.4 The role of tectal inhibition compared to other animals

Local tectal inhibition has been extensively studied within the other animal models, such as the lamprey (Phongphanphanee *et al.*, 2014; Kardamakis *et al.*, 2015). In lampreys, a local GABAergic system is present which regulates incoming excitatory sensory information to so-called deep layer output neurons. In particular, stimuli which are either temporally or spatially offset are suppressed by this system (Kardamakis *et al.*, 2016). Local interneurons are involved in this system, which is carried across the optic tectum by both short-range and long-range connection (Phongphanphanee *et al.*, 2014). Within the lamprey system, two origins for inhibition have been proposed; either an independent local inhibition or an exogenous source which provides global inhibition via GABAergic neurons projecting from the nucleus isthmi (Mysore and Knudsen, 2013). In regards to local interneurons within the lamprey optic tectum, they are activated by either retinal or electroreceptive afferents – similarly to the activation of deep layer optic tectum output neurons (Kardamakis *et al.*, 2016).

Similarly, to the situation found in mammals, studies in the lamprey brain suggest that the organization of the optic tectum is columnar, where deep layer output neurons and interneurons receive retinal excitation from the same ocular quadrant. Additionally, the pattern of excitation was shown to be retinotopically arranged. However, no clear

detailed arrangement of the suggested columnar structure or their function has been proposed yet (Kardamakis *et al.*, 2016). In mammals, bimodal suppression was described during vision (Meredith & Stein, 1996; Kadunce *et al.*, 1997).

4.5 Top-down modulation of the optic tectum

In mammals, midbrain neurons of the superior colliculus receive a combination of inhibitory and excitatory projections from the forebrain (Wurtz & Albano, 1980; Wurtz & Hikosaka, 1986). In lampreys, deep layer output neurons can perform stimulus selection without external modulation from other brain areas, however strong influence and modulation from other forebrain-structures are present. It was suggested, that basal ganglia disinhibition works in tandem with the excitatory projection from the pallium/cortex, as suggested that in both mechanism projections are targeted at the somata of the neurons, rather than the dendrites (Kardamakis *et al.*, 2016).

5. Summary

The vertebrate brain is a highly dynamic and complex network, permitting animals to process their environments, detect object within their visual field and make decisions. The midbrain-optic tectum is the main visuomotor integration centre in the amphibian brain. Additionally, it receives input from several other brain areas, mainly the diencephalon, such as the nucleus isthmi and pretectum. This thesis aimed to investigate findings that showed neurons of the optic tectum are influenced by the diencephalon. Object processing was represented by stimulation of the optic nerve. Thalamic influence was also measured by stimulation of the dorsal thalamus. Thalamic EPSP differed in their latency distribution, suggesting a di- or oligosynaptic projection from the dorsal thalamus to the optic tectum. Likely thalamic neurons of the type TH3 or TH5 mediate such a connection. Even though no significant difference in amplitude was found, action potential latency increased significantly when stimulating the optic nerve or the thalamus and the optic nerve simultaneously. This 'temporal inhibition' is likely another mechanism within the tecto-thalamic-feedback-loop, which acts as an attentional system during a paired-object-presentation task in amphibians. Tectal neurons responded commonly with IPSP after thalamic stimulation. Biocytin labelling showed that both tectal projection neurons and interneurons respond with IPSP to thalamic stimulation. These results suggest that inhibition, mediated by the thalamus is achieved by GABAergic interneurons, activating local inhibitory networks. In order to both record the membrane potential of tectal neurons and investigate top-down modulation of the diencephalon, a novel brain preparation was conceived. The tectal bulb was manually opened, allowing a sloped, flat area, where neurons are visible through a microscope. Additionally, the entire forebrain, including the optic nerve and descending fibres are still present in this preparation. Using this preparation, the optic nerve was stimulated and the membrane potential of tectal neurons recorded using the whole-cell current-clamp method. The short latency, likely monosynaptic EPSP were ablated after application of 100 µM DL-AP5, but still present after application of 10 µM NBQX. These results suggest that retinal ganglion cell projections are mainly mediated by NMDA receptors. IPSP resulting from thalamic stimulation could be ablated by application of 100 µM gabazine, both in terms of amplitude and probability, suggesting GABAergic projections from the thalamus. This thesis proposes that tectal interneurons, which are influenced by thalamic neurons, modulate tectal projection neurons, who directly receive retinal inputs.

6. Literature

Akopian, A. (2000). Neuromodulation of ligand- and voltage-gated channels in the amphibian retina. *Microsc Res Tech, 50*(5), 403-410.

Alvarado, J. C., Rowland, B. A., Stanford, T. R., & Stein, B. E. (2008). A neural network model of multisensory integration also accounts for unisensory integration in superior colliculus. *Brain Res, 1242*, 13-23.

amphibiaweb.org. (2019). https://amphibiaweb.org/taxonomy/AW_FamilyPhylogeny.html.

an der Heiden, U., & Roth, G. (1987). Mathematical model and simulation of retina and tectum opticum of lower vertebrates. *Acta Biotheor, 36*(3), 179-212.

Antal, M. (1991). Distribution of GABA immunoreactivity in the optic tectum of the frog: a light and electron microscopic study. *Neuroscience, 42*(3), 879-891.

Antal, M., Matsumoto, N., & Szekely, G. (1986). Tectal neurons of the frog: intracellular recording and labeling with cobalt electrodes. *J Comp Neurol, 246*(2), 238-253.

Antal, M., Tornai, I., & Szekely, G. (1980). Longitudinal extent of dorsal root fibres in the spinal cord and brain stem of the frog. *Neuroscience, 5*(7), 1311-1322.

Asteriti, S., Grillner, S., & Cangiano, L. (2015). A Cambrian origin for vertebrate rods. *Elife, 4*.

Barker, A. J., & Baier, H. (2013). SINs and SOMs: neural microcircuits for size tuning in the zebrafish and mouse visual pathway. *Front Neural Circuits, 7*, 89.

Basso, M. A., & Wurtz, R. H. (1997). Modulation of neuronal activity by target uncertainty. *Nature, 389*(6646), 66-69.

Baugh, A. T., & Ryan, M. J. (2010). The development of sexual behavior in tungara frogs (Physalaemus pustulosus). *J Comp Psychol, 124*(1), 66-80.

Bennett, M. V. (1997). Gap junctions as electrical synapses. *J Neurocytol, 26*(6), 349-366.

Bodznick, D. (1990). Elasmobranch vision: multimodal integration in the brain. *J Exp Zool Suppl, 5*, 108-116.

Boulenger, G. (1890). *The fauna of British India, including Ceylon and Burma: reptilia and Batrachia*: Taylor & Francis.

Cline, H. T., Debski, E. A., & Constantine-Paton, M. (1987). N-methyl-D-aspartate receptor antagonist desegregates eye-specific stripes. *Proc Natl Acad Sci U S A, 84*(12), 4342-4345.

Cornell-Bell, A. H., Finkbeiner, S. M., Cooper, M. S., & Smith, S. J. (1990). Glutamate induces calcium waves in cultured astrocytes: long-range glial signaling. *Science, 247*(4941), 470-473.

Dale, H. (1935). Pharmacology and Nerve-endings (Walter Ernest Dixon Memorial Lecture): (Section of Therapeutics and Pharmacology). *Proc R Soc Med, 28*(3), 319-332.

Dean, P., Redgrave, P., & Westby, G. W. (1989). Event or emergency? Two response systems in the mammalian superior colliculus. *Trends Neurosci, 12*(4), 137-147.

Debski, E. A., Cline, H. T., McDonald, J. W., & Constantine-Paton, M. (1991). Chronic application of NMDA decreases the NMDA sensitivity of the evoked tectal potential in the frog. *J Neurosci, 11*(9), 2947-2957.

Dicke, U., Heidorn, A., & Roth, G. (2011). Aversive and non-reward learning in the fire-bellied toad using familiar and unfamiliar prey stimuli. *Current Zoology, 57*(6), 709-716.

Dicke, U., & Muhlenbrock-Lenter, S. (1998). Primary and secondary somatosensory projections in direct-developing plethodontid salamanders. *J Morphol, 238*(3), 307-326.

Dicke, U., & Roth, G. (1996). Similarities and differences in the cytoarchitecture of the tectum of frogs and salamanders. *Acta Biol Hung, 47*(1-4), 41-59.
Dicke, U., & Roth, G. (2007). 2.04 - Evolution of the Amphibian Nervous System. In J. H. Kaas (Ed.), *Evolution of Nervous Systems* (pp. 61-124). Oxford: Academic Press.
Dicke, U., & Roth, G. (2009). Evolution of the Visual System in Amphibians. In M. Binder, N. Hirokawa, & U. Windhorst (Eds.), *Encyclopedia of Neuroscience* (pp. 1455-1459): Springer Berlin Heidelberg.
Dowling, J. E., & Werblin, F. S. (1969). Organization of retina of the mudpuppy, Necturus maculosus. I. Synaptic structure. *J Neurophysiol, 32*(3), 315-338.
Dudkin, E. A., & Gruberg, E. R. (2003). Nucleus isthmi enhances calcium influx into optic nerve fiber terminals in Rana pipiens. *Brain Res, 969*(1-2), 44-52.
Dunlop, S. A., & Beazley, L. D. (1987). Cell death in the developing retinal ganglion cell layer of the wallaby Setonix brachyurus. *J Comp Neurol, 264*(1), 14-23.
Edwards, F. A., Konnerth, A., Sakmann, B., & Takahashi, T. (1989). A thin slice preparation for patch clamp recordings from neurones of the mammalian central nervous system. *Pflugers Arch, 414*(5), 600-612.
Endepols, H., Walkowiak, W., & Luksch, H. (2000). Chemoarchitecture of the anuran auditory midbrain. *Brain Res Brain Res Rev, 33*(2-3), 179-198.
Ewert, J.-P. (1968). Der Einfluß von Zwischenhirndefekten auf die Visuomotorik im Beute- und Fluchtverhalten der Erdkröte (Bufo bufo L.). *Zeitschrift für vergleichende Physiologie, 61*(1), 41-70.
Feger, H. (1978). *Konflikterleben und Konfliktverhalten : psychologische Untersuchungen zu alltäglichen Entscheidungen*. Bern: H. Huber.
Feng, A. S., Hall, J. C., & Gooler, D. M. (1990). Neural basis of sound pattern recognition in anurans. *Progress in Neurobiology, 34*(4), 313-329.
Finkenstadt, T. (1980). Disinhibition of prey-catching in the salamander following thalamic-pretectal lesions. *Naturwissenschaften, 67*(9), 471-472.
Finkenstädt, T., & Ewert, J. P. (1983). Visual pattern discrimination through interactions of neural networks: a combined electrical brain stimulation, brain lesion, and extracellular recording study inSalamandra salamandra. *Journal of comparative physiology, 153*(1), 99-110.
Fite, K. V., Bengston, L. C., & Montgomery, N. M. (1988). Anuran accessory optic system: evidence for a dual organization. *J Comp Neurol, 273*(3), 377-384.
Franzoni, M. F., & Morino, P. (1989). The distribution of GABA-like-immunoreactive neurons in the brain of the newt, Triturus cristatus carnifex, and the green frog, Rana esculenta. *Cell and Tissue Research, 255*(1), 155-166.
Fritzsch, B. (1980). Retinal projections in European Salamandridae. *Cell and Tissue Research, 213*(2), 325-341.
Fritzsch, B., & Himstedt, W. (1980). Anatomy of visual afferents in salamander brain. *Naturwissenschaften, 67*(4), 203-204.
Frost, D. R., Grant, T., Faivovich, J., Bain, R. H., Haas, A., Haddad, C. F. B., De Sa, R. O., Channing, A., Wilkinson, M., Donnellan, S. C., Raxworthy, C. J., Campbell, J. A., Blotto, B. L., Moler, P., Drewes, R. C., Nussbaum, R. A., Lynch, J. D., Green, D. M., & Wheeler, W. C. (2006). The amphibian tree of life. *Bulletin of the American Museum of Natural History*(297), 8-370.
Gabriel, R., & Straznicky, C. (1995). Synapses of optic axons with GABA- and glutamate-containing elements in the optic tectum of Bufo marinus. *J Hirnforsch, 36*(3), 329-340.

Gabriel, R., Straznicky, C., & Wye-Dvorak, J. (1992). GABA-like immunoreactive neurons in the retina of Bufo marinus: evidence for the presence of GABA-containing ganglion cells. *Brain Res, 571*(1), 175-179.
Gale, S. D., & Murphy, G. J. (2016). Active Dendritic Properties and Local Inhibitory Input Enable Selectivity for Object Motion in Mouse Superior Colliculus Neurons. *J Neurosci, 36*(35), 9111-9123.
Gaze, R. M. (1958). The representation of the retina on the optic lobe of the frog. *Q J Exp Physiol Cogn Med Sci, 43*(2), 209-214.
Gias, C., Hewson-Stoate, N., Jones, M., Johnston, D., Mayhew, J. E., & Coffey, P. J. (2005). Retinotopy within rat primary visual cortex using optical imaging. *Neuroimage, 24*(1), 200-206.
Glagow, M., & Ewert, J. P. (1997). Dopaminergic modulation of visual responses in toads. I. Apomorphine-induced effects on visually directed appetitive and consummatory prey-catching behavior. *Journal of Comparative Physiology A, 180*(1), 1-9.
Grillner, S. (2003). The motor infrastructure: from ion channels to neuronal networks. *Nat Rev Neurosci, 4*(7), 573-586.
Grusser-Cornehls, U., Grusser, O. J., & Bullock, T. H. (1963). Unit Responses in the Frog's Tectum to Moving and Nonmoving Visual Stimuli. *Science, 141*(3583), 820-822.
Hamodi, A. S., & Pratt, K. G. (2014). Region-specific regulation of voltage-gated intrinsic currents in the developing optic tectum of the Xenopus tadpole. *J Neurophysiol, 112*(7), 1644-1655.
Hickmott, P. W., & Constantine-Paton, M. (1993). The contributions of NMDA, non-NMDA, and GABA receptors to postsynaptic responses in neurons of the optic tectum. *J Neurosci, 13*(10), 4339-4353.
Hille, B. (2001). *Ion channels of excitable membranes* (Vol. 507): Sinauer Sunderland, MA.
Hollis, D. M., & Boyd, S. K. (2005). Distribution of GABA-like immunoreactive cell bodies in the brains of two amphibians, Rana catesbeiana and Xenopus laevis. *Brain Behav Evol, 65*(2), 127-142.
Hughes, T. E. (1990). A light- and electron-microscopic investigation of the optic tectum of the frog, Rana pipiens, I: The retinal axons. *Vis Neurosci, 4*(6), 499-518.
Ingle, D. (1973a). Selective Choice between Double Prey Objects by Frogs. *Brain Behavior and Evolution, 7*(2), 127-144.
Ingle, D. (1973b). Two visual systems in the frog. *Science, 181*(4104), 1053-1055.
Ingle, D. (1975). Focal attention in the frog: behavioral and physiological correlates. *Science, 188*(4192), 1033-1035.
Isa, T., & Hall, W. C. (2009). Exploring the superior colliculus in vitro. *J Neurophysiol, 102*(5), 2581-2593.
Jenkin, S. M., & Laberge, F. (2010). Visual discrimination learning in the fire-bellied toad Bombina orientalis. *Learning & Behavior, 38*(4), 418-425.
Jetz, W., & Pyron, R. A. (2018). The interplay of past diversification and evolutionary isolation with present imperilment across the amphibian tree of life. *Nat Ecol Evol, 2*(5), 850-858.
Kaas, J. H., & Lyon, D. C. (2007). Pulvinar contributions to the dorsal and ventral streams of visual processing in primates. *Brain Research Reviews, 55*(2), 285-296.
Kadunce, D. C., Vaughan, J. W., Wallace, M. T., Benedek, G., & Stein, B. E. (1997). Mechanisms of within- and cross-modality suppression in the superior colliculus. *J Neurophysiol, 78*(6), 2834-2847.
Kandel, E. R. (2013). *Principles of neural science* (5th ed.). New York: McGraw-Hill.

Kardamakis, A. A., Perez-Fernandez, J., & Grillner, S. (2016). Spatiotemporal interplay between multisensory excitation and recruited inhibition in the lamprey optic tectum. *Elife, 5*.

Kardamakis, A. A., Saitoh, K., & Grillner, S. (2015). Tectal microcircuit generating visual selection commands on gaze-controlling neurons. *Proc Natl Acad Sci U S A, 112*(15), E1956-1965.

Kim, J., & Hetherington, T. E. (1993). Distribution and morphology of motoneurons innervating different muscle fiber types in an amphibian muscle complex. *J Morphol, 216*(3), 327-338.

Kostyk, S. K., & Grobstein, P. (1982). Visual Orienting Deficits in Frogs with Various Unilateral Lesions. *Behavioural Brain Research, 6*(4), 379-388.

Kottick, A., Baghdadwala, M. I., Ferguson, E. V., & Wilson, R. J. (2013). Transmission of the respiratory rhythm to trigeminal and hypoglossal motor neurons in the American Bullfrog (Lithobates catesbeiana). *Respir Physiol Neurobiol, 188*(2), 180-191.

Kozicz, T., & Lazar, G. (2001). Colocalization of GABA, enkephalin and neuropeptide Y in the tectum of the green frog Rana esculenta. *Peptides, 22*(7), 1071-1077.

Kuhlenbeck, H. (1967). *The central nervous system of vertebrates; a general survey of its comparative anatomy with an introduction to the pertinent fundamental biologic and logical concepts*. New York,: Academic Press.

Kulik, A., & Matesz, C. (1997). Projections from the nucleus isthmi to the visual and auditory centres in the frog, Rana esculenta. *J Hirnforsch, 38*(3), 299-307.

Laberge, F., Muhlenbrock-Lenter, S., Dicke, U., & Roth, G. (2008). Thalamo-telencephalic pathways in the fire-bellied toad Bombina orientalis. *J Comp Neurol, 508*(5), 806-823.

Landwehr, S., & Dicke, U. (2005). Distribution of GABA, glycine, and glutamate in neurons of the medulla oblongata and their projections to the midbrain tectum in plethodontid salamanders. *J Comp Neurol, 490*(2), 145-162.

Larsen, J. H., Jr., & Guthrie, D. J. (1975). The feeding system of terrestrial tiger salamanders (Ambystoma tigrinum melanostictum baird). *J Morphol, 147*(2), 137-153.

Lazar, G. (1969). Efferent pathways of the optic tectum in the frog. *Acta Biol Acad Sci Hung, 20*(2), 171-183.

Lazar, G. (1988). Columnar organization of the optic tectum in the frog. *Acta Biol Hung, 39*(2-3), 211-216.

Luksch, H., & Roth, G. (1996). Pretecto-tectal interactions: effects of lesioning and stimulating the pretectum on field potentials in the optic tectum of salamanders in vitro. *Neurosci Lett, 217*(2–3), 137-140.

Luthardt, G., & Roth, G. (1979). The influence of prey experience on movement pattern preference in Salamandra salamandra (L.). *Z Tierpsychol, 51*(3), 252-259.

Masino, T., & Grobstein, P. (1989). The organization of descending tectofugal pathways underlying orienting in the frog, Rana pipiens. I. Lateralization, parcellation, and an intermediate spatial representation. *Experimental Brain Research, 75*(2), 227-244.

Matesz, C., & Szekely, G. (1978). The motor column and sensory projections of the branchial cranial nerves in the frog. *J Comp Neurol, 178*(1), 157-176.

Matsumoto, N., & Bando, T. (1980). Excitatory synaptic potentials and morphological classification of tectal neurons of the frog. *Brain Res, 192*(1), 39-48.

Maturana, H. R. (1959). Number of fibres in the optic nerve and the number of ganglion cells in the retina of anurans. *Nature, 183*(4672), 1406-1407.

Maturana, H. R., Lettvin, J. Y., McCulloch, W. S., & Pitts, W. H. (1959). Evidence That Cut Optic Nerve Fibers in a Frog Regenerate to Their Proper Places in the Tectum. *Science, 130*(3390), 1709-1710.

McConville, J., Sterritt, L., & Laming, P. R. (2006). Behavioural responses to electrical and visual stimulation of the toad tectum. *Behavioural Brain Research, 170*(1), 15-22.

Meredith, M. A., Nemitz, J. W., & Stein, B. E. (1987). Determinants of multisensory integration in superior colliculus neurons. I. Temporal factors. *J Neurosci, 7*(10), 3215-3229.

Meredith, M. A., & Ramoa, A. S. (1998). Intrinsic circuitry of the superior colliculus: pharmacophysiological identification of horizontally oriented inhibitory interneurons. *J Neurophysiol, 79*(3), 1597-1602.

Meredith, M. A., & Stein, B. E. (1996). Spatial determinants of multisensory integration in cat superior colliculus neurons. *J Neurophysiol, 75*(5), 1843-1857.

Montgomery, N., & Fite, K. V. (1989). Retinotopic organization of central optic projections in Rana pipiens. *J Comp Neurol, 283*(4), 526-540.

Moschovakis, A. K., Scudder, C. A., & Highstein, S. M. (1996). The microscopic anatomy and physiology of the mammalian saccadic system. *Prog Neurobiol, 50*(2-3), 133-254.

Muhlenbrock-Lenter, S., Roth, G., & Grunwald, W. (2005). Connectivity and cytoarchitecture of telencephalic centers in the fire-bellied toad Bombina orientalis. *Brain Res Bull, 66*(4-6), 270-276.

Muntz, W. R. (1963). The development of phototaxis in the frog (Rana temporaria). *J Exp Biol, 40*, 371-379.

Naujoks-Manteuffel, C., & Niemann, U. (1994). Microglial cells in the brain of Pleurodeles waltl (Urodela, Salamandridae) after wallerian degeneration in the primary visual system using Bandeiraea simplicifolia isolectin B4-cytochemistry. *Glia, 10*(2), 101-113.

Neary, T. J., & Northcutt, R. G. (1983). Nuclear organization of the bullfrog diencephalon. *Journal of Comparative Neurology, 213*(3), 262-278.

Nieuwenhuys, R., Donkelaar, H. J. t., & Nicholson, C. (1998). *The central nervous system of vertebrates*. Berlin ; New York: Springer.

Nieuwenhuys, R., Hans, J., & Nicholson, C. (2014). *The central nervous system of vertebrates*: Springer.

Northcutt, R. G. (1974). Some histochemical observations on the telencephalon of the bullfrog, Rana catesbeiana Shaw. *J Comp Neurol, 157*(4), 379-389.

Numberger, M., & Draguhn, A. (1996). *Patch-Clamp-Technik*: Spektrum Akademischer Verlag

Olsen, R. W., & Sieghart, W. (2009). GABA A receptors: subtypes provide diversity of function and pharmacology. *Neuropharmacology, 56*(1), 141-148.

Panzanelli, P., Mulatero, B., Lazarus, L. H., & Fasolo, A. (1991). Neuromedin B-like immunoreactivity in the brain of the green frog (Rana esculenta L.). *Eur J Basic Appl Histochem, 35*(4), 359-370.

Papini, M. R., Muzio, R. N., & Segura, E. T. (1995). Instrumental learning in toads (Bufo arenarum): reinforcer magnitude and the medial pallium. *Brain Behav Evol, 46*(2), 61-71.

Phongphanphanee, P., Marino, R. A., Kaneda, K., Yanagawa, Y., Munoz, D. P., & Isa, T. (2014). Distinct local circuit properties of the superficial and intermediate layers of the rodent superior colliculus. *Eur J Neurosci, 40*(2), 2329-2343.

Potter, H. D. (1969). Structural characteristics of cell and fiber populations in the optic tectum of the frog (Rana catesbeiana). *J Comp Neurol, 136*(2), 203-231.

Pough, F. H. (2016). *Herpetology* (Fourth edition. ed.). Sunderland, Massachusetts, USA: Sinauer Associates, Inc., Publishers.
Puelles, L., Javier Milan, F., & Martinez-de-la-Torre, M. (1996). A segmental map of architectonic subdivisions in the diencephalon of the frog Rana perezi: acetylcholinesterase-histochemical observations. *Brain Behav Evol, 47*(6), 279-310.
Recanzone, G. H. (2003). Auditory influences on visual temporal rate perception. *J Neurophysiol, 89*(2), 1078-1093.
Reiner, A., Medina, L., & Veenman, C. L. (1998). Structural and functional evolution of the basal ganglia in vertebrates. *Brain Res Brain Res Rev, 28*(3), 235-285.
Rettig, G., & Roth, G. (1986). Retinofugal Projections in Salamanders of the Family Plethodontidae. *Cell and Tissue Research, 243*(2), 385-396.
Ricciuti, A. J., & Gruberg, E. R. (1985). Nucleus isthmi provides most tectal choline acetyltransferase in the frog Rana pipiens. *Brain Res, 341*(2), 399-402.
Roberts, A., & Perrins, R. (1995). Positive feedback as a general mechanism for sustaining rhythmic and non-rhythmic activity. *J Physiol Paris, 89*(4-6), 241-248.
Robertson, B., Saitoh, K., Menard, A., & Grillner, S. (2006). Afferents of the lamprey optic tectum with special reference to the GABA input: combined tracing and immunohistochemical study. *J Comp Neurol, 499*(1), 106-119.
Roth, G. (1987). *Visual behavior in salamanders*. Berlin Heidelberg: Springer-Verlag.
Roth, G., Dicke, U., & Grunwald, W. (1999). Morphology, axonal projection pattern, and response types of tectal neurons in plethodontid salamanders. II: intracellular recording and labeling experiments. *J Comp Neurol, 404*(4), 489-504.
Roth, G., Grunwald, W., & Dicke, U. (2003). Morphology, axonal projection pattern, and responses to optic nerve stimulation of thalamic neurons in the fire-bellied toad Bombina orientalis. *J Comp Neurol, 461*(1), 91-110.
Roth, G., Laberge, F., Muhlenbrock-Lenter, S., & Grunwald, W. (2007). Organization of the pallium in the fire-bellied toad Bombina orientalis. I: Morphology and axonal projection pattern of neurons revealed by intracellular biocytin labeling. *J Comp Neurol, 501*(3), 443-464.
Roth, G., Muhlenbrock-Lenter, S., Grunwald, W., & Laberge, F. (2004). Morphology and axonal projection pattern of neurons in the telencephalon of the fire-bellied toad Bombina orientalis: an anterograde, retrograde, and intracellular biocytin labeling study. *J Comp Neurol, 478*(1), 35-61.
Roth, G., Nishikawa, K., Dicke, U., & Wake, D. B. (1988). Topography and cytoarchitecture of the motor nuclei in the brainstem of salamanders. *J Comp Neurol, 278*(2), 181-194.
Rowland, B. A., Stanford, T. R., & Stein, B. E. (2007). A model of the neural mechanisms underlying multisensory integration in the superior colliculus. *Perception, 36*(10), 1431-1443.
Ruhl, T., & Dicke, U. (2012). The role of the dorsal thalamus in visual processing and object selection: a case of an attentional system in amphibians. *Eur J Neurosci, 36*(11), 3459-3470.
Ruhl, T., Hanslian, S., & Dicke, U. (2016). Lesions of the dorsal striatum impair orienting behaviour of salamanders without affecting visual processing in the tectum. *Eur J Neurosci, 44*(8), 2581-2592.
Rybicka, K. K., & Udin, S. B. (1994). Ultrastructure and GABA immunoreactivity in layers 8 and 9 of the optic tectum of Xenopus laevis. *Eur J Neurosci, 6*(10), 1567-1582.
Saitoh, K., Menard, A., & Grillner, S. (2007). Tectal control of locomotion, steering, and eye movements in lamprey. *J Neurophysiol, 97*(4), 3093-3108.

San Mauro, D., Vences, M., Alcobendas, M., Zardoya, R., & Meyer, A. (2005). Initial diversification of living amphibians predated the breakup of Pangaea. *Am Nat, 165*(5), 590-599.

Satou, M., & Ewert, J. P. (1984). Specification of tecto-motor outflow in toads by antidromic stimulation of tecto-bulbar/spinal pathways. *Naturwissenschaften, 71*(1), 52-53.

Scalia, F., & Fite, K. (1974). A retinotopic analysis of the central connections of the optic nerve in the frog. *J Comp Neurol, 158*(4), 455-477.

Scalia, F., Gallousis, G., & Roca, S. (1991). Differential projections of the main and accessory olfactory bulb in the frog. *J Comp Neurol, 305*(3), 443-461.

Schindelin, J., Arganda-Carreras, I., Frise, E., Kaynig, V., Longair, M., Pietzsch, T., Preibisch, S., Rueden, C., Saalfeld, S., Schmid, B., Tinevez, J. Y., White, D. J., Hartenstein, V., Eliceiri, K., Tomancak, P., & Cardona, A. (2012). Fiji: an open-source platform for biological-image analysis. *Nat Methods, 9*(7), 676-682.

Schofield, P. R., Darlison, M. G., Fujita, N., Burt, D. R., Stephenson, F. A., Rodriguez, H., Rhee, L. M., Ramachandran, J., Reale, V., Glencorse, T. A., & *et al.* (1987). Sequence and functional expression of the GABA A receptor shows a ligand-gated receptor super-family. *Nature, 328*(6127), 221-227.

Schuelert, N., & Dicke, U. (2005). Dynamic response properties of visual neurons and context-dependent surround effects on receptive fields in the tectum of the salamander Plethodon shermani. *Neuroscience, 134*(2), 617-632.

Singman, E. L., & Scalia, F. (1990). Quantitative study of the tectally projecting retinal ganglion cells in the adult frog: I. The size of the contralateral and ipsilateral projections. *J Comp Neurol, 302*(4), 792-809.

Singman, E. L., & Scalia, F. (1991). Quantitative study of the tectally projecting retinal ganglion cells in the adult frog. II. Cell survival and functional recovery after optic nerve transection. *J Comp Neurol, 307*(3), 351-369.

Skorina, L. K., Recktenwald, E. W., Dudkin, E. A., Saidel, W. M., & Gruberg, E. R. (2016). Representation of the visual field in the anterior thalamus of the leopard frog, Rana pipiens. *Neurosci Lett, 621*, 34-38.

Standen, N. B., Davies, N. W., & Langton, P. D. (1987). *Separation and analysis of macroscopic currents.* Paper presented at the Microelectrode Techniques, The Plymouth Workshop Handbook. 1st ed. Standen NB, Gray PTA, Whitaker MJ, Eds. Cambridge, UK, Company of Biologists.

Stein, B. E., & Stanford, T. R. (2008). Multisensory integration: current issues from the perspective of the single neuron. *Nat Rev Neurosci, 9*(4), 255-266.

Stirling, R. V., & Merrill, E. G. (1987). Functional morphology of frog retinal ganglion cells and their central projections: the dimming detectors. *J Comp Neurol, 258*(4), 477-495.

Straka, H., & Dieringer, N. (1993). Electrophysiological and pharmacological characterization of vestibular inputs to identified frog abducens motoneurons and internuclear neurons in vitro. *Eur J Neurosci, 5*(3), 251-260.

Szekely, G., Setalo, G., & Lazar, G. (1973). Fine structure of the frog's optic tectum: optic fibre termination layers. *J Hirnforsch, 14*(1), 189-225.

Thexton, A. J., Wake, D. B., & Wake, M. H. (1977). Tongue function in the salamander Bolitoglossa occident alis. *Arch Oral Biol, 22*(6), 361-366.

Thoreson, W. B., & Bryson, E. J. (2004). Chloride equilibrium potential in salamander cones. *BMC Neurosci, 5*, 53.

Unwin, N. (1993). Neurotransmitter action: opening of ligand-gated ion channels. *Cell, 72 Suppl*, 31-41.

Ursino, M., Cuppini, C., Magosso, E., Serino, A., & di Pellegrino, G. (2009). Multisensory integration in the superior colliculus: a neural network model. *J Comput Neurosci, 26*(1), 55-73.

Wada, M., Urano, A., & Gorbman, A. (1980). A stereotaxic atlas for diencephalic nuclei of the frog, Rana pipiens. *Arch Histol Jpn, 43*(2), 157-173.

Wake, D. B., Nishikawa, K. C., Dicke, U., & Roth, G. (1988). Organization of the motor nuclei in the cervical spinal cord of salamanders. *J Comp Neurol, 278*(2), 195-208.

Wallace, M. T., Ricciuti, A. J., & Gruberg, E. R. (1990). Nucleus isthmi: its contribution to tectal acetylcholinesterase and choline acetyltransferase in the frog Rana pipiens. *Neuroscience, 35*(3), 627-636.

Wallace, M. T., Wilkinson, L. K., & Stein, B. E. (1996). Representation and integration of multiple sensory inputs in primate superior colliculus. *J Neurophysiol, 76*(2), 1246-1266.

Wallstein, W., & Dicke, U. (1996). Distribution of glutamate-, GABA- and glycine-like immunoreactivity in the optic tectum of plethodontid salamanders. In N. E. a. H. U. Schnitzler (Ed.), *Proceedings of the 24th Gottingen Neurobiology Conference (I)*: Thieme.

Wenz, E., & Himstedt, W. (1990). Telencephalic structures are involved in learning and memory in the newt Triturus alpestris. *Naturwissenschaften, 77*(5), 239-240.

Westhoff, G., & Roth, G. (2002). Morphology and projection pattern of medial and dorsal pallial neurons in the frog Discoglossus pictus and the salamander Plethodon jordani. *J Comp Neurol, 445*(2), 97-121.

Wiggers, W. (1999). Projections of single retinal ganglion cells to the visual centers: an intracellular staining study in a plethodontid salamander. *Vis Neurosci, 16*(3), 435-447.

Wiggers, W., & Roth, G. (1994). Depth perception in salamanders: the wiring of visual maps. *Eur J Morphol, 32*(2-4), 311-314.

Wilczynski, W. (1981). Afferents to the midbrain auditory center in the bullfrog, rana catesbeiana. *J Comp Neurol, 198*(3), 421-433.

Wurtz, R. H., & Albano, J. E. (1980). Visual-motor function of the primate superior colliculus. *Annu Rev Neurosci, 3*, 189-226.

Wurtz, R. H., & Hikosaka, O. (1986). Role of the basal ganglia in the initiation of saccadic eye movements. *Prog Brain Res, 64*, 175-190.

Yang, S., & Feng, A. S. (2007). Heterogeneous biophysical properties of frog dorsal medullary nucleus (cochlear nucleus) neurons. *J Neurophysiol, 98*(4), 1953-1964.

Yang, S., Lin, W., & Feng, A. S. (2009). Wide-ranging frequency preferences of auditory midbrain neurons: Roles of membrane time constant and synaptic properties. *Eur J Neurosci, 30*(1), 76-90.

Zhu, S., Noviello, C. M., Teng, J., Walsh, R. M., Jr., Kim, J. J., & Hibbs, R. E. (2018). Structure of a human synaptic GABAA receptor. *Nature, 559*(7712), 67-72.

7. Appendix

7.1 Figures

7.2 Tables

7. 3 Supplementary Information

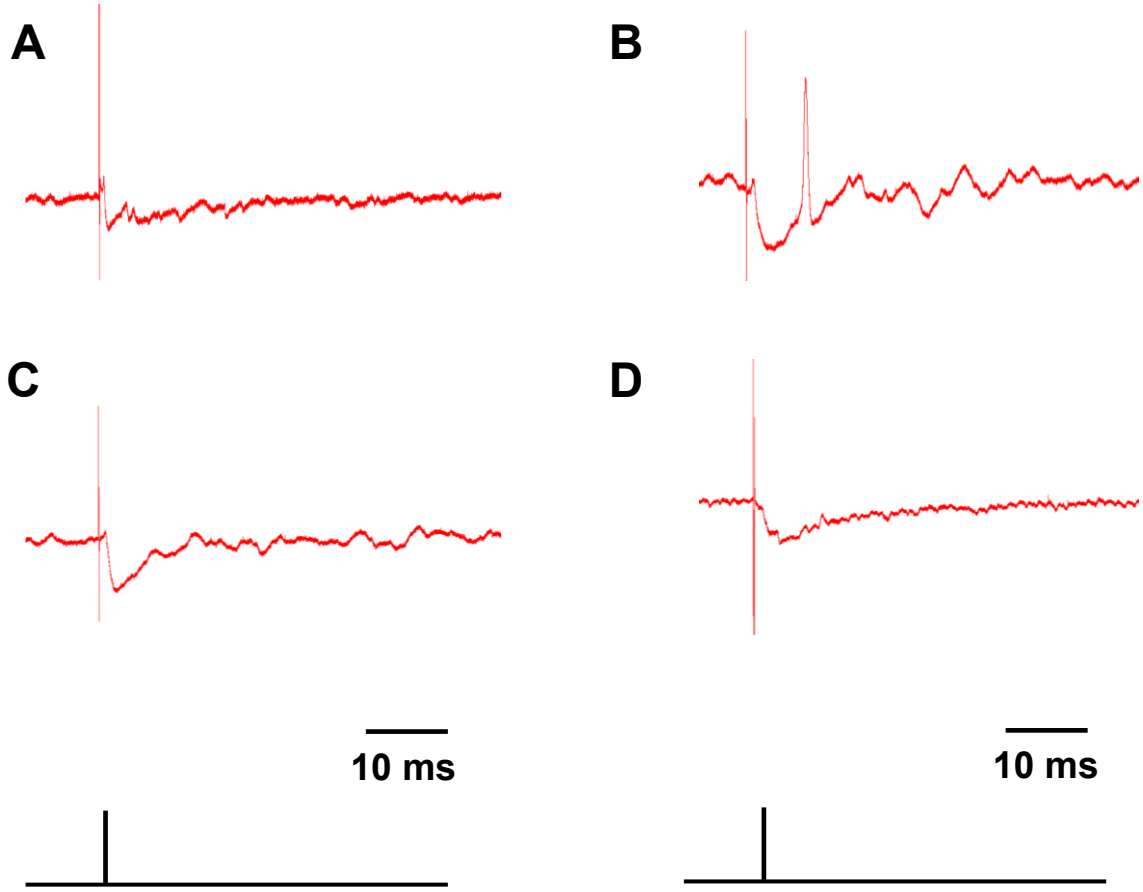

Figure 30 Representative double inhibition or inhibition followed by excitation after TH STIM.

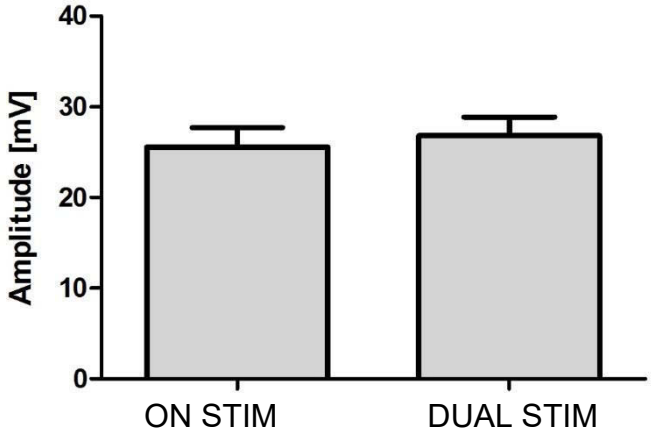

Figure 31 Average amplitude for action potentials after optic nerve stimulation (ON STIM) and double stimulation of the thalamus and optic nerve (DUAL STIM). *Whiskers represent SD, n = 12.*

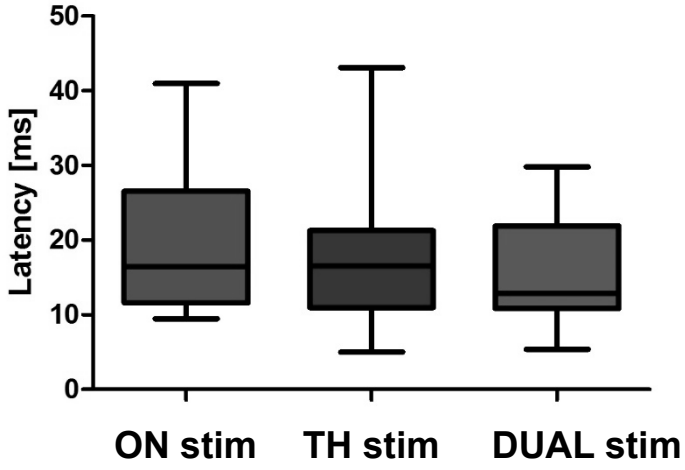

Figure 32 Average IPSP latencies during stimulation of the optic nerve (ON stim), the thalamus (TH stim) and both simultaneously (DUAL stim). *Middle black bar represents the average, while the grey box represents 50% of datapoints, black whiskers represent the distance to the highest and lowest recorded values.*

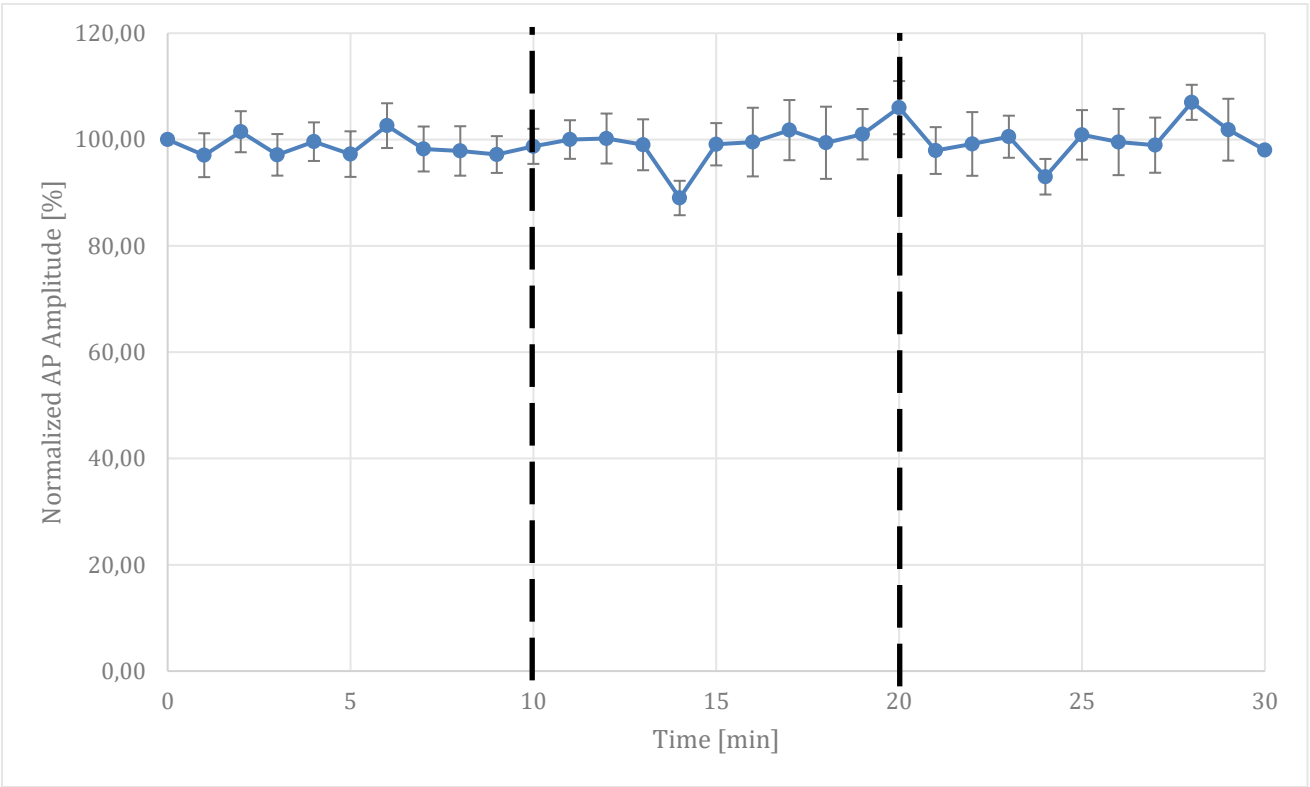

Figure 33 Time course of action potential amplitude during pharmacological agent application. *Representative normalized AP amplitudes in relation to the average amplitude of AP during minute 0. Dashed lines indicate application of Gabazine or wash-out.*

Zusammenfassung (deutsche Übersetzung)

Das Gehirn von Wirbeltieren ist ein hochdynamisches und komplexes Netzwerk, welches Lebewesen erlaubt, die Reize aus ihrer Umwelt zu verarbeiten, verschiedene Objekte innerhalb ihres visuellen Feldes zu detektieren und Entscheidungen zu treffen. Das Mittelhirn – optisches Tectum ist das Hauptzentrum der visuomotorischen Integration im Amphibiengehirn. Zusätzlich erreichen es zahlreiche Eingänge aus anderen Hirnarealen, darunter Areale aus dem Zwischenhirn, wie dem Nucleus Isthmi oder dem Prätectum. Diese Thesis zeigte, dass Neuronen aus dem optischen Tectum durch den Thalamus beeinflusst werden. Die Verarbeitung von Objektinformationen wurde durch Stimulation des optischen Nervens simuliert. Der Einfluss des Thalamus wurde durch die Stimulation des dorsalen Thalamus simuliert. EPSP, die durch Stimulation des Thalamus ausgelöst wurden, unterschieden sich in der Verteilung ihrer Latenz. Dies suggeriert eine di- oder oligosynaptische Projektion des dorsalen Thalamus zum optischen Tectum. Wahrscheinlich vermitteln Neuronen des Typs TH3 oder TH5 solch eine Projektion. Obwohl keine statistischen signifikanten Unterschiede in der Amplitude zwischen beiden Versuchsbedingungen gefunden wurde, unterschied sich die Latenz der Aktionspotentiale nach Stimulation des optischen Nerven und nach gleichzeitiger Stimulation des Thalamus und des optischen Nerven statistisch signifikant. Diese ‚zeitliche Inhibition' ist wahrscheinlich ein Mechanismus innerhalb eines tecto-thalamischen-Rückkopplungsmechanismus, welcher als Aufmerksamkeitssystem bei Aufgaben einer gepaarten-Objekt-Präsentationen bei Amphibien dient. Häufig reagierten tectale Neuronen mit IPSP nach Stimulation des Thalamus. Markierung von Neuronen mit Biocytin zeigte, dass sowohl Projektionsneurone als auch Interneurone des Tectum mit Inhibition auf Thalamusstimulation reagierten. Diese Ergebnisse suggerieren, dass Inhibition, vermittelt durch den Thalamus und GABAergen Interneuronen, welche dann lokale inhibitorische Netzwerke aktivieren, erreicht wird. Damit sowohl das Membranpotential von tectalen Neuronen aufgezeichnet und die Top-down Modulation durch das Zwischenhirn untersucht werden kann, wurde eine neue Präparationsmethode entwickelt. Die Mittelhirnsphäre wurde manuell eröffnet, um eine geneigte Gewebefläche zu schaffen, die zu mikroskopieren ist. Zusätzlich blieben die gesamte Vorderhirnhälfte, inklusive optischem Nerv und absteigenden Fasern erhalten. Mithilfe dieser Präparation wurde der optische Nerv stimuliert und das Membranpotential von tektalen Neuronen durch ‚Whole-Cell Patch Clamp' Technik aufgenommen. EPSP mit kurzen Latenzen, welche wahrscheinlich monosynaptischen Ursprungs sind, wurden mit der Badapplikation von 100 µM DL-AP5 unterdrückt. Diese waren aber noch präsent nach der Applikation von 10 µM NBQX. Diese Ergebnisse zeigen, dass die Projektionen der retinalen Ganglienzellen durch NMDA Rezeptoren vermittelt werden. IPSP, die von Thalamusstimulation in dieser Präparation aufgenommen wurden, konnten durch die Badapplikation von 100 µM Gabazin sowohl in Amplitude als auch in Auftrittswahrscheinlichkeit unterdrückt werden. Dies deutet auf hauptsächlich GABAerge Projektionen, welchem vom Thalamus stammen, hin. Diese Thesis schlägt vor, dass tecale Interneurone, welche von Thalamusneuronen moduliert werden, wiederrum tectale Projektionsneurone beeinflussen, die Eingänge von der Retina erhalten.

7.4. Affidavit

Anlage 1 zur Promotionsordnung

Versicherung an Eides Statt

Ich, Nikola Misevic, Kunkelstr. 9, Berlin 13347, 2135676, versichere an Eides Statt durch meine Unterschrift, dass ich die vorstehende Arbeit selbständig und ohne fremde Hilfe angefertigt und alle Stellen, die ich wörtlich dem Sinne nach aus Veröffentlichungen entnommen habe, als solche kenntlich gemacht habe, mich auch keiner anderen als der angegebenen Literatur oder sonstiger Hilfsmittel bedient habe.

Ich versichere an Eides Statt, dass ich die vorgenannten Angaben nach bestem Wissen und Gewissen gemacht habe und dass die Angaben der Wahrheit entsprechen und ich nichts verschwiegen habe.

Die Strafbarkeit einer falschen eidesstattlichen Versicherung ist mir bekannt, namentlich die Strafandrohung gemäß § 156 StGB bis zu drei Jahren Freiheitsstrafe oder Geldstrafe bei vorsätzlicher Begehung der Tat bzw. gemäß § 161 Abs. 1 StGB bis zu einem Jahr Freiheitsstrafe oder Geldstrafe bei fahrlässiger Begehung.

_____ _____

Ort, Datum Unterschrift